


8-2018

# Strong Evidence for the Density-wave Theory of Spiral Structure from a Multi-wavelength Study of Disk Galaxies

Hamed Pour-Imani

*University of Arkansas, Fayetteville*

Follow this and additional works at: <http://scholarworks.uark.edu/etd>

 Part of the [Physical Processes Commons](#), and the [Stars, Interstellar Medium and the Galaxy Commons](#)

---

## Recommended Citation

Pour-Imani, Hamed, "Strong Evidence for the Density-wave Theory of Spiral Structure from a Multi-wavelength Study of Disk Galaxies" (2018). *Theses and Dissertations*. 2864.

<http://scholarworks.uark.edu/etd/2864>

This Dissertation is brought to you for free and open access by ScholarWorks@UARK. It has been accepted for inclusion in Theses and Dissertations by an authorized administrator of ScholarWorks@UARK. For more information, please contact [scholar@uark.edu](mailto:scholar@uark.edu), [ccmiddle@uark.edu](mailto:ccmiddle@uark.edu).

Strong Evidence for the Density-wave Theory of Spiral Structure from a Multi-wavelength  
Study of Disk Galaxies

A dissertation submitted in partial fulfillment  
of the requirements for the degree of  
Doctor of Philosophy in Physics

by

Hamed Pour-Imani  
University of Isfahan  
Bachelor of Science in Physics, 2004  
University of Arkansas  
Master of Science in Physics, 2016

August 2018  
University of Arkansas

This dissertation is approved for recommendation to the Graduate Council.

---

Daniel Kennefick, Ph.D.  
Dissertation Director

---

Vincent Chevrier, Ph.D.  
Committee Member

---

Claud Lacy, Ph.D.  
Committee Member

---

Julia Kennefick, Ph.D.  
Committee Member

---

William Oliver, Ph.D.  
Committee Member

## ABSTRACT

The density-wave theory of spiral structure, though first proposed as long ago as the mid-1960s by C.C. Lin and F. Shu (Lin & Shu, 1964; Bertin & Lin, 1996; Shu, 2016), continues to be challenged by rival theories, such as the manifold theory. One test of these theories which has been proposed is that the pitch angle of spiral arms for galaxies should vary with the wavelength of the image in the density-wave theory, but not in the manifold theory. The reason is that stars are born in the density wave but move out of it as they age. In this dissertation, I combined large sample size with a wide range of wavelengths to investigate this issue. For each galaxy, I used wavelength FUV151nm,  $u$ -band, H- $\alpha$ , optical wavelength  $B$ -band and infrared 3.6 and 8.0  $\mu\text{m}$ . I measured the pitch angle with the 2DFFT and Spirality codes (Davis et al., 2012; Shields et al., 2015). I find that the  $B$ -band and 3.6  $\mu\text{m}$  images have smaller pitch angles than the infrared 8.0  $\mu\text{m}$  image in all cases, in agreement with the prediction of the density-wave theory. I also find that the pitch angle at FUV and H- $\alpha$  are close to the measurements made at 8.0  $\mu\text{m}$ . The Far-ultraviolet wavelength at 151nm shows very young, very bright UV stars still in the star-forming region (they are so bright as to be visible there and so short-lived that they never move out of it). I find that for both sets of measurements (2DFFT and Spirality) the 8.0  $\mu\text{m}$ , H- $\alpha$  and ultraviolet images agree in their pitch angle measurements, suggesting that they are, in fact, sensitive to the same region. By contrast, the 3.6  $\mu\text{m}$  and  $B$ -band images are uniformly tighter in pitch angle measurements than these wavelengths, suggesting that the density-wave picture is correct.

## DEDICATION

To my parents, my wife and my beloved family.

## EPIGRAPH

*We should do astronomy because it is beautiful and because it is fun. We should do it because people want to know. We want to know our place in the universe and how things happen.*

John N. Bahcall

## ACKNOWLEDGEMENTS

The last seven years of my life has truly been an amazing experience, and for this, I am grateful to a number of individuals, both for helping me finish this research, as well as making the journey enjoyable.

Thank you to my parents and to the rest of my family and friends, for all of their encouragement and support that has brought me to this point. I would like express appreciation to my beloved wife, Maryam, for being with me every step of my graduate career and my life.

Thank you to my advisor, Dr. Daniel Kenefick, and Dr. Julia Kenefick for consistently supporting my research with the Arkansas Galaxy Evolution Survey (AGES). Your informal approach towards advising me has made all of this research possible.

Thank you to my doctoral committee members, Dr. Cluad Lacy, Dr. William Oliver and Dr. Vincent Chevrier, for their insightful comments, encouragement, feedback, wisdom, and support.

Thank you to all my fellow students in AGES for your collaboration and friendship. Thank you to Dr. Benjamin Davis and Dr. Douglas Shields for teaching me the technique and providing me with the software necessary to perform 2DFFT and Spirality pitch angle measurements. Without your guidance, my graduate student career would have been entirely different.

Thank you, Physics Department, for giving me the opportunity to pursue a doctoral degree in physics at the University of Arkansas.

This research has made use of NASA's Astrophysics Data System and the NASA/IPAC Extragalactic Database, which is operated by the Jet Propulsion Laboratory, California Insti-

tute of Technology, under contract with the National Aeronautics and Space Administration.

## TABLE OF CONTENTS

<b>Chapter 1. Spiral Galaxies and Spiral Structure</b>	<b>1</b>
1.1 Introduction . . . . .	1
1.2 Spiral Galaxies . . . . .	2
1.3 Logarithmic Spiral Pitch Angle . . . . .	6
1.4 Hypotheses for Spiral Structure . . . . .	6
1.4.1 Winding Problem . . . . .	6
1.4.2 The Density-wave Theory . . . . .	7
1.4.3 SSPSF Model . . . . .	10
1.5 Thesis Outline . . . . .	10
Bibliography . . . . .	12
<b>Chapter 2. The Density-wave Theory of Spiral Structure and Pitch Angle Variations</b>	<b>13</b>
2.1 Introduction . . . . .	13
2.2 The Density-wave Theory and Pitch Angle Variations . . . . .	13
2.3 Previous Works . . . . .	16
2.4 Galaxies Imaged at Different Wavelengths of Light . . . . .	16
2.4.1 Spitzer Space Telescope . . . . .	18
2.4.1.1 IRAC 3.6 $\mu\text{m}$ . . . . .	18
2.4.1.2 IRAC 8.0 $\mu\text{m}$ . . . . .	18
2.4.2 <i>B</i> -band 445 nm . . . . .	19
2.4.3 Far-ultraviolet 151 nm (FUV) . . . . .	19
2.5 Methods for Pitch Angle Measurements . . . . .	19
2.5.1 2DFFT Code . . . . .	19
2.5.2 Spirality Code . . . . .	20
2.6 Conclusion . . . . .	20
Bibliography . . . . .	21
<b>Chapter 3. Strong Evidence for the Density-wave Theory of Spiral Structure in Disk Galaxies</b>	<b>23</b>
3.1 Abstract . . . . .	23
3.2 Introduction . . . . .	24
3.3 Data . . . . .	34
3.4 2DFFT Results . . . . .	34
3.5 Spirality Results . . . . .	41
3.6 Discussion . . . . .	48
3.7 Conclusion . . . . .	55
3.8 Acknowledgments . . . . .	56
Bibliography . . . . .	57
<b>Chapter 4. Spiral Structure Through a Multi-wavelength Study</b>	<b>59</b>
4.1 Abstract . . . . .	59
4.2 Introduction . . . . .	59
4.3 Data . . . . .	66
4.4 Results . . . . .	69
4.5 The Location of the Density-wave . . . . .	70



4.6	Pitch Angle Differences Between Optical and NIR Wavelengths . . . . .	76
4.7	Evidence From the <i>u</i> -band . . . . .	81
4.8	Conclusion . . . . .	86
	Bibliography . . . . .	87
<b>Chapter 5. The Connection Between Shear and Pitch Angle Variation in Different Wavelength</b>		<b>89</b>
5.1	Abstract . . . . .	89
5.2	Introduction . . . . .	89
5.3	Shear Rate, Mass Distribution, and Pitch Angle . . . . .	91
5.4	Data . . . . .	94
5.5	Shear rate and pitch angle variation for <i>B</i> -band, 3.6 and 8.0 $\mu\text{m}$ . . . . .	96
	5.5.1 Unbarred, Intermediate, and Barred Galaxies . . . . .	96
	5.5.2 Unbarred Galaxies . . . . .	100
5.6	Conclusion . . . . .	103
	Bibliography . . . . .	104
<b>Chapter 6. Conclusions</b>		<b>106</b>
	Bibliography . . . . .	109
<b>Appendix</b>		<b>111</b>
	American Astronomical Society Copyright Agreement . . . . .	111
	Vitæ . . . . .	112

## LIST OF FIGURES

Figure 1.1:	The Spitzer Infrared Nearby Galaxies Survey (SINGS) Hubble Tuning-Fork (Poster and Composite images created from SINGS observations (Kennicutt et al., 2003) by Karl D. Gordon). . . . .	4
Figure 1.2:	Illustration of the definition of logarithmic spiral arm pitch angle. There are four elements in the plot above: blue - a logarithmic spiral with $\phi = 25^\circ$ , teal - a circle with $r = 2.08$ intersecting the logarithmic spiral at $(0, 2.08)$ , red - a line tangent to the circle at $(0, 2.08)$ , and green - a line tangent to the logarithmic spiral at $(0, 2.08)$ . The angle subtended between the line tangent to circle and the line tangent to the logarithmic spiral is $25^\circ$ , which is equivalent to the pitch angle of the logarithmic spiral (Davis, 2015). . . . .	5
Figure 1.3:	Left: cartoon of density-wave moving through a rotating disk compared to, right: NGC1566, an intermediate spiral galaxy (Photo by Hubble Space Telescope). . . . .	9
Figure 2.1:	Predictions of density-wave theory for spiral-arm structure with old stars, blue stars, gas, and dust. (Figure created by H.Pour Imani). . . . .	15
Figure 3.1:	Predictions of density-wave theory for spiral-arm structure with old stars, blue stars, gas, and dust. On the left is a scenario where star formation occurs after gas clouds pass through the minimum of the potential of the density wave. On the right is a scenario in which star formation occurs as the gas clouds approach this minimum of the potential. . . . .	26
Figure 3.2:	Comparisons between pitch angles measured by 2DFFT code at wavelength $8.0 \mu\text{m}$ and $3.6 \mu\text{m}$ . Each point on the plots represents an individual galaxy positioned according to the measurement of its spiral-arm pitch angle at two different wavelengths. The histograms show the distribution of pitch angle differences in terms of the number of galaxies found in each bin. The greatest number of galaxies have a pitch angle difference of between $2^\circ.5$ and $5^\circ$ (see the relevant histograms), with very few found below $2^\circ.5$ . Images of 41 galaxies were used from SINGS survey. . . . .	36
Figure 3.3:	Comparisons between pitch angles measured by 2DFFT code at wavelength $3.6 \mu\text{m}$ and $B$ -band $445 \text{ nm}$ . The histograms show that the $B$ -band with $3.6 \mu\text{m}$ wavelengths are fundamentally equal since the greatest number of galaxies have pitch angles at these wavelengths that agree to better than $2^\circ.5$ . Images of 41 galaxies were used from SINGS survey. . . . .	37
Figure 3.4:	Comparisons between pitch angles measured by 2DFFT code at wavelength $B$ -band $445 \text{ nm}$ and FUV $151 \text{ nm}$ . The histograms show the greatest number of galaxies have a pitch angle difference of between $2^\circ.5$ and $5^\circ$ , with very few found below $2^\circ.5$ . Images of 28 galaxies were used from SINGS survey. . . . .	38

Figure 3.5:	Comparisons between pitch angles measured by 2DFFT code at wavelength $8.0 \mu\text{m}$ and FUV $151 \text{ nm}$ . The histograms show that the $8.0 \mu\text{m}$ and far ultraviolet (FUV) wavelengths are fundamentally equal since the greatest number of galaxies have pitch angles at these wavelengths that agree to better than $2^\circ.5$ . Images of 28 galaxies were used from SINGS survey. . . . .	39
Figure 3.6:	Pitch angle for NGC 3184 with different wavelengths. Left to right: $-11^\circ.92$ ( $3.6 \mu\text{m}$ ), $-18^\circ.30$ ( $B$ -band), $-23^\circ.40$ ( $8.0 \mu\text{m}$ ), $-26^\circ.75$ (FUV). . . .	40
Figure 3.7:	Comparisons between pitch angles measured by Spirality code at wavelength $8.0 \mu\text{m}$ and $B$ -band $445 \text{ nm}$ . . . . .	42
Figure 3.8:	Comparisons between pitch angles measured by Spirality code at wavelength $3.6 \mu\text{m}$ and $B$ -band $445 \text{ nm}$ . . . . .	43
Figure 3.9:	Comparisons between pitch angles measured by Spirality code at wavelength $8.0 \mu\text{m}$ and $3.6 \mu\text{m}$ . . . . .	44
Figure 3.10:	Comparisons between pitch angles measured by Spirality and 2DFFT code at wavelength $3.6 \mu\text{m}$ . . . . .	45
Figure 3.11:	Comparisons between pitch angles measured by Spirality and 2DFFT code at wavelength $8.0 \mu\text{m}$ . . . . .	46
Figure 3.12:	Comparisons between pitch angles measured by Spirality and 2DFFT code at wavelength $B$ -band $445 \text{ nm}$ . . . . .	47
Figure 4.1:	Predictions of density-wave theory for the spiral-arm structure at the different wavelength of light.(Pour-Imani et al., 2016) . . . . .	62
Figure 4.2:	Star-formation may be initiated as gas clouds approach the location of the spiral density-wave. In this scenario, newly born stars seen downstream of the star-forming region will be found close to the position of the density-wave. . . . .	63
Figure 4.3:	B Vs NIR, Hamed (Pour-Imani et al., 2016), Ben(Davis et al., 2012), Patsis (Grosbol & Patsis, 1998), Martinez (Martinez-Garcia, 2012), Seigar (Seigar et al., 2006) . . . . .	65
Figure 4.4:	Comparisons between pitch angles measured at different wavelengths. Each point on the plots represents an individual galaxy positioned according to the measurement of its spiral-arm pitch angle at two different wavelengths. The histograms show the distribution of pitch angle differences in terms of the number of galaxies found in each bin. The histograms for the top plot shows that the $u$ -band and far ultraviolet (FUV) wavelengths are fundamentally equal since the greatest number of galaxies have pitch angles at these wavelengths that agree to better than $3^\circ$ . The same is true for the second plot, comparing $B$ -band with $u$ -band images. In contrast, we can see that $u$ -band pitch angles and $3.6 \mu\text{m}$ pitch angles (bottom plot) are different from each other, since in both cases the greatest number of galaxies have a pitch angle difference of more than $3^\circ$ (see the relevant histograms), with very few found below $3^\circ$ . Images of 29 galaxies were used at $355 \text{ nm}$ , $445 \text{ nm}$ , $3.6 \mu\text{m}$ and 28 of these also had images at FUV ( $151 \text{ nm}$ ). . . . .	71

Figure 4.5:	Comparisons between pitch angles measured at different wavelengths. Each point on the plots represents an individual galaxy positioned according to the measurement of its spiral-arm pitch angle at two different wavelengths. The histograms show the distribution of pitch angle differences in terms of the number of galaxies found in each bin. The histograms for the top plot shows that the H- $\alpha$ and far ultraviolet (FUV) wavelengths are fundamentally equal since the greatest number of galaxies have pitch angles at these wavelengths that agree to better than 3°. The same is true for the second plot, comparing H- $\alpha$ with 8.0 $\mu\text{m}$ images. In contrast, we can see that H- $\alpha$ pitch angles and <i>B</i> -band pitch angles (bottom plot) are different from each other, since in both cases the greatest number of galaxies have a pitch angle difference of more than 5° (see the relevant histograms), with very few found below 5°. Images of 14 galaxies were used at H- $\alpha$ , 445 nm, 8.0 $\mu\text{m}$ . . . . .	72
Figure 4.6:	The Evolution of Pitch Angle from FUV (151 nm) to 3.6 $\mu\text{m}$ . . . . .	73
Figure 4.7:	Comparison between our results and Grosbol & Patsis (1998) for the same galaxies (NGC3223, 5085, 5247, 7083). The pitch angles measured at <i>B</i> -band (445 nm), <i>K</i> -band (2190 nm), <i>H</i> -band (1630 nm) and <i>J</i> -band (1220 nm). . . . .	79
Figure 4.8:	Spectral evolution for a single burst of star formation, for a Kroupa IMF and Solar metallicity, $Z=0.02$ . The total initial stellar mass is normalized to 1M. Solid lines show photospheric emission from the stellar population. Spectra are color-coded, with respective ages shown in the upper-right corner. Models with nebular continuum emission are shown with the same color-coding. Only the youngest age shows significant difference due to its large ionizing photon rate. Figure by Eufrazio (2015). . . . .	85
Figure 5.1:	Spiral arm pitch angle versus rotation curve shear rate, showing a strong correlation. The solid squares present the galaxies with data measured by Block et al. (1999), the open squares are galaxies from Seigar (2005) and the open triangles represent the data from Seigar et al. (2006). . . .	92
Figure 5.2:	Pitch angle variation, <i>B</i> -band versus difference between <i>B</i> -band and 8.0 $\mu\text{m}$	98
Figure 5.3:	Pitch angle variation, 3.6 $\mu\text{m}$ versus difference between 3.6 $\mu\text{m}$ and 8.0 $\mu\text{m}$	99
Figure 5.4:	Pitch angle variation for unbarred galaxies, <i>B</i> -band versus difference between <i>B</i> -band and 8.0 $\mu\text{m}$ . . . . .	101
Figure 5.5:	Pitch angle variation for unbarred galaxies, 3.6 $\mu\text{m}$ versus difference between 3.6 $\mu\text{m}$ and 8.0 $\mu\text{m}$ . . . . .	102

## LIST OF TABLES

Table 1.1: Spiral Galaxy Type and its Description . . . . .	3
Table 2.1: Galaxy in Different Wavelength of Light and its Pitch Angle . . . . .	17
Table 3.1: Spiral Galaxies and its Measured Pitch Angle at Different Wavelength of Light . . . . .	31
Table 4.1: Spiral Galaxies and its Measured Pitch Angle at Different Wavelength of Light . . . . .	67
Table 5.1: Pitch Angle and Shear Rate For 31 Spiral Galaxies, Reported by Seigar et al. (2006) . . . . .	93
Table 5.2: Pitch Angle's Variation for <i>B</i> -band, 3.6 and 8.0 $\mu\text{m}$ . . . . .	95

## LIST OF ABBREVIATIONS

**2DFFT** — Two-Dimensional Fast Fourier Transform

**A&A** — Astronomy and Astrophysics

**A&AS** — Astronomy and Astrophysics, Supplement

**AAS** — American Astronomical Society

**AGN** — Active Galactic Nuclei

**AGES** — Arkansas Galaxy Evolution Survey

**AJ** — Astronomical Journal

**Ap&SS** — Astrophysics and Space Science

**ApJ** — Astrophysical Journal

**ApJL** — Astrophysical Journal, Letters

**ApJS** — Astrophysical Journal, Supplement

**ARA&A** — Annual Review of Astronomy and Astrophysics

**Astron.** — Astronomy

**Astrophys.** — Astrophysics

**B-band** — Blue light wavelength filter ( $\lambda_{eff} = 445$  nm)

**B. S.** — Bachelor of Science

**deg.** — Degree ( $^{\circ}$ )

**Dr.** — Doctor

**e.g.** — exempli grātia

**Eq.** — Equation

**ESO** — European Southern Observatory

**et al.** — et alii

**etc.** — et cetera

**Fig.** — Figure

**FFT** — Fast Fourier Transform

**GOODS** — Great Observatories Origins Deep Survey

**H $\alpha$**  — Hydrogen Balmer spectral line

**I-band** — Infrared light wavelength filter ( $\lambda_{eff} = 806$  nm)

**i.e.** — id est

**J.** — Journal

**K'** — Infrared Light wavelength filter ( $\lambda_{eff} = 2190$  nm)

**m** — Meter

**mag** — Magnitude

**max** — Maximum

**min** — Minimum

**MNRAS** — Monthly Notices of the Royal Astronomical Society

**NASA** — National Aeronautics and Space Administration

**NED** — NASA/IPAC Extragalactic Database

**NGC** — New General Catalogue of Nebulae and Clusters of Stars

**NIR** — Near-Infrared

**FIR** — Far-Infrared

**uv,UV** — Ultraviolet

**NUV** — Near-Ultraviolet

**FUV** — Far-Ultraviolet

**IRAC** — The Infrared Array Camera

**GALEX** — Galaxy Evolution Explorer

**nm** — Nanometer

**No.** — Number

**PA** — Position Angle

**PASP** — Publications of the Astronomical Society of the Pacific

**pc** — Parsec

**Ph. D.** — Doctor of Philosophy

**Phys.** — Physics

**SDSS** — Sloan Digital Sky Survey

**SSPSF** — Stochastic Self-Propagating Star Formation

**Univ.** — University

**US** — United States

**Vol.** — Volume



## LIST OF PUBLICATIONS

Chapter 3 — Strong Evidence for the Density-wave Theory of Spiral Structure in Disk Galaxies. **Pour-Imani, Hamed**, Kenefick, D., Kenefick, J., Davis, B. L., Shields, D. W., & Abdeen, M. 2015, The Astrophysical Journal Letters, 827, L12

## Chapter 1

### Spiral Galaxies and Spiral Structure

#### 1.1 Introduction

Spiral structure in disk galaxies has been studied for decades. An important tool for studying spiral structure is the pitch angle of spiral arms in disk galaxies. The density wave theory is a theory proposed by C.Lin and F.Shu in the mid-1960s to explain spiral arm structure (Lin & Shu, 1964). A prediction of this theory is that the pitch angle of spiral arms for galaxies imaged in the different wavelength should be different. Martinez-Garcia et al. (2014) investigate the behavior of the pitch angle of spiral arms depending on optical wavelength. They examined five galaxies in two optical bandpasses and their results show that just three of those five galaxies comply with density wave theory. Their results and sample size are very similar to an earlier paper by Grosbol & Patsis (1998). In this research, we combined large sample size with the wide range of wavelengths, from the ultraviolet to the infrared to investigate a prediction of the density-wave theory. We have three main research areas within this overall program:

- The first is to use images of normal spiral galaxies with different wavelength and measure the pitch angle. To do this, we made use of two completely independent methods of measuring pitch angles. One is an established algorithm involving a 2DFFT (Davis et al., 2012) decomposition of the galactic image and the other is a new approach that compares the spiral pattern to templates based upon a spiral coordinate system

(Shields et al., 2015).

- The second is analyze the 2DFFT and Spirality results to define the pitch angle with an error bar for each individual spiral galaxy at the different wavelength.
- The third research area is to investigate the theoretical prediction for spiral structure by different theories and compare with experimental and observational data to find strong evidence for a prediction of the density-wave theory.

## 1.2 Spiral Galaxies

The spiral galaxy is the most common type of galaxy in the universe described by Edwin Hubble in 1936 (Hubble, 1926). About 77% of observed galaxies are spiral, such as our own galaxy, Milky-Way. Spiral galaxies are defined by their different parts. A flat rotating disk containing stars, gas, and dust, a bulge at the center includes a concentration of stars; and all of these surrounded by a diffuse halo of stars. The arms of spiral galaxies extend from the center into the galactic disk and they have lots of brighter stars, gas, and dust, and refer to the star formation region. By the visual appearance, we have the different galaxy morphological classification. The most famous classification is the Hubble sequence devised by Edwin Hubble and later expanded by other astrophysicists. By the shape and size of central bulge, galaxies are divided into three major type: Barred (SB), Intermediate (SO) and Unbarred (S) spiral galaxies, elliptical (E) and irregular (Irr) galaxies. Figure 1.1 shows our samples from SINGS survey and it shows clearly the presence of spirals of different types (Kennicutt et al., 2003). A further subdivision is based on how tightly wound the spirals are. Type "a" is a galaxy with very tightly wound arms, type "b" with more loosely wound

Table 1.1. Spiral Galaxy Type and its Description

Galaxy Type	Description
(1)	(2)
Sa	Spiral Galaxy, Type a, Very tightly wound arms
Sb	Spiral Galaxy, Type b, More loosely wound arms
Sc	Spiral Galaxy, Type c, Very loosely wound arms
SBa	Barred Spiral Galaxy, Type a
SBb	Barred Spiral Galaxy, Type b
SBc	Barred Spiral Galaxy, Type c

Note. — *Columns:* (1) Classification symbol (2) Description

arms and type "c" with very loosely wound arms. Table 1.1 shows a general description of the different type of spiral galaxy based on visual appearance.



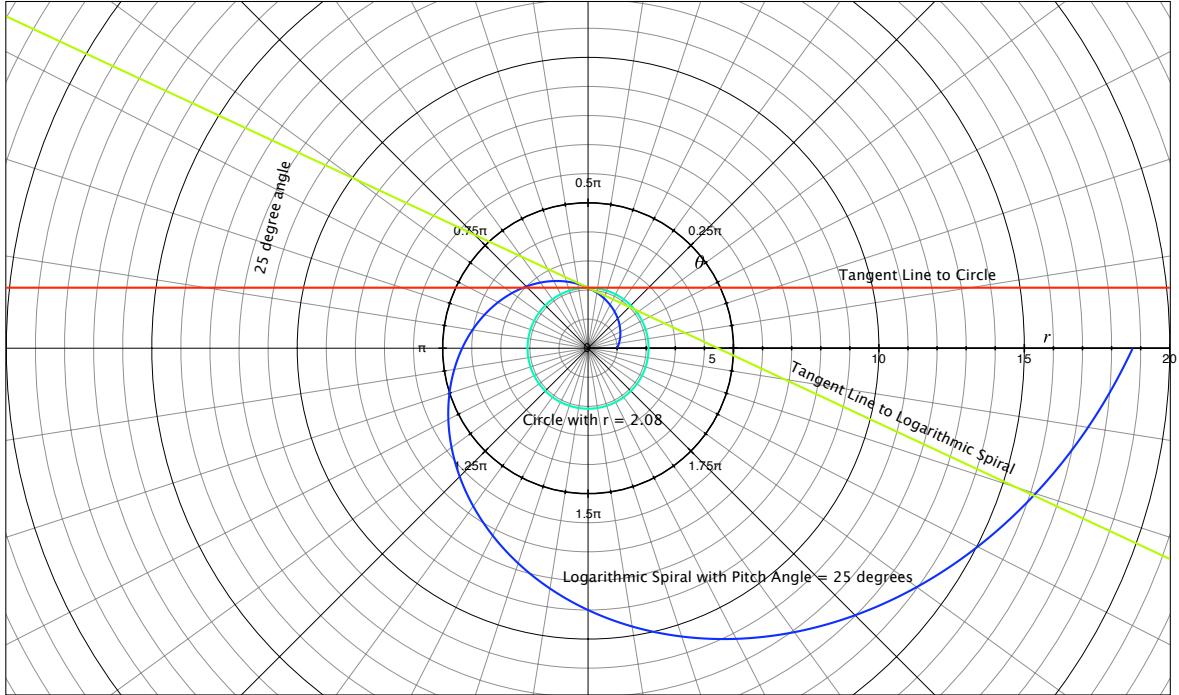


**Figure 1.2** Illustration of the definition of logarithmic spiral arm pitch angle. There are four elements in the plot above: blue - a logarithmic spiral with  $\phi = 25^\circ$ , teal - a circle with  $r = 2.08$  intersecting the logarithmic spiral at  $(0, 2.08)$ , red - a line tangent to the circle at  $(0, 2.08)$ , and green - a line tangent to the logarithmic spiral at  $(0, 2.08)$ . The angle subtended between the line tangent to circle and the line tangent to the logarithmic spiral is  $25^\circ$ , which is equivalent to the pitch angle of the logarithmic spiral (Davis, 2015).

### 1.3 Logarithmic Spiral Pitch Angle

Logarithmic spiral arms form self-similar spiral curves. These spirals were described by Descartes and later Jacob Bernoulli. In nature, we have several phenomena in which we can see curves close to being logarithmic spirals. The pitch angle of a logarithmic spiral arm at any radius is defined as the angle between a line tangent to the arm and a line tangent to a circle with the same radius and center as the spiral. Figure 1.2 illustrates the definition of the pitch angle. To a good approximation, the shape of the spiral arms in a spiral galaxy is a logarithmic spiral (Seigar & James, 1998). The limiting values of the pitch angle are  $0^\circ$  and  $90^\circ$ . The angle  $0^\circ$  produces a circle and  $90^\circ$  produces a line. Loosely wound spirals have larger pitch angle than tightly wound spirals. The positive pitch angle is for a clockwise outward winding and negative pitch angle describes counterclockwise.

### 1.4 Hypotheses for Spiral Structure

#### 1.4.1 Winding Problem

The first idea for spiral structure was that the arms of the spiral galaxy are material which form as the galaxy spins. The stars, gas, and dust near the center of a galaxy rotate faster than the materials at the edge of the galaxy. This means that the arms would quickly become curved and wind up as the galaxy rotates and become indistinguishable from the rest of the disk after a few orbits. If this was the case we would expect to see some tightly wound arms but we don't. This is called the "Winding Problem". The spiral cannot be a rigid mass concentration. If this was the case, the galaxy must rotate as a whole around its center. According to the Lindblad's observations and physics, this is not the right theory.

Since the 1960s there have been different models to explain the spiral structure. Three leading hypotheses are Density-wave theory (Lin & Shu, 1964), Stochastic Self-Propagating Star Formation (SSPSF) Mueller & Arnett (1976) and the Manifold theory (Athanasoula et al., 2010).

#### 1.4.2 The Density-wave Theory

The density-wave theory was developed by C.Lin and F.Shu in the mid-1960s to explain spiral arm structure (Lin & Shu, 1964). They proposed that the arms cannot be material. They said the arms are the areas with a greater concentration of stars, gas, and dust. Spiral arms are not actually a set of stars that all move together. This is where stars are clumped up together, closer together, where they are being formed at a faster rate. In fact, it's a traffic jam of stars, similar to a traffic jam on a highway. In a traffic jam, the positions and speed of cars may change with time. But the traffic jam itself remains stable (more or less) as the cars move down the highway. The cars make up the jam as they flow through it. The lead cars accelerate away and the other cars come in, to take their place. The members of traffic jam always change but the traffic jam remains at the same place on the highway. It is the same thing with the stars that move through the galaxy. The Density-wave in the galaxy is not caused by a traffic jam. instead, it is caused by a gravitational resonance. For example, a disturbance caused by a passing nearby galaxy or a bar at the center of the galaxy can create a resonance. Spiral arms are the result of density waves propagating through the galaxy. As it moves through the galaxy the stars, gas, and dust don't move with it, instead, the waves move through them. When the clouds of gas and dust pass through the density wave, they are compressed triggering star formation. So,



the materials of the galaxy are being constantly stirred and new stars are born. Figure 1.3, shows the spiral pattern as a region formed by the density-waves as they move radially out from the center of the galaxy through the rotating disk.

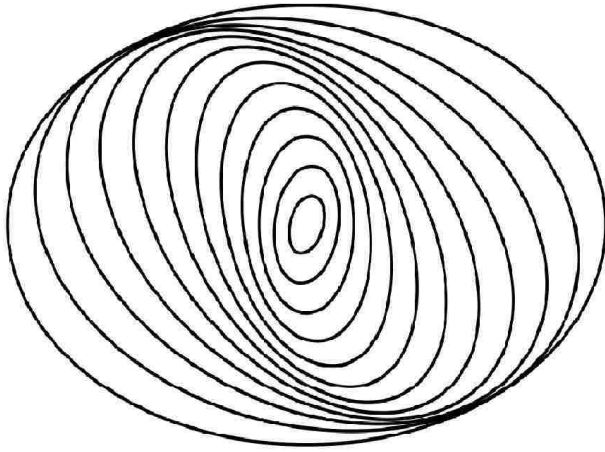


**Figure 1.3** Left: cartoon of density-wave moving through a rotating disk compared to, right: NGC1566, an intermediate spiral galaxy (Photo by Hubble Space Telescope).

### 1.4.3 SSPSF Model

The Stochastic Self-Propagating Star Formation (SSPSF) model was proposed by Mueller & Arnett (1976) and later by Gerola & Seiden (1978). In this model, the propagation of star formation is caused by the action of shock waves from stellar winds and supernovae that compose the interstellar medium. The idea is the star formation begins in a uniform disk randomly. At some point some cloud collapses and stars begin to form. Supernovae explosions create shock waves which propagate through the cloud and trigger more star formation. Shearing due to the differential rotation gives such random patches of star formation a spiral appearance. In 1999, the density-wave model was combined with SSPSF model by Auer (1999). The Manifold theory described spiral arms as being due to stars which move in chaotic highly eccentric orbits which confine them to narrow tracks through the galaxy's disk known as manifolds

## 1.5 Thesis Outline

The focus of this thesis is on investigating the density-wave theory of spiral structure in disk galaxies. I use theoretical, observational and computational methodologies to study the structure of spiral galaxies. This doctoral thesis is comprised of my lead-author publication in a peer-reviewed scientific journal published and copyrighted by the American Astrophysical Society (AAS) <sup>1</sup>. In Chapter 2, “The Density-wave Theory of Spiral Structure and Pitch Angle Variation”, I detail the density-wave theory of spiral structure and discuss a prediction of this theory for pitch angle variation when we look at the galaxies through

---

<sup>1</sup>The AAS permits the use of material from its journals by lead authors, especially when material is being reproduced for a doctoral thesis.

different wavelengths. In Chapter 3, “Strong Evidence for the density-wave Theory of Spiral Structure in Disk Galaxies” (Pour-Imani et al., 2016), I detail the results for spiral arm pitch angle measurements in different wavelengths of light to investigate a prediction of the density-wave theory. In Chapter 4, “Spiral Structure Through a Multi-wavelength Study”, I combined a larger sample size with a wide range of wavelengths to investigate more predictions of the density-wave theory. In Chapter 5, “The Connection Between Shear and Pitch Angle’s Variation in Different Wavelength”, I detail the correlation between the shear rate and pitch angle’s variation. In Chapter 6, I summarize the overall results of this research and its implications.

## Bibliography

- Athanassoula, E., Romero-Gómez, M., Bosma, A. and Masdemont, J. J. 2010, MNRAS, 407, 1433-1448
- Auer, R., A spiral galaxy model combining the density wave and self-propagating star formation., Univ. (Germany). Naturwissenschaftlich-Mathematische Gesamtfakultät, Dec 1999
- Davis, B. L., Berrier, J. C., Shields, D. W., Kenefick, J., Kenefick, D., Seigar, M. S., Lacy, C. H. S., & Puerari, I. 2012, ApJS, 199, 33
- Davis, Benjamin Lee, "Logarithmic Spiral Arm Pitch Angle of Spiral Galaxies: Measurement and Relationship to Galactic Structure and Nuclear Supermassive Black Hole Mass" (2015). Theses and Dissertations. 1041. <http://scholarworks.uark.edu/etd/1041>
- Gerola, H. and Seiden, P. E. 1978, ApJ, 223, 129
- Grosbol, P. J. & Patsis, P. A. 1998, A&A, 336, 840
- Hubble, E. P. 1926, ApJ, 64, 321
- Kennicutt, R. C., Bendo, G., Engelbracht, C., Gordon, K. and Li, A., Rieke, G. H., Rieke, M. J., Smith, J. D., Armus, L. and Helou, G., Jarrett, T. H., Roussel, H., Calzetti, D., Leitherer, C., Malhotra, S., Meyer, M., Regan, M. W., Dale, D. A., Draine, B., Grauer, A. D., Hollenbach, D. J., Kewley, L. J., Murphy, E., Thornley, M. D. & Walter, F. 2003, in American Astronomical Society Meeting Abstracts, Bulletin of the American Astronomical Society, Vol. 35, 1351
- Lin, C. C. & Shu, F. H. 1964, ApJ, 140, 646
- Mueller, M. W. & Arnett, W. D. 1976, ApJ, 210, 670
- Martínez-García, E. E. and Puerari, I. and Rosales-Ortega, F. F. and González-Lópezlira, R. A. and Fuentes-Carrera, I. and Luna, A. 2014, ApJ, 793, L19
- Pour-Imani, H., Kenefick, D., Kenefick, J., Davis, B. L., Shields, D. W., & Shameer Abdeen, M. 2016, ApJ, 827, L2
- Shields, D. W., Davis, B. L., Pour-Imani, Hamed., Abdeen, M.S., Kenefick, D., & Kenefick, J. 2015, arXiv:1511.06365
- Seigar, M. S. & James, P. A. 1998, MNRAS, 299, 685

## Chapter 2

### The Density-wave Theory of Spiral Structure and Pitch Angle Variations

#### 2.1 Introduction

As we discussed in Chapter 1, since the 1960s, there have been different models to explain the spiral structure. The density-wave theory of galactic spiral-arm structure (Lin & Shu, 1964) makes a striking prediction that the pitch angle of spiral arms should vary with the wavelength of the galaxy's image. The reason is that the spiral arm is a pattern which rotates rigidly, while the physical components of the galactic disk (including stars and gas clouds) rotate differentially. Thus density-wave theory predicts that the pitch angle of the spiral pattern where star formation is actually occurring should be greater (looser arms) than the pitch angle of the spiral pattern traced by the stars recently born in that region. Thus we expect tighter spiral arms in optical and near-infrared wavebands associated with the stars born in the spiral arm than we observe in UV or far infrared bands associated with light from the spiral arm. Stars are born in the spiral arms of the galaxies. Other theories such as SSPSF model and the Manifold theory don't predict any variations of pitch angle with image wavelength.

#### 2.2 The Density-wave Theory and Pitch Angle Variations

In the density-wave theory, Stars form in arms and move through the density wave as they age. Thus density wave theory predicts that the pitch angle of the spiral pattern where

star formation is actually occurring should be greater (looser arms) than the pitch angle of the spiral pattern traced by the stars recently born in that region. Thus we expect tighter spiral arms in optical and near-infrared wavebands associated with the stars born in the spiral arm than we observe in UV or far infrared bands associated with light from the spiral arm, while the other theories don't predict any variations in pitch angle. Very luminous but short-lived stars will die before leaving the density wave. Faster moving materials which orbit the center of galaxy move into the density wave region, become compressed and move out the other side continuing its orbit. The co-rotation radius  $R_c$ , is a radius where the stars and density waves move together. The rotation speed of the spiral arms is defined as  $\Omega_{gp}$ , the global pattern speed. Inside the co-rotation radius  $R_c$ , stars move faster than the spiral arm ( $\Omega > \Omega_{gp}$ ) and outside of the co-rotation radius, stars move more slowly ( $\Omega < \Omega_{gp}$ ). The stars move through the density wave as they age. This implies that the pitch angle of galactic spiral arms should vary with the wavelength of the image (Figure 2.1). Logarithmic spirals are characterized by a constant pitch angle which governs the radial evolution of the spiral as one rotates around the galaxy. Pitch angle is, in the density wave theory, directly related to the wavelength of the waves, which is governed by a dispersion relation which depends upon the galaxy's bulge mass and disk density. Previous work has confirmed a correlation between spiral arm pitch angle, bulge mass and gas density in the disk, which is consistent with the basic scheme of density wave theory (Davis et al., 2015). Since pitch angle is a quantifiable feature of the spiral pattern, it has been proposed as a quantifiable feature suitable for theory testing between different explanations for galactic spiral structure (Athanasoula et al., 2010; Martinez-Garcia, 2012; Davis et al., 2015).

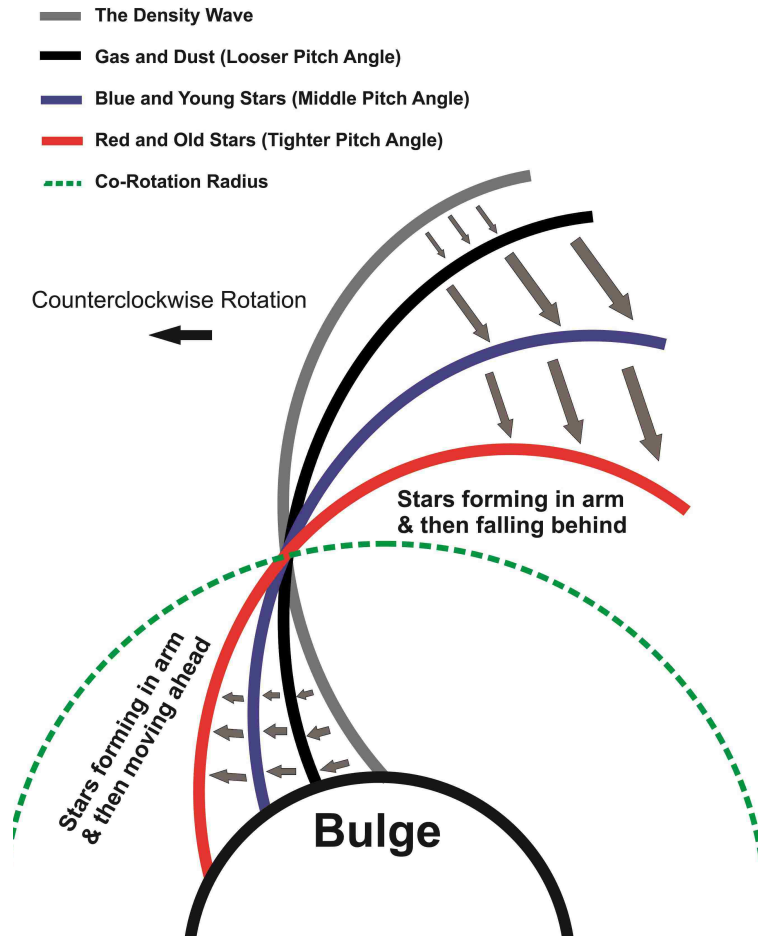


**Figure 2.1** Predictions of density-wave theory for spiral-arm structure with old stars, blue stars, gas, and dust. (Figure created by H.Pour Imani).



### 2.3 Previous Works

E. M Garcia et al (Martinez-Garcia et al., 2014) investigated the behavior of the pitch angle of spiral arms depending on optical wavelength. They examined five galaxies in two optical bandpasses and their results show that just three of those five galaxies comply with density wave theory. Their results and sample size are very similar to an earlier paper by Grosbol and Patsis (Grosbol & Patsis, 1998).

Davis et al (Davis et al., 2012) consider the possibility of different pitch angles arising in different wavebands of light. Their results show a comparison of their pitch angle measurements for 49 NGC galaxies in optical and NIR wavelengths (*B*-band: 445 nm, *I*-band: 806 nm) and found a consistent difference in pitch angle behaves these two wavelengths. We used a larger sample size than any previously used to study this issue.

### 2.4 Galaxies Imaged at Different Wavelengths of Light

Every time we look at the sky through different wavelengths, we get a different picture of the universe. By looking at spiral arms in spiral galaxies over a range of wavelengths we gain clues to the generation of spiral density waves and star formation mechanisms. Galaxy images at different wavelengths tell us about stars of different age or show us gas, and dust in star formation burst. For example in the *Spitzer* survey (Figure 1.1), we have images of galaxies taken at 8 and 3.6  $\mu\text{m}$ . At 8.0  $\mu\text{m}$ , which images warmed dust in clouds where star formation is occurring, we are capable of seeing the region of star formation in the gaseous spiral arm. Spiral arm properties of galaxies were measured at 3.6  $\mu\text{m}$ , where extinction is small and the old stars dominate. With a deeper range in infrared band-pass 8.0  $\mu\text{m}$  we can

Table 2.1. Galaxy in Different Wavelength of Light and its Pitch Angle

Wavelength (1)	Reference (2)	Pitch Angle (3)
3.6 $\mu\text{m}$ , Spitzer IRAC 3.6	Red Stars (Old Stars)	Tigher arms
<i>B</i> -band, 445 nm	Blue Stars (Young Stars)	Loser arms
8.0 $\mu\text{m}$ , Spitzer IRAC 8.0	Gas and Dust, Star formation region	More loser arms
Far Ultraviolet 151 nm, GALEX 1510	Short-Lived Stars, Close to star formation region	More Loser arms

Note. — *Columns:* (1) Wavelength (2) Wevelength refer to (3) Pitch angle prediction by Density-wave theory

see more details of gas and dust and star formation region in spiral arm (Elmegreen et al., 2011). The far-ultraviolet images from the *Galaxy Evolution Explorer (GALEX)* show the same region since they are sensitive to stars so young and bright that they are seen while still in their star-forming nurseries. The near-infrared and *B*-band (445 nm) images are sensitive to starlight and young stars. Table 2.1 shows more details for different wavelengths and their references.

### 2.4.1 Spitzer Space Telescope

The *Spitzer* space telescope is looking at the universe in a new way through infrared light. The Infrared Array Camera (IRAC) is one of *Spitzer's* three focal plane instruments (Fazio et al., 2004). It is a camera that provides images at near-,mid-infrared wavelengths. This camera is a four-channel camera and it's able to take images at wavelengths of 3.6, 4.5, 5.8, and 8.0  $\mu\text{m}$ . IRAC's high sensitivity and its large field of view make this telescope a powerful survey instrument for astronomers.

#### 2.4.1.1 IRAC 3.6 $\mu\text{m}$

IRAC 3.6  $\mu\text{m}$  is sensitive to light at wavelength 3.6  $\mu\text{m}$ . This waveband is sensitive to starlight and for the images at this bandpass, it is expected that small and older stars dominate (Elmegreen et al., 2011). As we discussed in Section 2.2, density-wave theory predicts the smallest pitch angle and tighter arms in spiral galaxies for this wavelength (see Figure 2.1).

#### 2.4.1.2 IRAC 8.0 $\mu\text{m}$

IRAC 8.0  $\mu\text{m}$  gives us the aromatic features from gas and dust grains/molecules. This waveband is sensitive to dust warmed by nearby star formation and we can see more details of gas and dust in spiral arms (Elmegreen et al., 2011). By a prediction of density-wave theory (Section 2.2), we should expect bigger pitch angle and looser arms in spiral galaxies for this wavelength (see Figure 2.1).

### 2.4.2 *B*-band 445 nm

This waveband filters the light with wavelength 445 nm. B-band is sensitive to starlight and the galaxy's image with this waveband is showing blue and young stars. Density-wave theory predicts a looser arm and bigger pitch angle than  $3.6 \mu\text{m}$  (older stars) in spiral galaxies (see Figure 2.1).

### 2.4.3 Far-ultraviolet 151 nm (FUV)

This waveband shows more details for the region of star formation at wavelength 151 nm. FUV is sensitive to stars so young and bright that they are seen while still in their star-forming nurseries. Density-wave theory predicts the biggest pitch angle for this waveband and at the same range of gas and dust  $8.0 \mu\text{m}$  (see Figure 2.1). The FUV images are from *Galaxy Evolution Explorer (GALEX)* (Bianchi & GALEX Team, 1999).

## 2.5 Methods for Pitch Angle Measurements

We made use of two completely independent methods of measuring pitch angles. One is an established algorithm involving a 2DFFT (Davis et al., 2012) decomposition of the galactic image and the other is a new approach that compares the spiral pattern to templates based upon a spiral coordinate system (Shields et al., 2015).

### 2.5.1 2DFFT Code

The 2DFFT code uses two-dimensional fast Fourier transformations of images of spiral galaxies, in order to isolate and measure the pitch angles of their spiral arms. This technique

provides a quantitative way to measure a galaxy’s morphological features. This will allow comparison of spiral galaxy pitch angle at different wavelength and test spiral arm genesis theories.

### 2.5.2 Spirality Code

Spirality code is a novel method for measuring spiral arm pitch angles by fitting galaxy images to spiral templates of known pitches. The code yielded correct results for all synthetic spirals with galaxy-like properties. The Spirality code package also includes GenSpiral, which produces FITS images of synthetic spirals, and SpiralArmCount, which uses a one-dimensional Fast Fourier Transform to count the spiral arms of a galaxy after its pitch is determined (Shields et al., 2015).

## 2.6 Conclusion

Density-wave theory is one of the lead theories for spiral structure in disk galaxies. A prediction of this theory is a co-relation between spiral arm pitch angle variations at different wavelengths of light. We make use of *Spitzer* images of galaxies taken at wavelengths 3.6 and 8.0  $\mu\text{m}$ , *GALEX* images taken at 151 (FUV) and images taken at *B*-band 445 nm, to test this prediction by density-wave theory. In order to measure the pitch angles of spiral galaxies, we made use of two different methods 2DFFT and Spirality.

## Bibliography

- Athanassoula, E., Romero-Gómez, M., Bosma, A. and Masdemont, J. J. 2010, MNRAS, 407, 1433-1448
- Bertin, G. & Lin, C. C. 1995, Spiral structure in galaxies a density wave theory, The MIT Press
- Bianchi, L. and GALEX Team. 1999, Mem. Soc. Astron. Italiana, 70
- Davis, B. L., Kenefick, D., Kenefick, J., Kyle, B. W., Shields, D. W. 2015, ApJ, 802, L13
- Davis, B. L., Berrier, J. C., Shields, D. W., Kenefick, J., Kenefick, D., Seigar, M. S., Lacy, C. H. S., & Puerari, I. 2012, ApJS, 199, 33
- Egusa, F. and Kohno, K. and Sofue, Y. and Nakanishi, H. and Komugi, S. 2009, ApJ, 697, 1870
- Elmegreen, D. M., Elmegreen, B. G., Yau, Andrew, et al. 2011, ApJ, 737, 32
- Fazio, G. G., Hora, J. L., Allen, L. E., et al. 2004, ApJS, 154, 10
- Gittins, D. M. and Clarke, C. J. 2004, MNRAS, 349, 909-921
- Grosbol, P. J. & Patsis, P. A. 1998, A&A, 336, 840
- Kendall, S. and Kennicutt, R. C. and Clarke, C. and Thornley, M. D. 2008, MNRAS, 387, 1007-1020
- Kennicutt, Jr., R. C. 1981, AJ, 86, 1847
- Kim, Y. and Kim, W.-T. 2013, MNRAS, 440, 208-224
- Lin, C. C. and Shu, F. H. 1964, ApJ, 140, 646
- Louie, M. and Koda, J. and Egusa, F. 2013, ApJ, 763, 94
- Martínez-García, E. E. 2012, ApJ, 744, 92
- Martínez-García, E. E. and Puerari, I. and Rosales-Ortega, F. F. and González-Lópezlira, R. A. and Fuentes-Carrera, I. and Luna, A. 2014, ApJ, 793, L19
- Roberts, W. W. 1969, ApJ, 158, 123
- Seigar, M. S., Bullock, J. S., Barth, A. J., & Ho, L. C. 2006, ApJ, 645, 1012
- Seigar, M. S., Kenefick, D., Kenefick, J., & Lacy, C. H. S. 2008, ApJ, 678, L93

Savchenko, S. S., and Reshetnikov, V. P. 2011, *AstL*, 37, 817

Shields, D. W., Davis, B. L., Pour-Imani, Hamed., Kennefick, D., & Kennefick, J. 2015, arXiv:1511.06365

Shu, Frank H. 2016, Six Decades of Spiral Density-Wave Theory, *Annual Review of Astronomy and Astrophysics*, Vol 54, Sep 2016

## Chapter 3

# Strong Evidence for the Density-wave Theory of Spiral Structure in Disk Galaxies

### 3.1 Abstract

The density-wave theory of galactic spiral-arm structure makes a striking prediction that the pitch angle of spiral arms should vary with the wavelength of the galaxy's image. The reason is that stars are born in the density wave but move out of it as they age. The spiral arm is a pattern which rotates rigidly, while the physical components of the galactic disk (including stars and gas clouds) rotate differentially. Thus density wave theory predicts that the pitch angle of the spiral pattern where star formation is actually occurring should be greater (looser arms) than the pitch angle of the spiral pattern traced out by the stars recently born in that region. Thus we expect tighter spiral arms in optical and near-infrared wavebands associated with the stars born in the spiral arm, than we observe in UV or far infrared bands associated with light from the spiral arm. Stars born in the spiral arms of the galaxies move ahead of the density wave inside the co-rotation radius, and fall behind outside of it, resulting in a tighter pitch angle at wavelengths that image stars (optical and near infrared) than those that are associated with star formation (far infrared and ultraviolet). In this study we combined large sample size with wide range of wavelengths, from the ultraviolet to the infrared to investigate this issue. For each galaxy we used an optical wavelength image (*B*-band: 445 nm) and images from the *Spitzer Space Telescope*



at two infrared wavelengths (infrared: 3.6 and 8.0  $\mu\text{m}$ ) and we measured the pitch angle with the 2DFFT and Spirality codes (Davis et al., 2012; Shields et al., 2015). We find that the  $B$ -band and 3.6  $\mu\text{m}$  images have smaller pitch angles than the infrared 8.0  $\mu\text{m}$  image in all cases, in agreement with the prediction of density-wave theory. We also used images in the ultraviolet from *Galaxy Evolution Explorer*, whose pitch angles agreed with the measurements made at 8  $\mu\text{m}$ . Because stars imaged at those wavelengths have not had time during their short lives to move out of the star-forming region.

### 3.2 Introduction

Spiral arm structure can serve as an indicator for several properties of galaxies including central bulge mass and disk surface density (Davis et al., 2015) and thus indirectly central black hole mass galaxies including central bulge mass and disk surface density (Davis et al., 2015) and thus indirectly central black hole mass (Seigar et al., 2008) as well as rotation shear (Seigar et al., 2006), rotational velocity (Savchenko et al., 2011) and weakly, bulge-to-disk ratio (Kennicutt, 1981). Evolution in spiral structure can provide clues about the evolution of the aforementioned properties.

The density-wave theory of spiral structure in disk galaxies was proposed in the mid 1960s by C.C. Lin and Frank Shu (Lin & Shu, 1964; Bertin & Lin, 1996; Shu, 2016). Their theory envisaged long-lived quasi-stationary density waves (also called heavy sound), which impose a semi-permanent spiral pattern on the face of the galactic disk. All subsequent versions of the theory agree that the density wave causes star formation to occur by compressing clouds of gas as they pass through the spiral arm.

The brightest stars created in this burst of star formation do not live long enough to travel far from the position of the spiral density waves and so the eye, when observing the galaxy in optical wavelengths, picks out the spiral pattern quite easily.

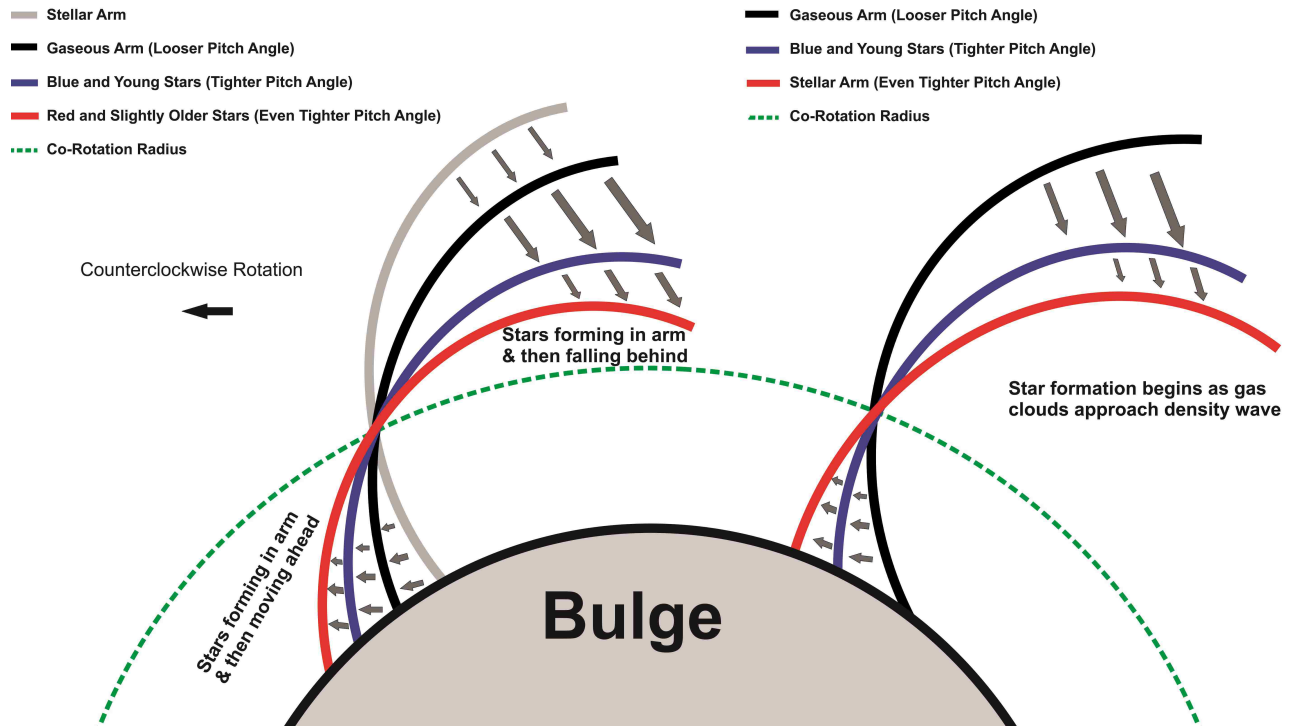


**Figure 3.1** Predictions of density-wave theory for spiral-arm structure with old stars, blue stars, gas, and dust. On the left is a scenario where star formation occurs after gas clouds pass through the minimum of the potential of the density wave. On the right is a scenario in which star formation occurs as the gas clouds approach this minimum of the potential.

Pitch angle is, in the density wave theory, directly related to the wavelength of the waves, which is governed by a dispersion relation which depends upon the galaxy's bulge mass and disk density. Previous work has confirmed a correlation between spiral arm pitch angle, bulge mass and gas density in the disk, which is consistent with the basic scheme of density wave theory (Davis et al., 2015).

The spiral arms predicted by this theory, and those actually observed in disk galaxies, are approximately logarithmic spirals. Logarithmic spirals are characterized by a constant pitch angle that has been proposed as a quantifiable feature suitable for theory testing between different explanations for galactic spiral structure (Athanasoula et al., 2010; Martinez-Garcia, 2012; Davis et al., 2015).

Because the spiral pattern moves as if it was a rigid pattern, it follows that the newly born stars, which are subject to differential rotation, will quickly move out of the spiral arm. In fact, since newly born stars are typically obscured from view by the warm dust-filled clouds associated with star formation (except for the very brightest UV stars), most of the new stars will be observed only when they leave the spiral arm. In the inner part of the disk, stars move faster than the spiral-arm pattern and move ahead of the density wave, while in the outer part of the disk, they fall behind (see Fig. 3.1). In between is the co-rotation radius where stars and the spiral arm move together.<sup>1</sup> It thus follows that the pitch angle of the pattern formed by the newly formed stars (the bluer stars), seen in the optical, is smaller than the pitch angle of spiral shape formed by the actual star formation region (we will refer to this region as the gaseous arm), seen in the far-infrared (which is sensitive to light from

---

<sup>1</sup>In practice, there are galaxies where the co-rotation radius is quite outside the region where we measure pitch angle, but the relation between pitch angles will still be as described.

the warmed dust of the star-forming region itself). In other words, the spiral pattern formed by the newly formed stars is tighter than the one formed by the gaseous arm or star-forming region (see either side of Figure 3.1).

The density-wave theory predicts that the pitch angle of galactic spiral arms should vary with the wavelength in which the spiral pattern is observed. This is in contrast to its main rival, the manifold theory of spiral structure, which posits that the spiral arms are the result of highly eccentric orbits of young stars (formed at the end of the galaxy's bars) that confine the stars to motion along manifolds - tubes running across the disk. A key aspect of this theory is that the pitch angle should not vary with wavelength (Athanasoula et al., 2010).

This is an excellent opportunity for theory testing and indeed several attempts have been made to do so, with mixed results. Three studies have looked at large samples using only two wavebands in the optical or near-infrared. Two of these studies have declared that there is no discernible variation in pitch angle considering only these wavelengths (Seigar et al., 2006; Davis et al., 2012). Another study by Martinez-Garcia (2012), drew the opposite conclusion. Though it is noteworthy that the majority of galaxies measured in that paper was close to, on or even over the line of equality from the smaller number that showed the reported trend (see Fig.11 of Martinez-Garcia (2012)). Two studies by Martinez-Garcia et al. (2014) and Grosbol & Patsis (1998) measured only five galaxies across several wavebands spanning the optical and extending into the near infrared or near ultraviolet. They did observe small differences in pitch angle in a majority of the galaxies they studied. In addition to these studies, there have been others that have looked for offsets in position between star-forming

regions, stellar arms, and recently formed stars, both in the radio (Egusa et al., 2009; Louie et al., 2013) and in the optical (Kendall et al., 2008). Thus, results to date on this important question have been inconclusive, though it would have to be said that the vast majority of galaxies studied have shown no significant difference in pitch angle across optical and infrared wavelengths.

This study makes several advances over previous efforts, most importantly, the much increased range of wavelengths over which measurements are made. We make use of *Spitzer* images of galaxies taken at 8.0 and 3.6  $\mu\text{m}$ . At 8.0  $\mu\text{m}$ , which images warmed dust in clouds where star formation is occurring, we are capable of seeing the region of star formation in the gaseous spiral arm. The uv images from *Galaxy Evolution Explorer (GALEX)* show the same region, since they are sensitive to stars so young and bright that they are seen while still in their star-forming nurseries. We do indeed find that the 8.0  $\mu\text{m}$  pitch angles agree with those measured in the uv for those galaxies (a majority) for which *GALEX* images are available (see Fig. 3.5). The near-infrared and *B*-band images are sensitive to starlight. We find that the pitch angles of these images are consistently tighter than those measured for the 8.0  $\mu\text{m}$  and uv images (see Fig. 3.5). It is clear that the *B*-band images are showing young stars that have recently left the gaseous arm where they were formed.

Another improvement on earlier work is the large sample size. The average error in pitch angle in our sample is  $2^\circ.5$ . To increase confidence in our results, we made use of two completely independent methods of measuring pitch angles. 2DFFT (Davis et al., 2012) and Spirality (Shields et al., 2015) code (see section 2.5). We found that the two codes agree well and that our results are independent of the method of measurement used. We took great

care to eliminate the bar from our measurement annulus, as discussed in Davis et al. (2012) and also used a function of Spirality (Shields et al., 2015) to check that the spiral arms in one image actually corresponded, in angular terms, to spiral arms in the other wavelength images of the same galaxy. We also made use of a third check on the results, electronically overlaying synthetic spiral arms of the measured pitch on the galaxy image to let the observer's eye provide a check on the validity of each measurement (see Fig. 3.6). A prediction of this theory is that the pitch angle of spiral arms for galaxies in blue-light wavelength images should be smaller than when imaged in deep infrared-light. Young (blue) stars born in the spiral arms of the galaxies move ahead of the density wave inside the co-rotation radius, and fall behind outside of it. The co-rotation radius is defined as the radius at which the density wave pattern speed is equal to the local rotation speed of stars (which rotate differentially with radius). This implies that blue stars should form slightly tighter arms than the density wave itself does. It means gas and dust involved in star formation should form looser arms with bigger pitch angles than blue and red stars, and blue stars should form bigger pitch angle than red and old stars (because they are short-lived and have less time in which to move ahead of and fall behind the density wave pattern). So the old stars form tighter arms in galaxies (Figure 3.1).

Table 3.1. Spiral Galaxies and its Measured Pitch Angle at Different Wavelength of Light

Galaxy Name	Type	P (IRAC 3.6)	P ( <i>B</i> -band)	P (IRAC 8.0)	P (FUV Band)	Image Source
(1)	(2)	(3)	(4)	(5)	(6)	(7)
NGC 0157	SABb	3.58 ± 0.13	8.66 ± 0.89	9.32 ± 1.01	...	IRAC3.60, INT4400, IRAC8.0
NGC 0289	SBbc	9.89 ± 1.20	19.71 ± 1.94	23.36 ± 2.61	...	IRAC3.6, CTIO4400, IRAC8.0
NGC 0613	SBbc	19.27 ± 2.22	21.57 ± 1.76	25.67 ± 2.30	...	IRAC3.6, ESO4400, IRAC8.0
NGC 0628	Sac	9.58 ± 0.60	9.20 ± 0.83	20.60 ± 2.28	21.43 ± 1.42	IRAC3.6, NOT4400, IRAC8.0, GALEX1516A
NGC 0925	SABd	4.45 ± 0.65	7.51 ± 3.81	20.10 ± 4.69	29.68 ± 3.75	IRAC3.6, PAL4400, IRAC8.0, GALEX1516A
NGC 1097	SBb	6.84 ± 0.21	7.54 ± 3.49	9.50 ± 1.28	16.25 ± 2.30	IRAC3.6, LCO4400, IRAC8.0, GALEX1516A
NGC 1353	SBb	11.14 ± 0.70	13.68 ± 2.31	17.96 ± 1.66	...	IRAC3.6, ESO4400, IRAC8.0
NGC 1512	SBab	4.70 ± 2.24	24.80 ± 3.43	30.20 ± 4.64	...	IRAC3.6, NOT4400, IRAC8.0
NGC 1566	SABbc	15.29 ± 2.37	31.20 ± 4.80	44.13 ± 11.94	45.80 ± 2.97	IRAC3.6, KPNO4400, IRAC8.0, GALEX1516A
NGC 2403	SABc	12.50 ± 1.62	19.35 ± 1.57	28.52 ± 6.73	23.54 ± 0.78	IRAC3.6, LCO4400, IRAC8.0, GALEX1516A
NGC 2841	SAb	16.13 ± 1.63	18.77 ± 1.66	22.25 ± 2.42	23.26 ± 2.31	IRAC3.6, LOWE4500, IRAC8.0, GALEX1516A
NGC 2915	SBab	7.42 ± 0.44	7.90 ± 0.75	10.40 ± 2.08	...	IRAC3.6, KPNO4400, IRAC8.0
NGC 2976	Sac	4.14 ± 0.34	5.13 ± 0.43	8.36 ± 0.40	10.68 ± 1.00	IRAC3.6, KPNO4400, IRAC8.0, SDSS3551A
NGC 3031	SAab	15.63 ± 6.99	16.19 ± 1.23	20.54 ± 2.21	20.14 ± 1.90	IRAC3.6, JKY4034, IRAC8.0, GALEX1516A
NGC 3049	SBab	8.60 ± 0.46	10.50 ± 2.05	16.10 ± 2.59	...	IRAC3.6, CFHT4400, IRAC8.0
NGC 3184	SABcd	11.92 ± 1.77	18.30 ± 3.45	23.40 ± 3.27	26.75 ± 0.55	IRAC3.6, KPNO4400, IRAC8.0, GALEX1516A
NGC 3190	SAap	16.39 ± 2.15	17.67 ± 2.34	18.35 ± 4.43	...	IRAC3.6, CTIO4400, IRAC8.0
NGC 3198	SBc	15.97 ± 1.38	18.95 ± 2.69	20.59 ± 5.95	23.98 ± 1.84	IRAC3.6, CTIO4400, IRAC8.0, GALEX1516A



Table 3.1 (cont'd)

Galaxy Name	Type	P (IRAC 3.6)	P ( <i>B</i> -band)	P (IRAC 8.0)	P (FUV Band)	Image Source
(1)	(2)	(3)	(4)	(5)	(6)	(7)
NGC 3351	SBb	4.60 ± 1.92	16.41 ± 1.93	22.21 ± 6.96	27.17 ± 2.11	IRAC3.6, CTIO4400, IRAC8.0, GALEX1516A
NGC 3513	SBc	19.35 ± 2.85	20.27 ± 1.67	22.20 ± 2.29	...	IRAC3.6, CTIO4400, IRAC8.0
NGC 3521	SABbc	16.74 ± 1.32	19.28 ± 1.92	21.48 ± 2.19	24.81 ± 2.40	IRAC3.6, CTIO4400, IRAC8.0, GALEX1516A
NGC 3621	SAd	17.22 ± 3.37	18.43 ± 3.12	20.81 ± 2.72	20.34 ± 1.98	IRAC3.6, ESO4400, IRAC8.0, GALEX1516A
NGC 3627	SABb	11.71 ± 0.78	16.97 ± 1.54	18.59 ± 2.85	40.29 ± 1.60	IRAC3.6, KPNO4400, IRAC8.0, GALEX1516A
NGC 3938	SAc	11.46 ± 2.32	12.22 ± 1.94	19.34 ± 3.80	21.45 ± 1.87	IRAC3.6, LOWE4500, IRAC8.0, GALEX1516A
NGC 4050	SBab	5.82 ± 0.51	6.32 ± 1.89	9.00 ± 1.01	...	IRAC3.6, LCO4050, IRAC8.0
NGC 4254	SAc	28.40 ± 4.04	30.01 ± 4.36	32.8 ± 1.45	38.66 ± 3.91	IRAC3.6, INT4034, IRAC8.0, GALEX2274A
NGC 4321	SABbc	18.60 ± 1.69	15.06 ± 1.20	24.46 ± 3.76	28.49 ± 1.26	IRAC3.6, KPNO4331, IRAC8.0, SWIFT2030A
NGC 4450	SAab	12.59 ± 2.63	16.62 ± 1.45	21.2 ± 3.87	22.99 ± 5.43	IRAC3.6, LOWE4500, IRAC8.0, GALEX2267A
NGC 4536	SABbc	17.3 ± 1.75	33.74 ± 4.8	52.22 ± 2.42	55.59 ± 2.75	IRAC3.6, KP4400, IRAC8.0, GALEX1516A
NGC 4569	SABab	8.64 ± 0.52	19.05 ± 2.42	38.55 ± 6.44	42.11 ± 5.80	IRAC3.6, PAL4050, IRAC8.0, GALEX1516A
NGC 4579	SABb	11.44 ± 0.57	13.8 ± 3.25	30.73 ± 4.73	33.98 ± 3.69	IRAC3.6, KPNO4400, IRAC8.0, SWIFT2030A
NGC 4725	SABab	3.04 ± 1.83	7.40 ± 0.35	10.80 ± 1.04	13.60 ± 1.29	IRAC3.6, KPNO400, IRAC8.0, GALEX2267A
NGC 4736	SAab	8.19 ± 2.94	8.41 ± 1.34	14.09 ± 5.11	14.98 ± 2.31	IRAC3.6, PAL4400, IRAC8.0, GALEX1516A
NGC 4939	SAbc	10.93 ± 3.60	11.20 ± 1.07	16.25 ± 4.94	...	IRAC3.6, CTIO4400, IRAC8.0
NGC 4995	SABb	12.40 ± 4.36	13.00 ± 2.87	15.90 ± 3.66	...	IRAC3.6, LCO4050, IRAC8.0
NGC 5033	SAc	7.09 ± 0.46	10.46 ± 2.66	13.91 ± 4.42	...	IRAC3.6, KPNO4400, IRAC8.0

Table 3.1 (cont'd)

Galaxy Name	Type	P (IRAC 3.6)	P ( <i>B</i> -band)	P (IRAC 8.0)	P (FUV Band)	Image Source
(1)	(2)	(3)	(4)	(5)	(6)	(7)
NGC 5055	SAbc	16.35 ± 1.78	19.31 ± 1.63	20.63 ± 2.11	20.29 ± 5.87	IRAC3.6, PAL4360, IRAC8.0, GALEX1516A
NGC 5474	SACd	12.11 ± 1.15	13.84 ± 6.22	19.12 ± 3.22	19.91 ± 2.65	IRAC3.6, JKY4034, IRAC8.0, GALEX1516A
NGC 5713	SABb	12.20 ± 0.32	18.76 ± 3.10	34.79 ± 5.01	27.40 ± 1.20	IRAC3.6, CTIO4400, IRAC8.0, GALEX1516A
NGC 7331	Sab	17.13 ± 2.63	20.10 ± 1.85	21.65 ± 2.15	22.54 ± 2.41	IRAC3.6, KPNO4400, IRAC8.0, GALEX1516A
NGC 7793	SAd	10.98 ± 1.6	12.16 ± 2.1	16.34 ± 5.47	16.89 ± 1.87	IRAC3.6, ESO4400, IRAC8.0, GALEX1516A

Note. — *Columns:* (1) Galaxy name; (2) Hubble morphological type; (3) Pitch angle in degrees for infrared 3.6  $\mu\text{m}$ ; (4) Pitch angle in degrees for *B*-band 445 nm; (5) Pitch angle in degrees for infrared 8.0  $\mu\text{m}$ ; (6) Pitch angle in degrees for FUV 1516 Å; (7) Telescope/literature source of imaging.

### 3.3 Data

Our sample of 41 galaxies is drawn from the *Spitzer* Infrared Nearby Galaxies Survey, which consists of imaging from the Infrared Array Camera (Fazio et al., 2004), selecting those galaxies with imaging at both 3.6 and 8.0  $\mu\text{m}$  and that had available optical imaging in the *B*-band (445 nm) as found in the NASA/IPAC Extragalactic Database (NED; see Table 3.1 for *B*-band image sources). Twenty-eight (28) of these galaxies also have available ultraviolet imaging from archived *GALEX* data at two wavelengths, far-UV (FUV) 1350-1780  $\text{\AA}$  and near-UV (NUV) 1770-2730  $\text{\AA}$ , as indicated in Table 3.1.

### 3.4 2DFFT Results

Spiral-arm pitch angles of our sample galaxies were measured in three or four wavelength bands using the 2DFFT code (Davis et al., 2012) and checked with the Spirality code of Shields et al. (2015) (see section 3.5). Figures 3.2 to 3.5 present comparisons between pitch angles measured by 2DFFT at different wavelengths. Each point on the plots represents an individual galaxy positioned according to the measurement of its spiral-arm pitch angle at two different wavelengths. The histograms show the distribution of pitch angle differences in terms of the number of galaxies found in each bin. The *B*-band images are sensitive primarily to newly born stars that have emerged from their stellar nurseries. For the images at 3.6  $\mu\text{m}$  it is expected that older stars dominate. By contrast, at 8.0  $\mu\text{m}$ , we can see details of gas and dust in spiral arms (Elmegreen et al., 2011), as this waveband is sensitive to dust warmed by nearby star formation. Finally, the *GALEX* images at 1516  $\text{\AA}$  are sensitive to the brightest O-type stars with the shortest lives, visible while still in the

star-forming region.

We find that the  $B$ -band images have smaller pitch angles (tighter spiral arms) than the infrared  $8.0 \mu\text{m}$  image in all cases. in agreement with the prediction of the density-wave theory, because  $8.0 \mu\text{m}$  images trace the gas and dust in spiral arms.

Our results for 28 local galaxies show that spiral arms for images at  $8.0\mu\text{m}$  are clearly very similar in pitch angle to the same spiral arms observed in the far-UV by *GALEX* (see Fig. 3.5, top panel). If they are different, as the histogram in Fig. 3.5 suggests, it is by less than  $2^\circ.5$  of pitch in most cases, which is the average error in our measurements. Similarly, as seen in the second panel of Fig. 3.3, the pitch angles of 41 galaxies (the entire sample) in the  $B$ -band and  $3.6 \mu\text{m}$  images are also close to the line of equality, clustered largely within  $2^\circ.5$  of it, as the histogram shows. By contrast, Figure 3.4 shows that the  $B$ -band and Far-UV images clearly disagree in pitch angle. The  $B$ -band images have consistently tighter pitch angles, with the histogram showing that they typically differ by  $5^\circ$  or more. Similarly, there is also a clear difference, in Figure 3.2, between the pitch angles in the two infrared bands. Once again it is the stellar waveband ( $3.6 \mu\text{m}$ ) that is consistently tighter in pitch angle than that associated with the star-forming region ( $8.0 \mu\text{m}$ ).

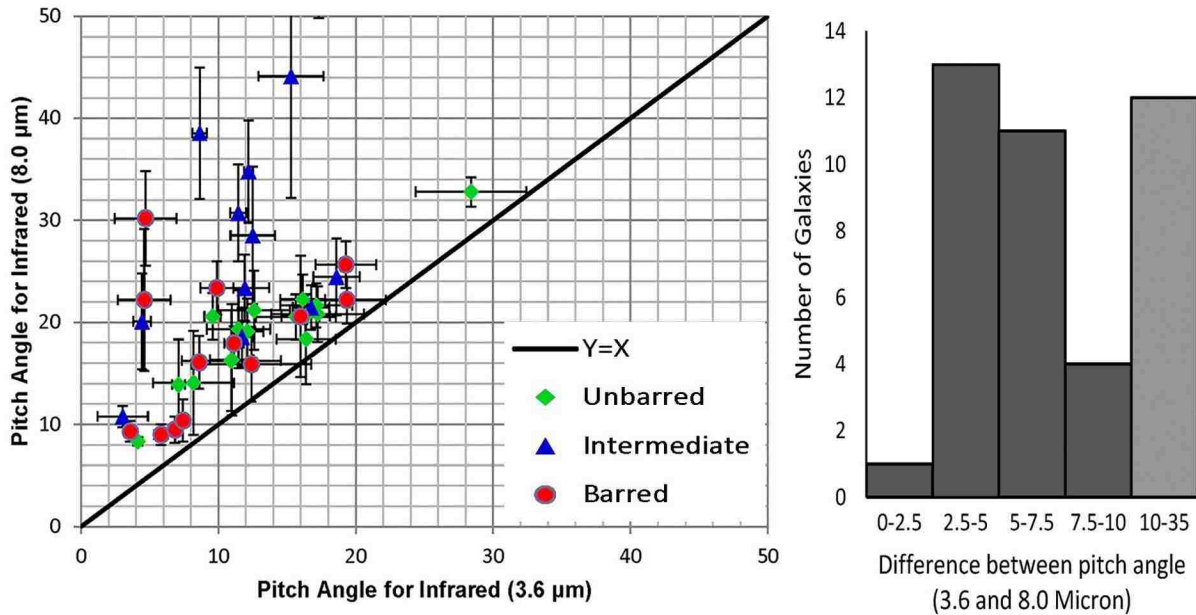


**Figure 3.2** Comparisons between pitch angles measured by 2DFFT code at wavelength 8.0  $\mu\text{m}$  and 3.6  $\mu\text{m}$ . Each point on the plots represents an individual galaxy positioned according to the measurement of its spiral-arm pitch angle at two different wavelengths. The histograms show the distribution of pitch angle differences in terms of the number of galaxies found in each bin. The greatest number of galaxies have a pitch angle difference of between 2°.5 and 5° (see the relevant histograms), with very few found below 2°.5. Images of 41 galaxies were used from SINGS survey.

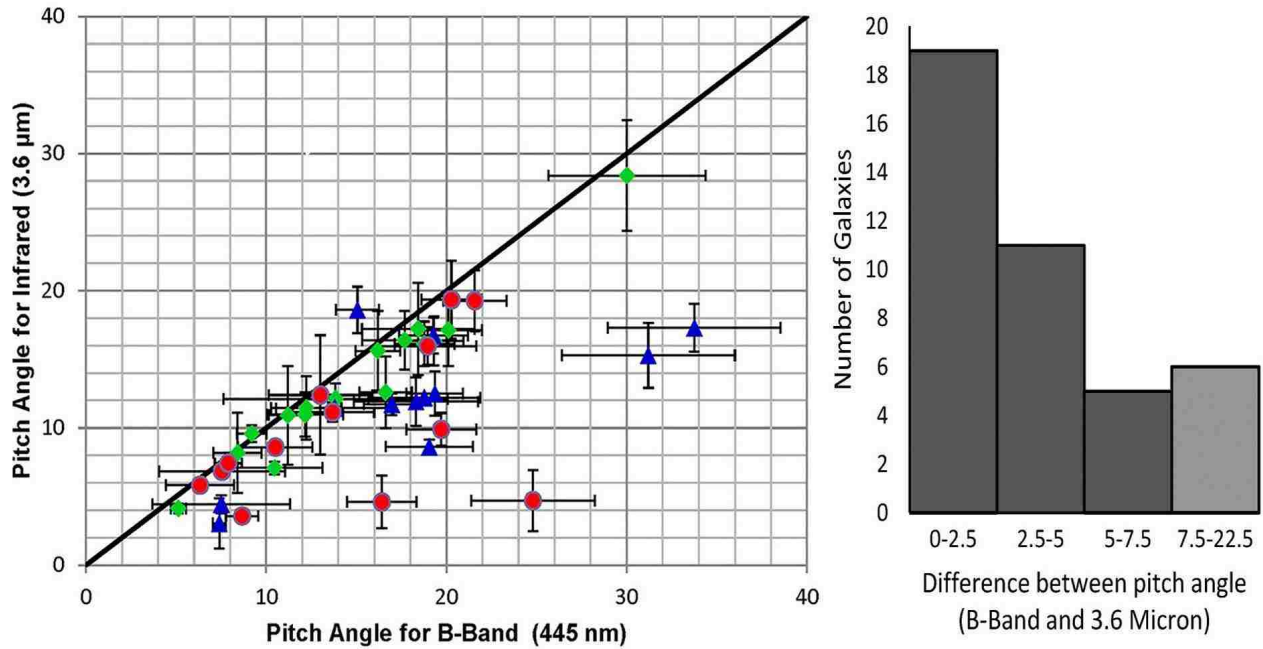


**Figure 3.3** Comparisons between pitch angles measured by 2DFFT code at wavelength 3.6  $\mu\text{m}$  and *B*-band 445 nm. The histograms show that the *B*-band with 3.6  $\mu\text{m}$  wavelengths are fundamentally equal since the greatest number of galaxies have pitch angles at these wavelengths that agree to better than  $2^\circ.5$ . Images of 41 galaxies were used from SINGS survey.

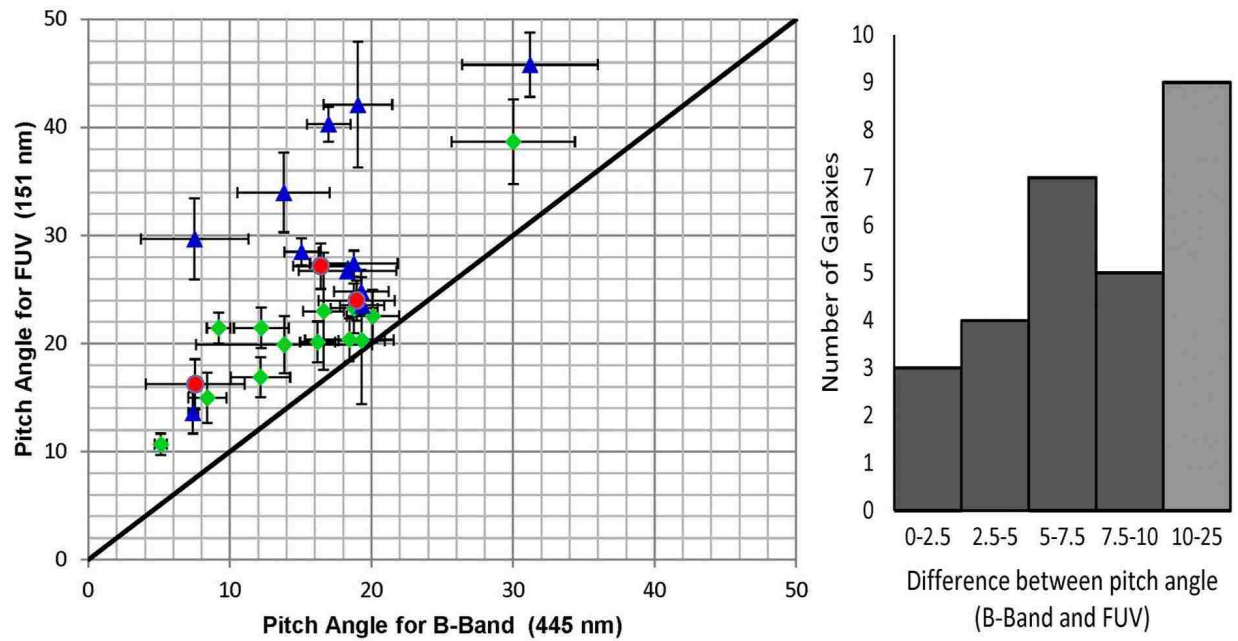


**Figure 3.4** Comparisons between pitch angles measured by 2DFFT code at wavelength *B*-band 445 nm and FUV 151 nm. The histograms show the greatest number of galaxies have a pitch angle difference of between  $2^{\circ}.5$  and  $5^{\circ}$ , with very few found below  $2^{\circ}.5$ . Images of 28 galaxies were used from SINGS survey.

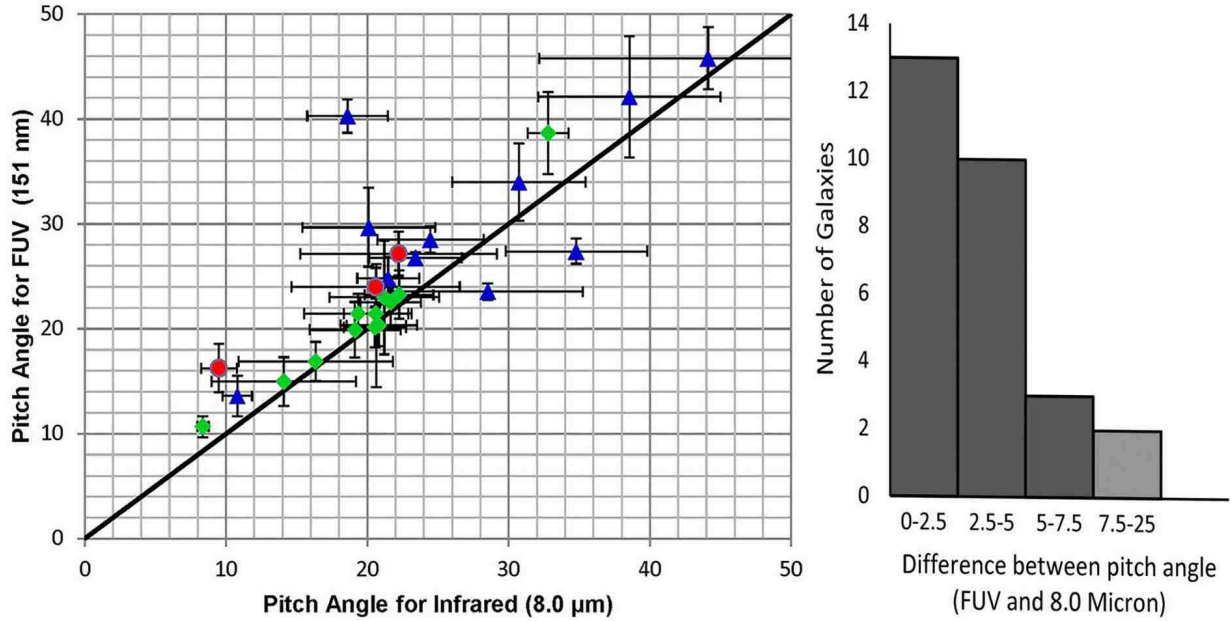


**Figure 3.5** Comparisons between pitch angles measured by 2DFFT code at wavelength 8.0  $\mu\text{m}$  and FUV 151 nm. The histograms show that the 8.0  $\mu\text{m}$  and far ultraviolet (FUV) wavelengths are fundamentally equal since the greatest number of galaxies have pitch angles at these wavelengths that agree to better than  $2^\circ.5$ . Images of 28 galaxies were used from SINGS survey.



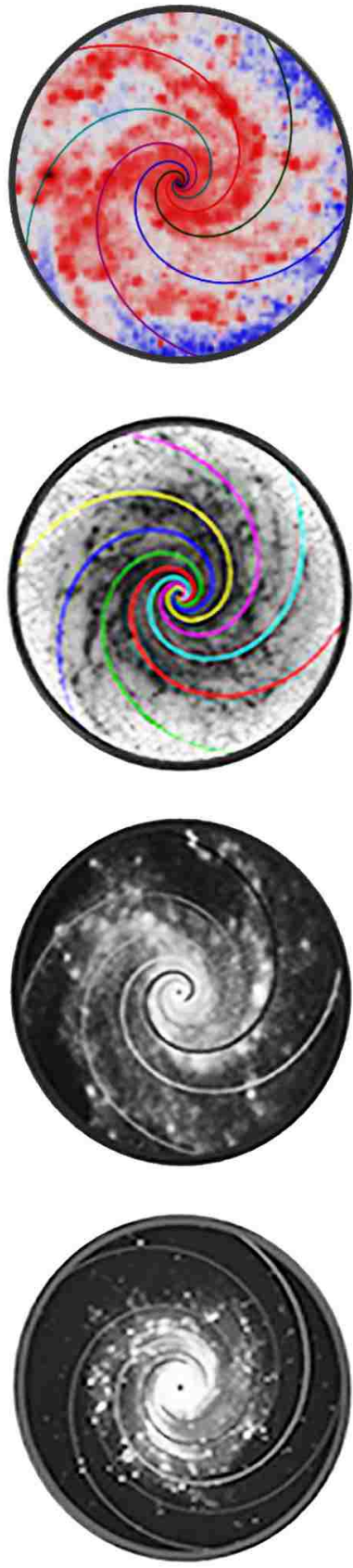


**Figure 3.6** Pitch angle for NGC 3184 with different wavelengths. Left to right:  $-11^\circ.92$  ( $3.6 \mu\text{m}$ ),  $-18^\circ.30$  ( $B$ -band),  $-23^\circ.40$  ( $8.0 \mu\text{m}$ ),  $-26^\circ.75$  (FUV).

### 3.5 Spirality Results

For  $B$ -band and  $3.6 \mu\text{m}$ , Spirality results shows slightly same pitch angle but systematically looser pitch angle than 2DFFT with average difference  $4.0^\circ$  for  $3.6 \mu\text{m}$  images and average difference  $3.1^\circ$  for  $B$ -band. In the  $8.0 \mu\text{m}$  images, the average difference is  $3.6^\circ$  and there is no systematic bias. The total average difference is  $3.5^\circ$  for 41 NGC galaxies (Unbarred, Intermediate and Barred) and  $1.8^\circ$  when we only consider 17 Unbarred galaxies. When we compare the results from both codes at a specific radius of a galaxy, the results are slightly same. Figures 3.7, 3.8 and 3.9 present the results from Spirality code for pitch angle measurements at different wavelengths. Figures 3.10, 3.11 and 3.12 present a comparison between pitch angle measured by 2DFFT and Spirality code at different wavelengths.

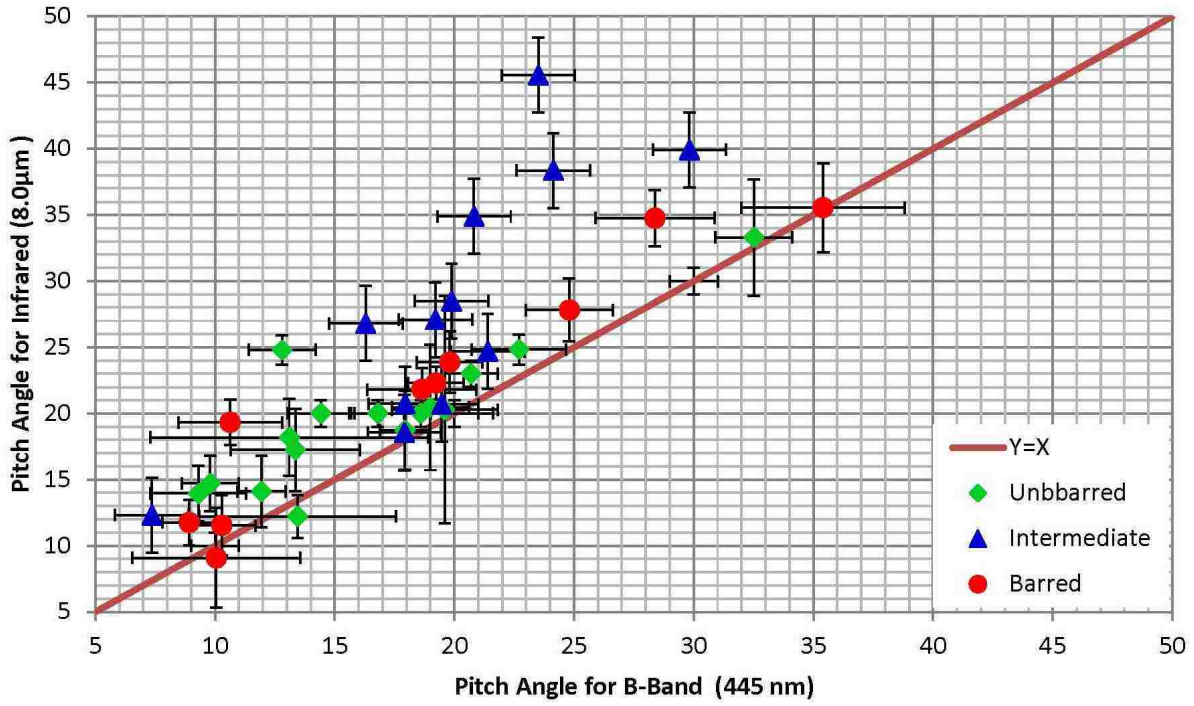


**Figure 3.7** Comparisons between pitch angles measured by Spirality code at wavelength 8.0  $\mu\text{m}$  and *B*-band 445 nm.

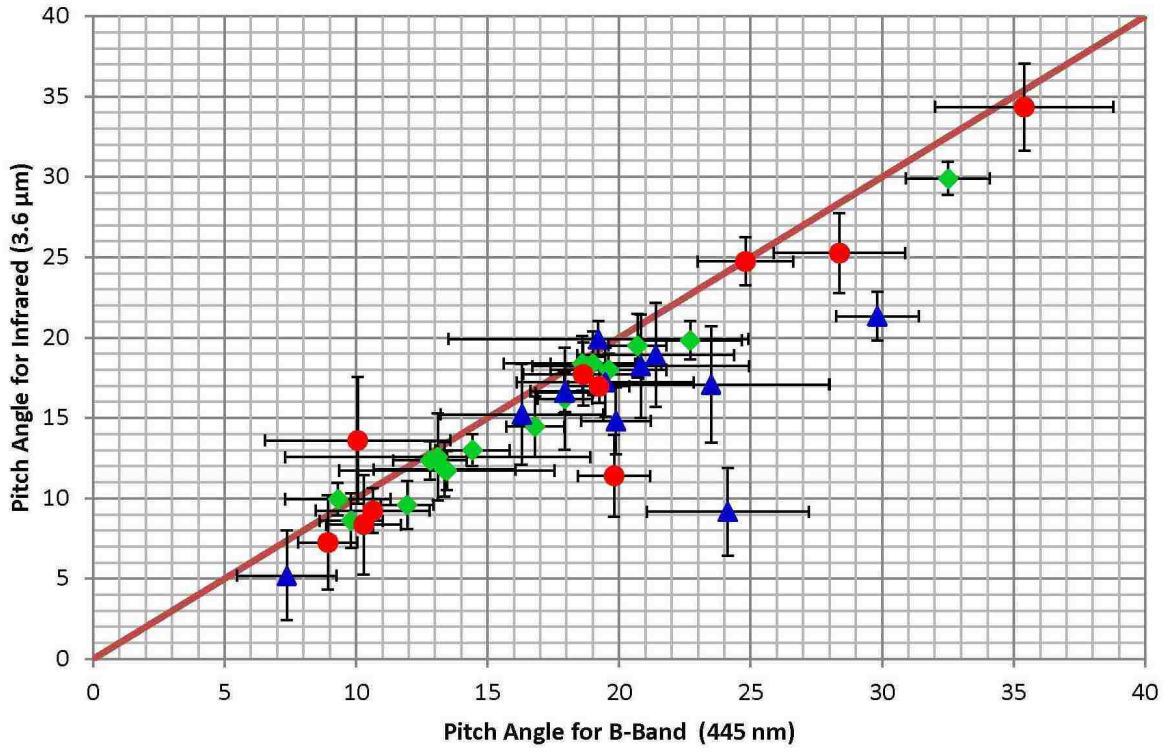


**Figure 3.8** Comparisons between pitch angles measured by Spirality code at wavelength  $3.6 \mu\text{m}$  and  $B$ -band  $445 \text{ nm}$ .

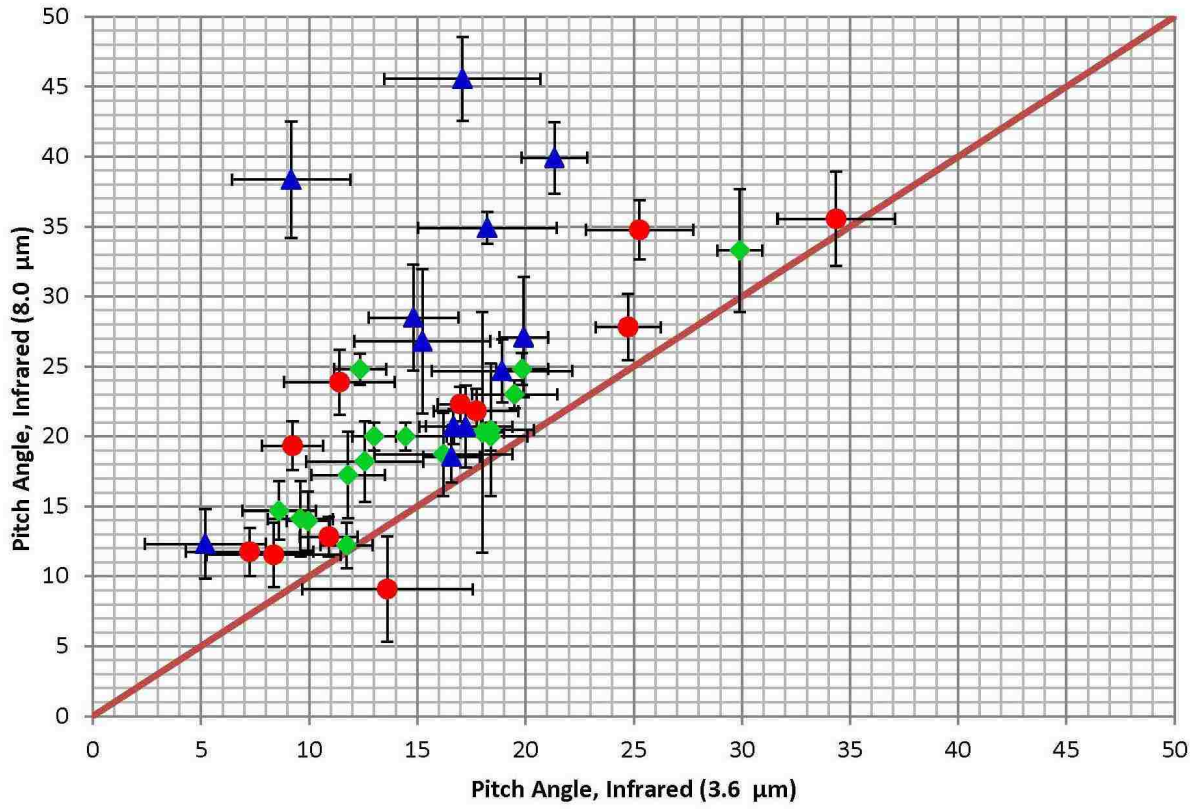


**Figure 3.9** Comparisons between pitch angles measured by Spirality code at wavelength 8.0  $\mu\text{m}$  and 3.6  $\mu\text{m}$ .

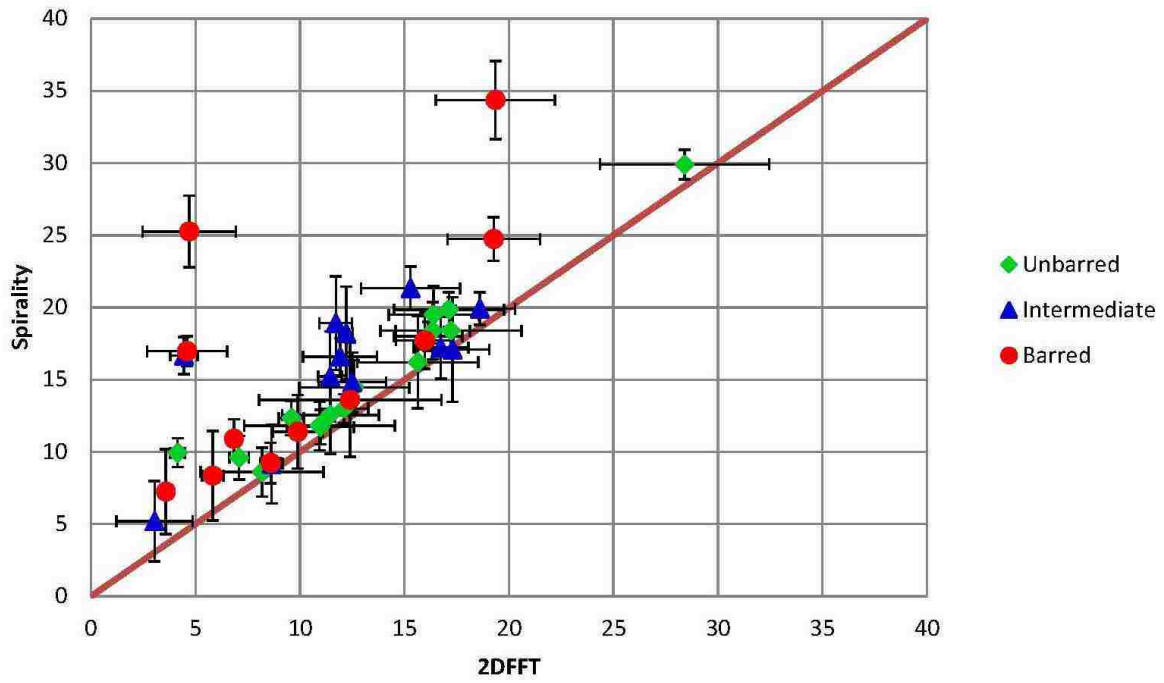


**Figure 3.10** Comparisons between pitch angles measured by Spirality and 2DFFT code at wavelength  $3.6 \mu\text{m}$ .

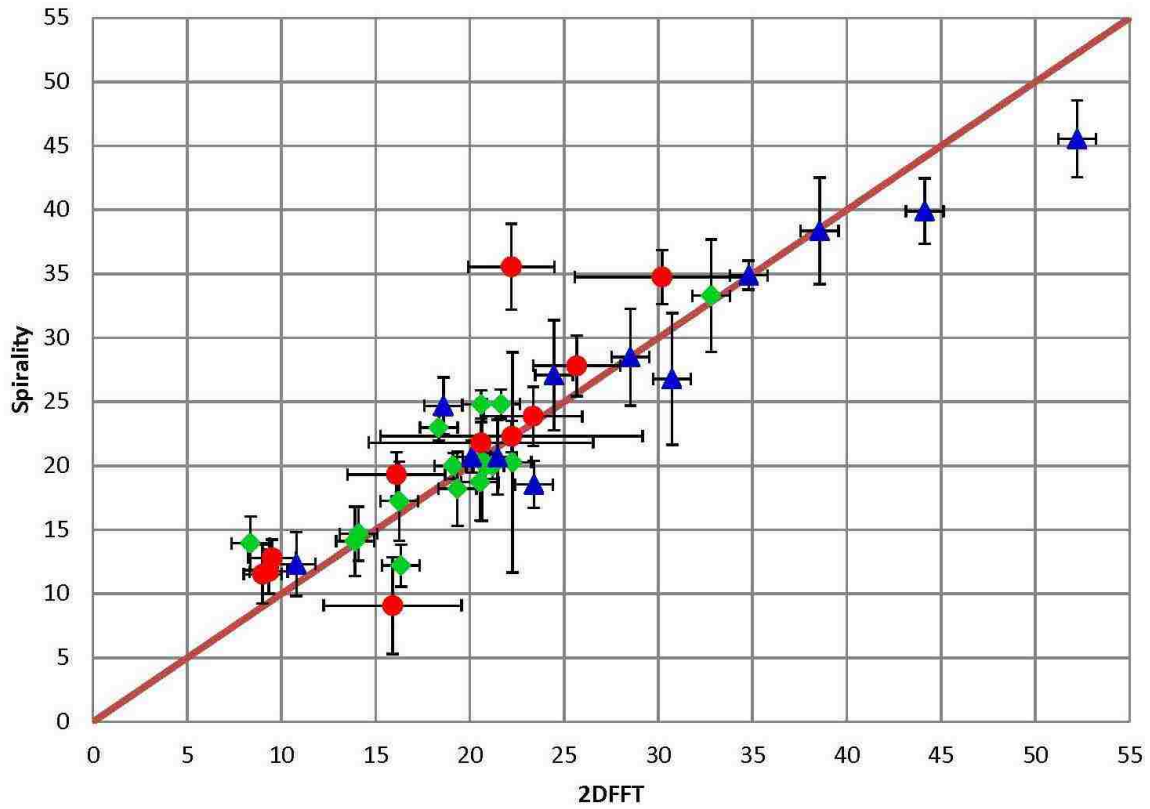


**Figure 3.11** Comparisons between pitch angles measured by Spirality and 2DFFT code at wavelength  $8.0 \mu\text{m}$ .

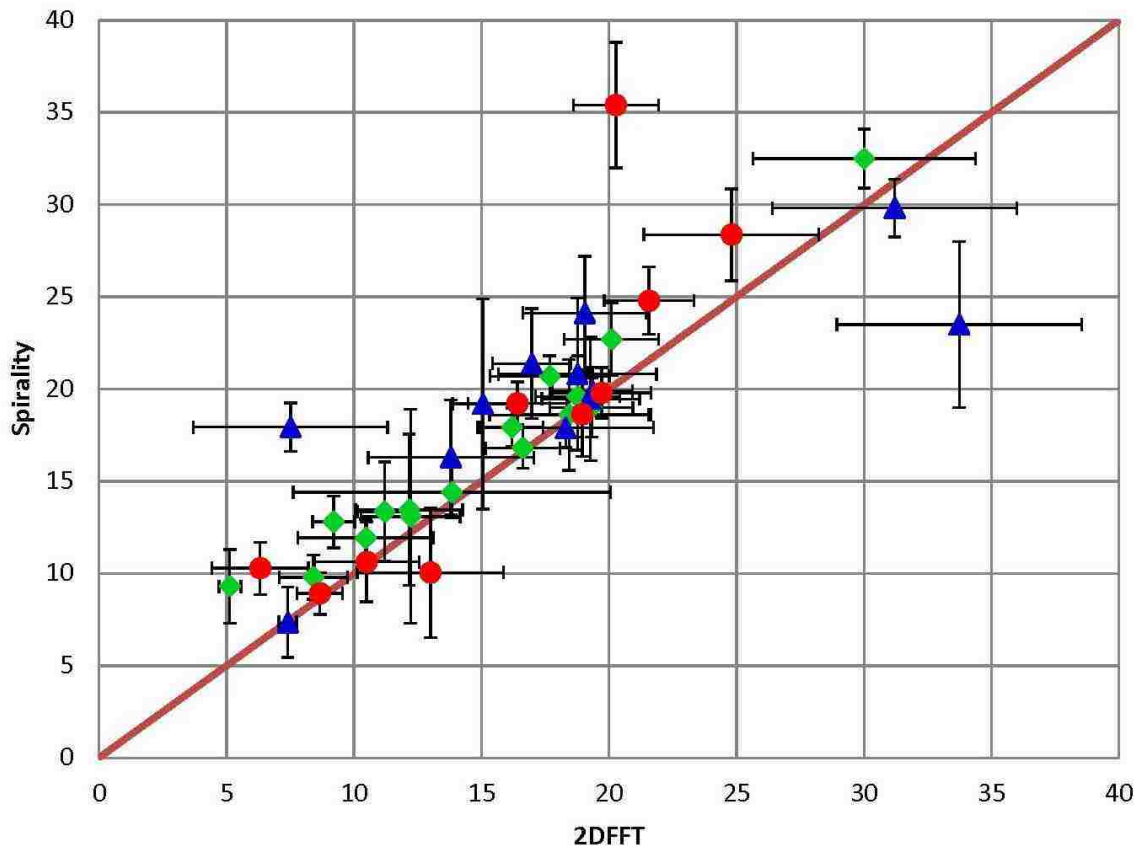


**Figure 3.12** Comparisons between pitch angles measured by Spirality and 2DFFT code at wavelength *B*-band 445 nm.



### 3.6 Discussion

It is apparent from Figure 3.5 that the far-UV and the 8.0  $\mu\text{m}$  images have essentially the same pitch angle. This supports our argument that these wavebands both image the star-forming region. It forms a spiral pattern that is noticeably looser than that formed in both the  $B$ -band and the 3.6  $\mu\text{m}$  images, which both image stars. Thus, we confirm the picture from the left-hand side of Figure 3.1, in which the star-forming region or gaseous arm (UV and 8.0  $\mu\text{m}$ ) has a larger pitch angle than that formed by the bluer stars ( $B$ -band) and the redder stars (3.6  $\mu\text{m}$ ). The region just downstream from the spiral arm has just as many old disk stars as any other region of the disk, but the population has been augmented by recently formed reddish stars. Thus, even in the red or infrared, the region associated with newly formed stars is brighter than other parts of the disk. For several intermediate and barred galaxies, the difference in pitch angle in the different wavebands is very high, which may mean that the pitch angle derived is biased by the presence of a bar.

We employed a Monte Carlo technique to generate two-dimensional Gaussians about each data point (based upon the associated measurement errors) to see what were the chances of finding counter-examples to our reported trend. We find that there is on the order of a 1% chance of contradicting the claim of tighter pitch angles for the stellar sources than for the star-forming regions (Figure 2, bottom two panels). For the cases where the two bands are both sampling stellar sources (Figure 2, second panel) or star-forming regions (Figure 2, top panel), the chance of finding a contradictory result are on the order of 10%.

Our results are compatible with those in Davis et al. (2012) and Seigar et al. (2006). Both claimed to see no noticeable change in pitch angle at wavebands that image stars,

Davis et al. between  $B$  and  $I$  bands and Seigar et al. between  $B$  on the one hand and either  $K'$  or  $H$  bands on the other. We believe this is consistent with our picture that there are fundamentally two discernible pitch angles, one that images the gaseous arm and one that images stars that have moved out from the star-forming region to form a tighter spiral pattern nearby and that crosses the gaseous arm at the co-rotation radius. We do see a modest difference between the bands at the extreme ends of this range, from  $B$ -band to  $3.6 \mu\text{m}$  (see Fig. 3.3), but it is small at best.

Another study is Martinez-Garcia (2012), which compares pitch angles in  $B$  and  $H$  for a good-sized sample of galaxies. Although Martinez-Garcia sees an overall tendency for the  $B$ -band pitches to be tighter than the  $H$ -band pitches (see Fig. 11 of Martinez-Garcia (2012)), we note (as stated above) that many of his objects are consistent with an equality between the pitch angles at optical and near-infrared images.

Our results are not compatible with the claim made by both Martinez-Garcia et al. (2014) and Grosbol & Patsis (1998) that they see a tendency for pitch angles to be tighter at blue wavelengths than at red. Broadly speaking, we see the opposite, looser spirals in the ultraviolet, growing tighter in the blue, and perhaps tightening a little further into the red. We find, nevertheless, that there is some important common ground between our work and that of Martinez-Garcia et al. (2014).

Grosbol and Patsis claim a difference in pitch angle, for four objects <sup>2</sup>, between the  $B$ -band and the  $I$  band, which is tighter in  $B$  for all four. Davis et al. also measures  $B$ -band versus  $I$ -band for a larger sample of galaxies. The reader will note that none of Grosbol

---

<sup>2</sup>Grosbol and Patsis measure five galaxies but only have  $B$ -band measurements for four of them.

and Patsis' objects are exceptional in this sample. They are close to galaxies with a similar difference between  $B$  and  $I$  as measured by Davis et al. But the over all spread of Davis et al's results straddles the line of equality. Thus we believe that a larger sample in Grosbol and Patsis would have shown a similar result, that there is no significant difference in pitch angle between the  $B$  and  $I$  bands. They claim an even larger difference between  $B$  and  $K'$ , in disagreement with the much larger sample of Seigar et al, who see no consistent tendency for  $B$  or  $K'$  to be tighter than the other. Our difference between  $B$  and  $3.6 \mu\text{m}$  is the opposite to that claimed between  $B$  and  $K'$  by Grosbol and Patsis (they see  $B$  as the tighter pitch, we see it as looser). We do not have high quality images in  $K'$  for a direct comparison. We do note that our measurements in  $B$  for two of their objects agree reasonably well with theirs, so this is not simply the result of two different methods of measuring pitch angle.

We agree completely with one key result of Martinez-Garcia et al. (2014): that pitch angles in images taken at the  $H\alpha$  line agree well with the pitch measured in the  $u$  band. They argue that these images are capturing the star-forming region. We agree since we have measured some of our objects in the  $u$  band and find results in agreement with those given here for the UV and  $8.0 \mu\text{m}$  bands. Therefore, it seems likely that both they and we are successfully imaging the gaseous arm in a number of different widely separated wavebands. However, they find that images in the  $g$ ,  $r$ ,  $i$ , and  $z$  bands tend to show tighter pitch angles, compared to  $u$  and  $H\alpha$ . So, contrary to us, they claim that the stellar pitch angles are tighter than the pitch angle of the gaseous arm where stars are formed.

Their analysis, which is based on the theoretical work of Kim & Kim (2013), is that their red bands are imaging the stellar spiral arm where the density wave causes old disk

stars to crowd closer together. The pitch angle of this “stellar arm” should be the largest because the density wave moves in a fixed pattern. Everything else moves ahead of the stellar arm when inside the co-rotation radius and falls behind outside of it, as illustrated in Fig. 3.1 (this is a simplified account, but qualitatively matches the more complex picture coming from density-wave theory, as seen in Kim & Kim (2013)). The stellar arm is where gas clouds passing through the density wave begin their collapse (gray arm in Fig. 3.1). A short while later their gravitational collapse has proceeded to the point where they are giving birth to stars. By this time they have moved to a new position that is referred to as the gaseous arm (black arm in Fig. 3.1). Because the stellar arm and the gaseous arm cross each other at the co-rotation radius, Martinez-Garcia et al. (2014) and Grosbol & Patsis (1998) are looking for a gradient of this type: red spiral arms tighter than blue. Equivalently, the stellar arm is tighter than the gaseous arm, as depicted in Fig. 7 of Kim & Kim (2013), which is based upon complex theoretical modeling of the dynamics within the spiral arm created by the density wave.

We interpret our results, in contrast, not as the result of a gradient across the spiral arm itself, but a gradient produced by migration of new stars, born inside the spiral arm, as they pass out of it. As Martinez-Garcia et al. (2014) say in their paper, speaking about the stars born in the spiral arm, “these young stars will then gradually age, as they leave the place where they were born, and produce a gradient toward the red in the opposite direction.” That is to say, when we image the stars that originate in the star-forming region, these stars will have moved further on from that region (ahead in the inner disk, behind in the outer disk) and so the pitch angle gradient will be, as they say, in the opposite direction:

UV stars will have the loosest pitch, blue stars a tighter pitch. This is, of course, exactly what we see in our sample. In fact, the reddest stars in our sample may have the tightest pitch angle of all. We conclude, therefore, that these are also stars born in the spiral arm that have migrated out of it. We stress, however, that this issue is not critical to the confirmation of the density-wave theory. It is sufficient to note the difference in pitch angle between the newly born blue stars and the 8.0  $\mu\text{m}$  and UV images that sample the gaseous spiral arm. These stars are part of the general disk population. The only thing distinguishing them from stars elsewhere in the disk is that they are a little closer together (because they are currently in the density wave). But the star-forming clouds which are beginning to gather about them must tend to obscure these stars and it seems unlikely that a slightly enhanced density will be noticeable, compared to the brightness of the new stars being born downstream. Certainly there should be no tendency at all for these old stars to be bluer than stars anywhere else in the disk. The fact that our  $B$ -band measurements have a tighter pitch angle than our UV and 8.0 micron images suggests that these are the newly born blue stars moving downstream from the star-forming region.

One possible interpretation is that our 3.6  $\mu\text{m}$  images are not capturing the old stars in the "stellar arm" (gray line in Fig. 3.1). These stars are part of the general disk population. The only thing distinguishing them from stars elsewhere in the disk is that they are a little closer together (because they are currently in the density wave). But the star-forming clouds which are beginning to gather about them must tend to obscure these stars and it seems unlikely that a slightly enhanced density will be noticeable, compared to the brightness of the new stars being born downstream. Certainly there should be no tendency at all for

these old stars to be bluer than stars anywhere else in the disk. The fact that our  $B$ -band measurements have a tighter pitch angle than our UV and  $8.0\ \mu\text{m}$  images suggests that these are the newly born blue stars moving downstream from the star-forming region. Since our  $3.6\ \mu\text{m}$  images are, if anything, slightly tighter than the  $B$ -band images, we might interpret this as evidence that these stars are also recently born. Of course, they mingle with and augment the light from a population of older disk stars that themselves just passed through the spiral arm. Thus, we are seeing the “gradient ... in the opposite direction” referred to in Martinez-Garcia et al. (2014). Rather than seeing a color gradient within the spiral arm itself we may be seeing a color gradient created by stars moving downstream from their formation within the spiral arm.

Another interpretation is possible, however, based upon the notion, proposed in some versions of density-wave theory (Roberts, 1969; Gittins & Clarke, 2004), that the star formation begins to occur as the gas clouds approach the density wave (see the right-hand side of Figure 3.1). In this case, the gaseous or star formation arm should have a looser pitch angle than the stellar arm consisting of old red disk stars concentrated by the density wave, which is what we see. New blue stars formed in the gaseous arm move downstream as described earlier and end up close to the position of the stellar arm. This scenario is clearly compatible with our results.

We hope that in future work we may decide between these two interpretations by studying individual galaxies and their dynamics in more detail to determine which fits better with observations. In this context, it is worth noting that a few galaxies in Figures 3.2 to 3.5, all barred, have very large changes in pitch angle that are hard to reconcile with either

scenario. These anomalies could be due to difficulties in measurement (pitch angles of these galaxies all have large error bars). Increasing the sample size may help in identifying the reason for these odd results.

We don't believe that any of our images are capturing the old disk stars in the spiral arm which would show the gradient they report. As stated above we would find it difficult to see such a gradient in a larger sample, because it is not easy to image those old stars (the stellar arm), and because the pitch angle difference sought for within the spiral arm itself is probably smaller than our codes' measurement error. Rather than seeing a colour gradient within the spiral arm itself we are seeing a colour gradient created by stars moving downstream from their formation within the spiral arm.

The colour gradient within the spiral arm sought for by Martinez-Garcia (2012); Grosbol & Patsis (1998) has also been the subject of studies by Choi et al. (2015); Yuan & Grosbol (1981) in an effort to confirm or test density wave theory. Although the effect we see is related, but different, Regardless of the interpretation, we find our results to be a strong confirmation of the density- wave theory. The model that our results support is one in which a star-forming region rotating with a fixed spiral pattern gives birth to stars that move downstream from the spiral arm, with a pitch angle altered by shear (differential rotation). This is a prediction of the density-wave theory that is not replicated by its rivals. The strongest competitor to the density-wave theory currently is the manifold theory. As noted by Athanassoula et al. (2010), this theory finds that the spiral patterns are formed by stars moving along orbital trajectories within certain elliptical manifolds. It predicts that all stars and gas should move together, with no color gradient. This is contrary to the evidence

we present in this letter.

### 3.7 Conclusion

Images from deep infrared wavelength (3.6 and 8.0  $\mu\text{m}$ ) unlike images taken at optical wavelengths show us the spiral arms patterns traced by old stars (near-infrared) and gas and dust (far-infrared). For each galaxy we used an optical wavelength image ( $B$ -band: 445 nm) and another image from the Spitzer Space Telescope in the deep infrared range and we measured the pitch angle with the 2DFFT code and a completely independent code called Spirality (which uses templates with Fourier transforms to measure pitch angle). Our results for 41 NGC galaxies show that spiral arms for images with optical wavelength 445 nm (more details of blue stars) are clearly tighter than spiral arms in infrared wavelength 8.0  $\mu\text{m}$  (more details of gas and dust (Elmegreen et al., 2011)) in all cases and spiral arms for images with infrared wavelength 3.6  $\mu\text{m}$  (more details of red and old stars (Elmegreen et al., 2011)) are clearly tighter than spiral arms in optical wavelength 445 nm (more details of blue stars), in agreement with the prediction of density wave theory (Figure 3.1). The results for pitch angle measurements by two different independent codes are slightly same with total average difference  $3.5^\circ$  for all 41 NGC galaxies (Unbarred, Intermediate and Barred) and average difference  $1.8^\circ$  for 17 unbarred NGC galaxies. When we consider the results for specific inner and outer radius, 2DFFT and Spirality results are becoming ever more closely satisfied.



### 3.8 Acknowledgments

The authors thank Matthew Bershad and Bret Lehmer for valuable suggestions that guided our research. This research has made use of the NASA/IPAC Extragalactic Database, which is operated by the Jet Propulsion Laboratory, California Institute of Technology, under contract with the National Aeronautics and Space Administration.

## Bibliography

- Athanassoula, E., Romero-Gómez, M., Bosma, A. and Masdemont, J. J. 2010, MNRAS, 407, 1433-1448
- Bertin, G. & Lin, C. C. 1995, Spiral structure in galaxies a density wave theory, The MIT Press
- Choi, Y. , Dalcanton, J. J. ,Williams, B. F. ,Weisz, D. R. ,Skillman, E. D. ,Fouesneau, M. and Dolphin, A. E 2015, ApJ, 810, 9
- Davis, B. L., Kennefick, D., Kennefick, J., Kyle, B. W., Shields, D. W. 2015, ApJ, 802, L13
- Davis, B. L., Berrier, J. C., Shields, D. W., Kennefick, J., Kennefick, D., Seigar, M. S., Lacy, C. H. S., & Puerari, I. 2012, ApJS, 199, 33
- Egusa, F. and Kohno, K. and Sofue, Y. and Nakanishi, H. and Komugi, S. 2009, ApJ, 697, 1870
- Elmegreen, D. M., Elmegreen, B. G., Yau, Andrew, et al. 2011, ApJ, 737, 32
- Fazio, G. G., Hora, J. L., Allen, L. E., et al. 2004, ApJS, 154, 10
- Gittins, D. M. and Clarke, C. J. 2004, MNRAS, 349, 909-921
- Grosbol, P. J. & Patsis, P. A. 1998, A&A, 336, 840
- Kendall, S. and Kennicutt, R. C. and Clarke, C. and Thornley, M. D. 2008, MNRAS, 387, 1007-1020
- Kennicutt, Jr., R. C. 1981, AJ, 86, 1847
- Kim, Y. and Kim, W.-T. 2013, MNRAS, 440, 208-224
- Lin, C. C. and Shu, F. H. 1964, ApJ, 140, 646
- Louie, M. and Koda, J. and Egusa, F. 2013, ApJ, 763, 94
- Martínez-García, E. E. 2012, ApJ, 744, 92
- Martínez-García, E. E. and Puerari, I. and Rosales-Ortega, F. F. and González-Lópezlira, R. A. and Fuentes-Carrera, I. and Luna, A. 2014, ApJ, 793, L19
- Roberts, W. W. 1969, ApJ, 158, 123
- Seigar, M. S., Bullock, J. S., Barth, A. J., & Ho, L. C. 2006, ApJ, 645, 1012
- Seigar, M. S., Kennefick, D., Kennefick, J., & Lacy, C. H. S. 2008, ApJ, 678, L93

Savchenko, S. S., and Reshetnikov, V. P. 2011, *AstL*, 37, 817

Shields, D. W., Davis, B. L., Pour-Imani, Hamed., Kennefick, D., & Kennefick, J. 2015, arXiv:1511.06365

Shu, Frank H. 2016, Six Decades of Spiral Density-Wave Theory, *Annual Review of Astronomy and Astrophysics*, Vol 54, Sep 2016

Yuan, C. and Grosbol, P. 1981, *ApJ*, 243, 432

## Chapter 4

### Spiral Structure Through a Multi-wavelength Study

#### 4.1 Abstract

The density-wave theory of spiral structure proposes that star formation occurs in or near a spiral-shaped region of higher density that rotates rigidly within the galactic disk at a fixed pattern speed. Newborn stars move downstream of this position as they come into view, forming a downstream spiral with a smaller pitch angle than the density wave (i.e. its spiral is tighter). A rival theory, the manifold theory, demands that pitch angle should not depend on wavelength. We measure the pitch angle of a large sample of galaxies at several wavelengths associated with star formation or very young stars (8.0 microns, H- $\alpha$  line and 151 nm in the FUV) and show that they all have the same pitch angle, which is larger than the pitch angle measured for the same galaxies at optical and NIR wavelengths. Our measurements in the *B*-band and at 3.6 microns have unambiguously tighter spirals than the star-forming wavelengths. In addition we have measured in the *u*-band, which seems to fall midway between these two extremes. Thus our results are consistent with a region of enhanced stellar light situated downstream of a star-forming region.

#### 4.2 Introduction

The density-wave theory has dominated the interpretation of spiral arms in disk galaxies since the mid-sixties (Lin & Shu, 1964; Bertin & Lin, 1996; Shu, 2016). The orig-

inal theory, with its disk-spanning standing-wave pattern created by resonant modes, has been challenged by numerical simulations which suggest that the waves should be subject to damping which might prevent long-lasting modes from generating semi-permanent spiral arms. An alternative theory, known as swing amplification (introduced by Goldreich & Lynden-Bell (1965) and Julian & Toomre (1966)), proposes that small local disturbances can be amplified to create transient patterns. Currently, the theoretical situation is such that quite diverse views co-exist and there is no consensus that a single mechanism is responsible for all of the observed spiral patterns in galaxies. While some experts insist that spiral patterns must last only a galactic rotation or two, other theorists argue that swing amplification can give rise to superposed modes of the system which can last for up to ten rotation periods (Sellwood & Calberg, 2014). In Chapter 3 (Pour-Imani et al., 2016), I confirmed a key prediction of the density-wave theory, that spiral arm pitch angle varies with observation wavelength. This is in contrast to the predictions of rival theories, such as the Manifold theory (for a discussion of this theory test see (Athanasoula et al., 2010)). The density-wave theory predicts that the density-wave gives rise (through compression of clouds approaching and passing through it) to a star-forming region and that newly born stars will move downstream of this star-forming region before they are observed. How this affects pitch angle depends crucially on the existence of a co-rotation radius, a point on the disk at which the rotational speed of stars equals the rotational speed of the fixed spiral pattern itself (the density-wave). Inside the co-rotation radius, stars move faster than the pattern speed and downstream means ‘in advance of the pattern.’ Outside the co-rotation radius stars move slower than the pattern speed and downstream means ‘falling behind the

pattern.’ Thus newly born stars should form a spiral arm which is tighter (with a smaller pitch angle) than the spiral density wave itself as shown in Fig.4.1. In Chapter 3 (Pour-Imani et al., 2016), I showed that for a sample of 41 galaxies there is a clear difference between the pitch angle of two wavelengths associated with stellar light,  $B$ -band and 3.6 microns and two wavelengths associated with star formation, 8.0 microns and 151 nm in the FUV. The stellar pitch angles are uniformly smaller (tighter spiral arms) than the star-formation pitch angles. In this chapter, I look at another wavelength associated with star-formation, the H- $\alpha$  line. In confirmation of the earlier result, the pitch angles for this wavelength agree well with those earlier measured for 8.0 microns and the FUV. In addition, I have added pitch angles measured in the  $u$ -band. This band lies midway between the FUV and the  $B$ -band, which though close in wavelength disagree in pitch angle. Not surprisingly, we find evidence that the pitch angle associated with the  $u$ -band appears to lie between these other two, suggesting that there are some stars that do not live long enough to move from the star forming region (seen in the FUV), stars which move a short distance away ( $u$ -band), and stars that live long enough to move clearly away from the star-forming region ( $B$ -band).

I find these new results to be further evidence in favor of the density-wave theory. One important point is that the  $B$ -band and 3.6 microns pitch angles agree reasonably well with each other. If anything we see the 3.6 micron pitch angle as being even a little tighter than the  $B$ -band. In short, there may be a steady gradient from blue to red of tightening pitch angles, moving through FUV,  $u$ -band,  $B$ -band to 3.6 microns. Other groups report a different result, in line with the expectation that in the NIR we are not seeing newly born stars but rather old red disk stars compressed together by the density-wave itself (Martinez-Garcia,

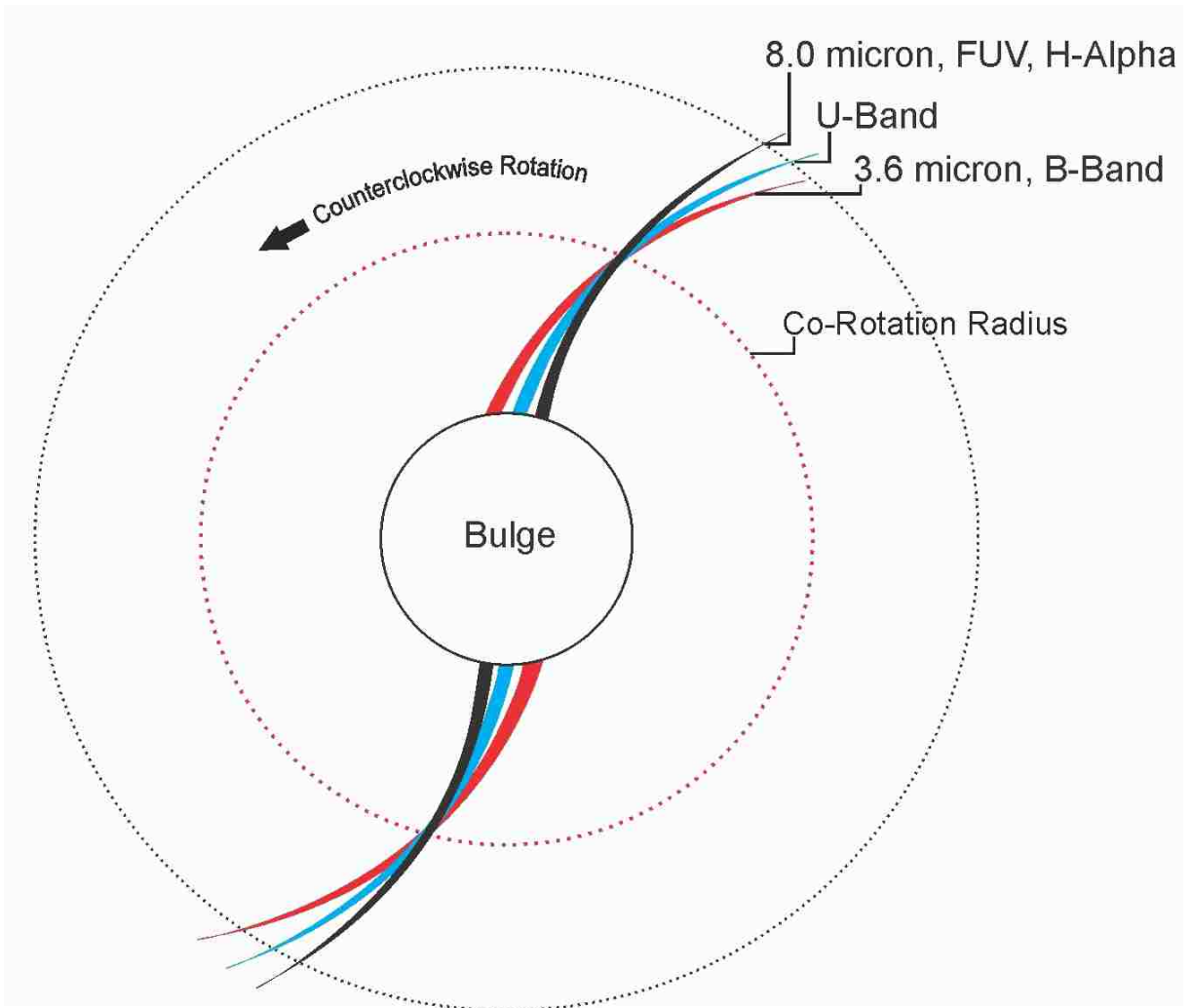


**Figure 4.1** Predictions of density-wave theory for the spiral-arm structure at the different wavelength of light.(Pour-Imani et al., 2016)

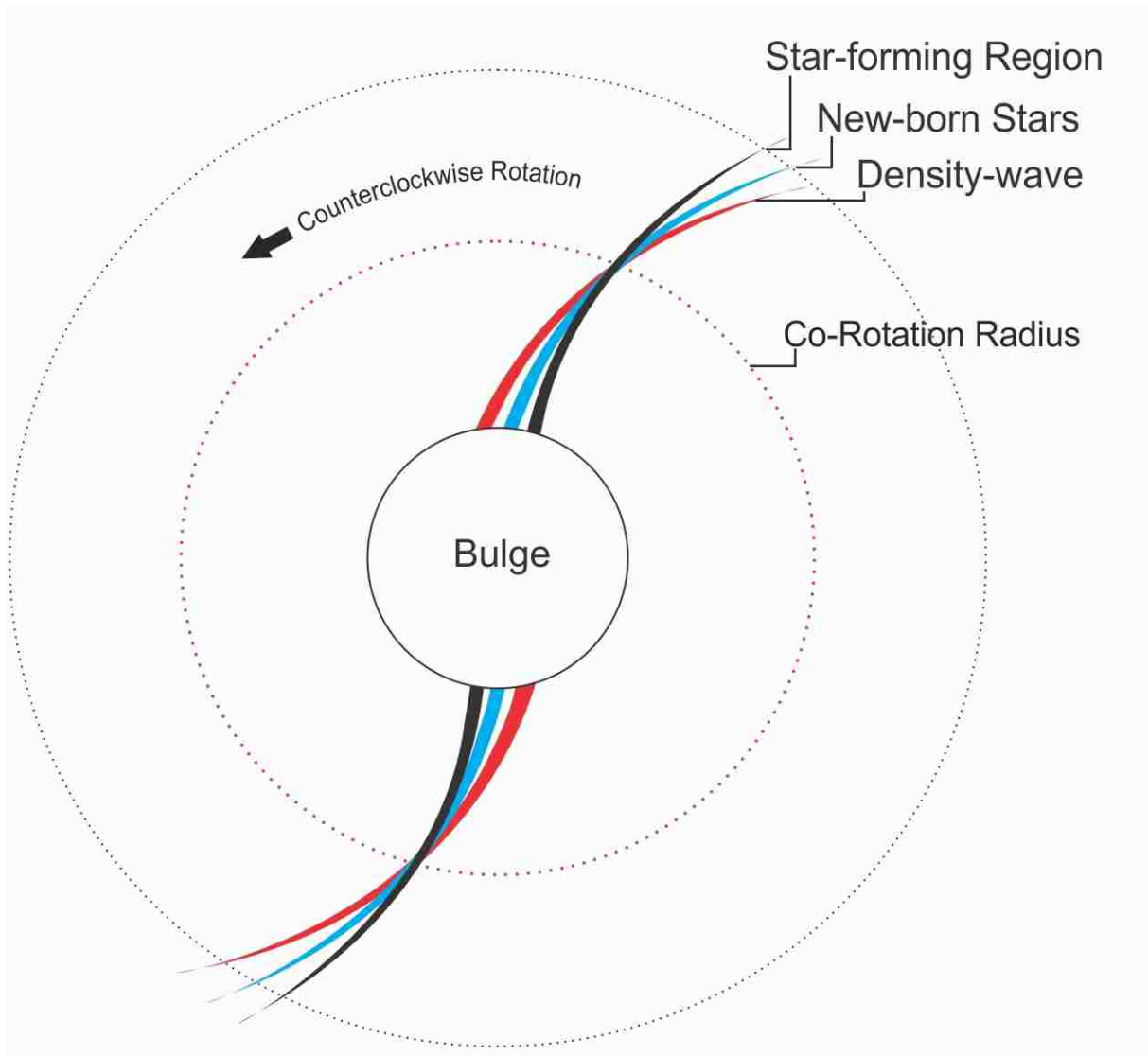


**Figure 4.2** Star-formation may be initiated as gas clouds approach the location of the spiral density-wave. In this scenario, newly born stars seen downstream of the star-forming region will be found close to the position of the density-wave.



2012; Martinez-Garcia et al., 2014; Grosbol & Patsis, 1998) (see Fig.4.3). In interpreting our results we would argue that each of the  $u$ -band,  $B$ -band and 3.6 microns measurements is seeing a spiral region created by newborn stars mingling with the old disk population to create a brighter spiral-shaped region downstream of the star-forming region. This is a very natural interpretation consistent with our understanding of stellar evolution. The question might be raised as to where the density-wave itself is to be found in this picture. Traditionally the expectation was that NIR images would show where the old red disk population was compressed together by the density-wave. Thus it might be expected that our 3.6 microns images should show the current position of the density-wave. As just noted, a natural interpretation would be that we see where new-born stars augment the red light of the old disk population. But it is also consistent with seeing the position of the density-wave if star-formation begins as clouds approach the density-wave, so that the star-formation region is to be found upstream of the density-wave as shown in Fig.4.2.

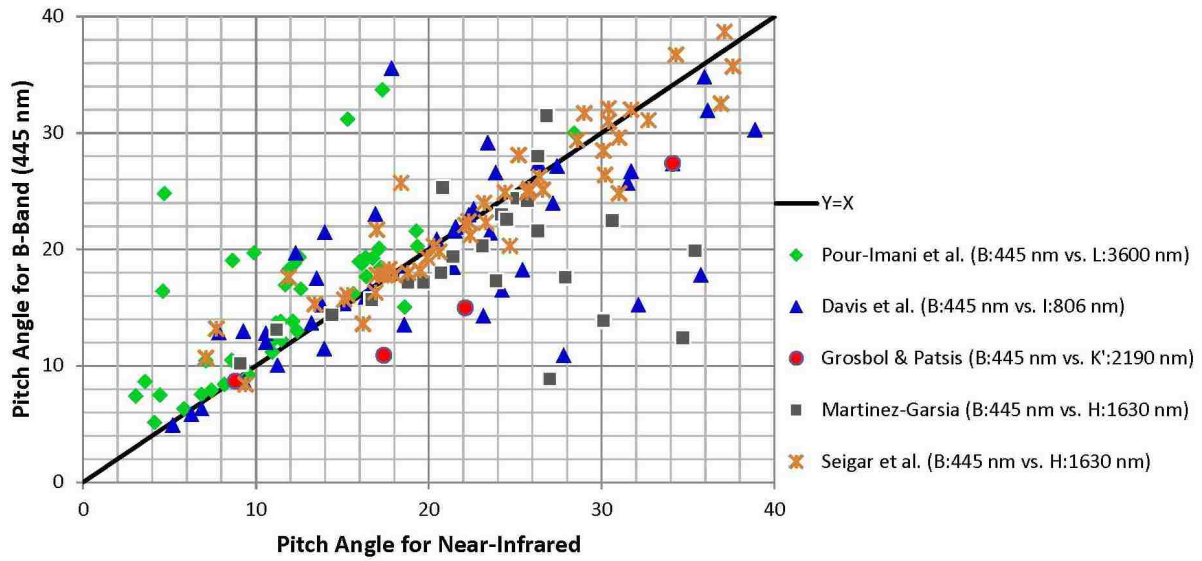


**Figure 4.3** B Vs NIR, Hamed (Pour-Imani et al., 2016), Ben(Davis et al., 2012), Patsis (Grosbol & Patsis, 1998), Martinez (Martinez-Garcia, 2012), Seigar (Seigar et al., 2006)

### 4.3 Data

My sample of 29 galaxies is drawn from the *Spitzer* Infrared Nearby Galaxies Survey, which consists of imaging from the Infrared Array Camera (Fazio et al., 2004). The sample is drawn from the sample found in Pour-Imani et al. (2016) selecting those objects for which images in the  $u$ -band and the H- $\alpha$  line were available. Thus the sample in this chapter selects those galaxies with imaging at  $3.6 \mu\text{m}$  that had available optical imaging in the  $B$ -band (445 nm) and ultraviolet imaging in the  $u$ -band (355 nm) as found in the NASA/IPAC Extragalactic Database (NED; see Table 4.1 for  $B$ -band and  $u$ -band image sources). Twenty-eight (28) of these galaxies also have available ultraviolet imaging from archived *GALEX* data in the far-UV (FUV)  $1516 \text{ \AA}$  and 14 galaxies with narrow-band H- $\alpha$  imaging as indicated in Table 4.1.

Table 4.1. Spiral Galaxies and its Measured Pitch Angle at Different Wavelength of Light

Galaxy Name	Type	$P$ (3.6 Micron)	$P$ ( $B$ -band)	$P$ ( $u$ -band)	$P$ (8.0 Micron)	$P$ (H- $\alpha$ )	$P$ ( $FUV$ )	Image Source
(1)	(2)	(3)	(4)	(5)	(6)	(7)	(8)	(9)
NGC 0628	Sac	$9.58 \pm 0.60$	$9.20 \pm 0.83$	$19.76 \pm 2.08$	$20.60 \pm 2.28$	—	$21.43 \pm 1.42$	IRAC3.6, NOT4400, GALEX
NGC 0925	SABd	$4.45 \pm 0.65$	$7.51 \pm 3.81$	$52.90 \pm 8.10$	$20.10 \pm 4.69$	$25.16 \pm 3.40$	$29.68 \pm 3.75$	IRAC3.6, PAL4400, Palomar, KPNO2, GALEX
NGC 1097	SBb	$6.84 \pm 0.21$	$7.54 \pm 3.49$	$11.62 \pm 2.70$	$9.50 \pm 1.28$	$12.10 \pm 3.10$	$16.25 \pm 2.3$	IRAC3.6, LCO4400, duPont, 2MASS, GALEX
NGC 1566	SABbc	$15.29 \pm 2.37$	$31.20 \pm 4.80$	$35.50 \pm 1.30$	$44.13 \pm 11.94$	—	$45.80 \pm 2.97$	IRAC3.6, KPNO4400, duPont, GALEX
NGC 2403	SABc	$12.50 \pm 1.62$	$19.35 \pm 1.57$	$20.33 \pm 2.10$	$28.52 \pm 6.73$	$28.07 \pm 2.80$	$23.54 \pm 0.78$	IRAC3.6, LCO4400, 2MASS, Palomar, GALEX
NGC 2841	SAb	$16.13 \pm 1.63$	$18.77 \pm 1.66$	$18.68 \pm 3.40$	$22.25 \pm 2.42$	—	$23.26 \pm 2.31$	IRAC3.6, LOWE4500, Palomar, GALEX
NGC 2976	Sac	$4.14 \pm 0.34$	$5.13 \pm 0.43$	$9.80 \pm 1.30$	$8.36 \pm 0.40$	—	$10.68 \pm 1$	IRAC3.6, KPNO4400, SDSS
NGC 3031	SAab	$15.63 \pm 6.99$	$16.19 \pm 1.23$	$19.70 \pm 1.50$	$20.54 \pm 2.21$	—	$20.14 \pm 1.90$	IRAC3.6, JKY4034, GALEX
NGC 3184	SABcd	$11.92 \pm 1.77$	$18.30 \pm 3.45$	$11.27 \pm 4.50$	$23.40 \pm 3.27$	$23.45 \pm 1.90$	$26.75 \pm 0.55$	IRAC3.6, KPNO4400, NOT, 2MASS, GALEX
NGC 3190	SAap	$16.39 \pm 2.15$	$17.67 \pm 2.34$	$26.75 \pm 7.02$	$18.35 \pm 4.43$	—	—	IRAC3.6, CTIO4400, SWIFT
NGC 3198	SBc	$15.97 \pm 1.38$	$18.95 \pm 2.69$	$20.46 \pm 4.10$	$20.59 \pm 5.95$	—	$23.98 \pm 1.84$	IRAC3.6, CTIO4400, SDSS, GALEX
NGC 3351	SBb	$4.60 \pm 1.92$	$16.41 \pm 1.93$	$17.45 \pm 1.60$	$22.21 \pm 6.96$	$20.89 \pm 5.10$	$27.17 \pm 2.11$	IRAC3.6, CTIO4400, SDSS, KPNO2, GALEX
NGC 3521	SABbc	$16.74 \pm 1.32$	$19.28 \pm 1.92$	$21.8 \pm 1.90$	$21.48 \pm 2.19$	—	$24.81 \pm 2.04$	IRAC3.6, CTIO4400, SDSS, GALEX
NGC 3621	SAd	$17.22 \pm 3.37$	$18.43 \pm 3.12$	$21.30 \pm 2.98$	$20.81 \pm 2.72$	—	$20.34 \pm 1.98$	IRAC3.6, ESO4400, GALEX
NGC 3627	SABb	$11.71 \pm 0.78$	$16.97 \pm 1.54$	$53.10 \pm 4.20$	$18.59 \pm 2.85$	—	$40.29 \pm 1.60$	IRAC3.6, KPNO4400, SDSS, GALEX
NGC 3938	SAc	$11.46 \pm 2.32$	$12.22 \pm 1.94$	$23.50 \pm 2.59$	$19.34 \pm 3.80$	$23.39 \pm 3.30$	$21.45 \pm 1.87$	IRAC3.6, LOWE4500, 2MASS, GALEX
NGC 4254	SAc	$28.40 \pm 4.04$	$30.01 \pm 4.36$	$39.32 \pm 6.92$	$32.8 \pm 1.45$	$33.40 \pm 4.50$	$38.66 \pm 3.91$	IRAC3.6, INT4034, 2MASS, GALEX
NGC 4321	SABbc	$18.60 \pm 1.69$	$15.06 \pm 1.20$	$23.17 \pm 3.10$	$24.46 \pm 3.76$	$21.18 \pm 2.50$	$28.49 \pm 1.26$	IRAC3.6, KPNO4331, 2MASS, GALEX

Table 4.1 (cont'd)

Galaxy Name	Type	$P$ (3.6 Micron)	$P$ ( $B$ -band)	$P$ ( $u$ -band)	$P$ (8.0 Micron)	$P$ (H- $\alpha$ )	$P$ (FUV)	Image Source
(1)	(2)	(3)	(4)	(5)	(6)	(7)	(8)	(9)
NGC 4450	SAab	12.59 $\pm$ 2.63	16.62 $\pm$ 1.45	21 $\pm$ 2.00	21.2 $\pm$ 3.87	—	22.99 $\pm$ 5.43	IRAC3.6, LOWE4500, GALEX
NGC 4536	SABbc	17.3 $\pm$ 1.75	33.74 $\pm$ 4.8	52.30 $\pm$ 1.90	52.22 $\pm$ 2.42	52.37 $\pm$ 4.80	55.59 $\pm$ 2.75	IRAC3.6, KP4400, SDSS,KPNO2, GALEX
NGC 4569	SABab	8.64 $\pm$ 0.52	19.05 $\pm$ 2.42	22.21 $\pm$ 3.6	38.55 $\pm$ 6.44	—	42.11 $\pm$ 5.80	IRAC3.6, PAL4050, SDSS, GALEX
NGC 4579	SABb	11.44 $\pm$ 0.57	13.80 $\pm$ 3.25	14.30 $\pm$ 1.60	30.73 $\pm$ 4.73	32.74 $\pm$ 4.10	33.98 $\pm$ 3.69	IRAC3.6, KPNO400, SDSS,KPNO2, SWIFT
NGC 4725	SABab	3.04 $\pm$ 1.83	7.40 $\pm$ 0.35	9.49 $\pm$ 2.50	10.80 $\pm$ 1.04	15.59 $\pm$ 4.90	13.6 $\pm$ 1.92	IRAC3.6, KPNO400, SDSS,KPNO2, GALEX
NGC 4736	SAab	8.19 $\pm$ 2.94	8.41 $\pm$ 1.34	16.31 $\pm$ 1.29	14.09 $\pm$ 5.11	—	14.98 $\pm$ 2.31	IRAC3.6, PAL4400, GALEX
NGC 5055	SABc	16.35 $\pm$ 1.78	19.31 $\pm$ 1.63	19.10 $\pm$ 4.80	20.63 $\pm$ 2.11	21.22 $\pm$ 2.21	20.29 $\pm$ 5.87	IRAC3.6, PAL4360,2MASS, GALEX
NGC 5474	SACd	12.11 $\pm$ 1.15	13.84 $\pm$ 6.22	18.62 $\pm$ 6.57	19.12 $\pm$ 3.22	—	19.91 $\pm$ 2.65	IRAC3.6, JKY4034, GALEX
NGC 5713	SABb	12.20 $\pm$ 0.32	18.76 $\pm$ 3.10	20.81 $\pm$ 3.80	34.79 $\pm$ 5.01	30.37 $\pm$ 4.10	27.40 $\pm$ 1.20	IRAC3.6, CTIO4400,2MASS, GALEX
NGC 7331	Sab	17.13 $\pm$ 2.63	20.10 $\pm$ 1.85	19 $\pm$ 1.70	21.65 $\pm$ 2.15	—	22.54 $\pm$ 2.41	IRAC3.6, KPNO4400, GALEX
NGC 7793	SAd	10.98 $\pm$ 1.60	12.16 $\pm$ 2.10	14.47 $\pm$ 3.30	16.34 $\pm$ 5.47	17.80 $\pm$ 3.90	16.89 $\pm$ 1.87	IRAC3.6, ESO400, CTIO,2MASS, GALEX

Note. — Columns: (1) Galaxy name; (2) Hubble morphological type; (3) Pitch angle in degrees for 3.6  $\mu$ m; (4) Pitch angle in degrees for  $B$ -band 445 nm; (5) Pitch angle in degrees for  $u$ -band 355 nm; (6) Pitch angle in degrees for 8.0  $\mu$ m; (7) Pitch angle in degrees for H- $\alpha$  (8) Pitch angle in degrees for far ultraviolet (FUV) 151 nm; (9) Telescope/literature source of imaging.

## 4.4 Results

Spiral-arm pitch angles of my sample galaxies were measured in three or four wavelength bands (depends on availability) using the 2DFFT code (Davis et al., 2012). The  $B$ -band images are sensitive primarily to newly born stars that have emerged from their stellar nurseries. For the images at  $3.6 \mu\text{m}$  it is expected that older stars would contribute more, but we must also keep in mind that stellar evolution models suggest that newborn stars also produce a lot of red light. By contrast, the *GALEX* images at  $1516 \text{ \AA}$  are sensitive to the brightest O-type stars with the shortest lives, visible while still in the star-forming region. The  $u$ -band ( $355 \text{ nm}$ ), we might expect to lie somewhere between this and the  $B$ -band, that is to say, we may image stars that are short-lived, but still, have time to move some distance from where they are born. My results show that the pitch angles of 28 galaxies in the FUV( $1516 \text{ \AA}$ ) are bigger than the  $u$ -band ( $355 \text{ nm}$ ) image in most of the cases (which corresponds, as expected to looser arms). However, as can be seen from the adjoining histogram (Fig. 4.3 and 4.4), the typical difference in pitch angle is less than the average measurement error. Therefore we cannot clearly distinguish between these two wavelengths. Similarly, as seen in the second panel of Fig. 4.4, the pitch angles of 29 galaxies (the entire sample) in the  $u$ -band ( $355 \text{ nm}$ ) are larger than measured from the  $B$ -band ( $445 \text{ nm}$ ) image. Again the difference is typically less than the measurement error, so that, as one might expect, we cannot clearly distinguish between these two wavelengths. But note that we can clearly distinguish between FUV and  $B$ -band (include this figure from previous paper), as argued in Chapter 3 (Pour-Imani et al., 2016). It seems clear that if FUV is decisively different from  $B$ -band, but  $u$ -band is not clearly separated from either, than logically  $u$ -band tends to lie

between these two (See Fig. 4.6). This makes sense if we imagine that what we are seeing is progressively longer-lived stars moving downstream from where they were formed. Finally, the last panel shows that the  $3.6 \mu\text{m}$  and  $u$ -band images clearly disagree in pitch angle. The  $3.6 \mu\text{m}$  images have consistently tighter pitch angles, with the histogram showing that they typically differ by  $4^\circ$  or more. Again this seems to add weight to our argument that we are seeing a gradual decrease in pitch angle from blue to red, beginning with the FUV, then with  $u$ -band, then  $B$ -band and finally the NIR. But note that the bulk of the change takes place within the  $uv$ . Within the entirety of the optical and NIR there is no change in pitch angle greater (on average) than our typical measurement error. Figure 4.6 shows the evolution of pitch angle from FUV (151 nm) to  $3.6 \mu\text{m}$  for our samples.

#### 4.5 The Location of the Density-wave

A careful analysis of our pitch angle measurements at different wavelengths suggests an overall picture very compatible with density-wave theory, but with one or two aspects that require closer examination.

The concise summary of our results is that examination of “stellar light” (optical and near-infrared wavelengths) produces pitch angles that are consistently tighter than those produce by wavelengths associated with the star-forming region. The wavelengths of light associated with the star-forming region include 8.0 microns infrared light produced by warmed dust from clouds undergoing gravitational collapse, light emitted at the frequency of the  $\text{H}\alpha$  line produced by hot gas heated by proto-stars forming within the gas clouds and far-UV light at 151 nm emitted by very bright young stars. The rationale for this last assertion

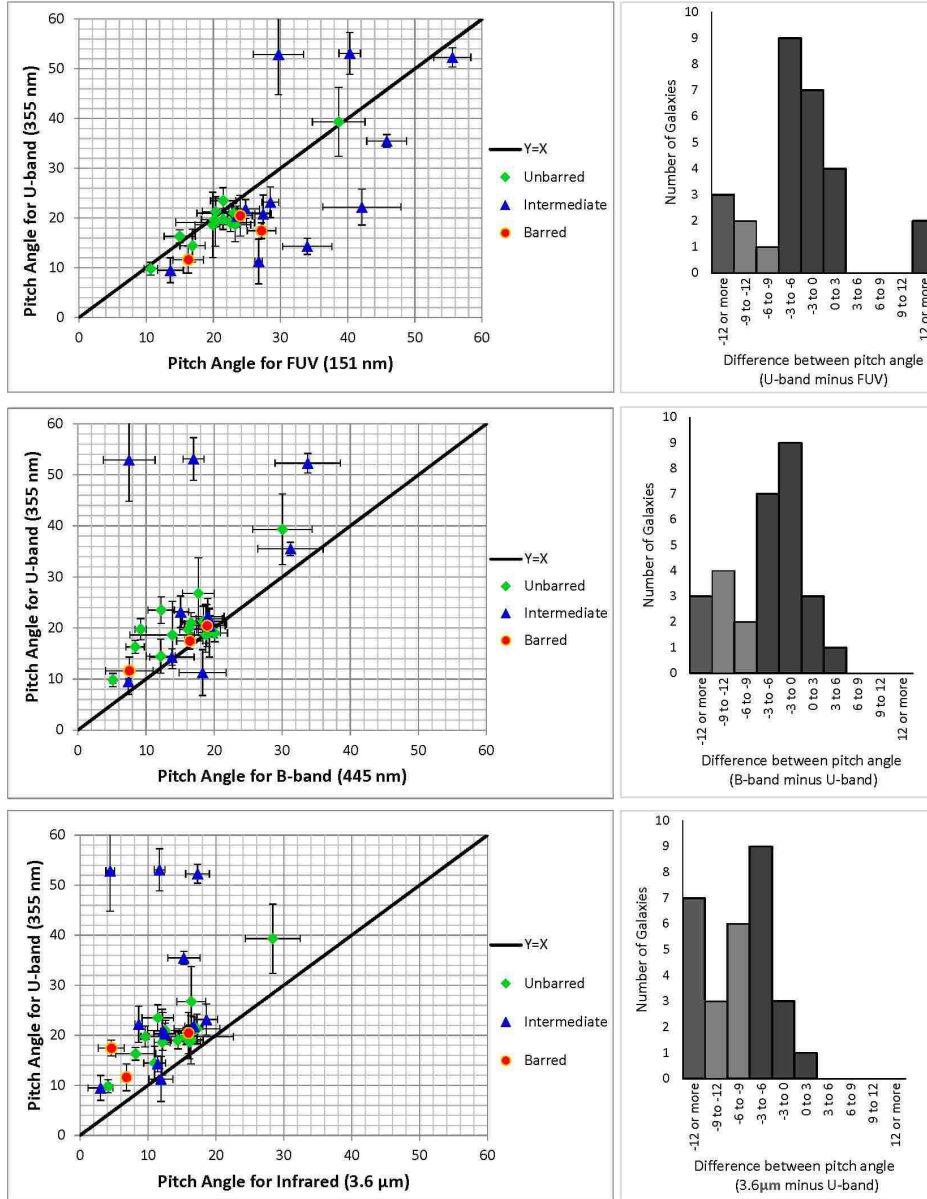


**Figure 4.4** Comparisons between pitch angles measured at different wavelengths. Each point on the plots represents an individual galaxy positioned according to the measurement of its spiral-arm pitch angle at two different wavelengths. The histograms show the distribution of pitch angle differences in terms of the number of galaxies found in each bin. The histograms for the top plot shows that the *u*-band and far ultraviolet (FUV) wavelengths are fundamentally equal since the greatest number of galaxies have pitch angles at these wavelengths that agree to better than  $3^\circ$ . The same is true for the second plot, comparing *B*-band with *u*-band images. In contrast, we can see that *u*-band pitch angles and  $3.6 \mu\text{m}$  pitch angles (bottom plot) are different from each other, since in both cases the greatest number of galaxies have a pitch angle difference of more than  $3^\circ$  (see the relevant histograms), with very few found below  $3^\circ$ . Images of 29 galaxies were used at 355 nm, 445 nm,  $3.6 \mu\text{m}$  and 28 of these also had images at FUV (151 nm).



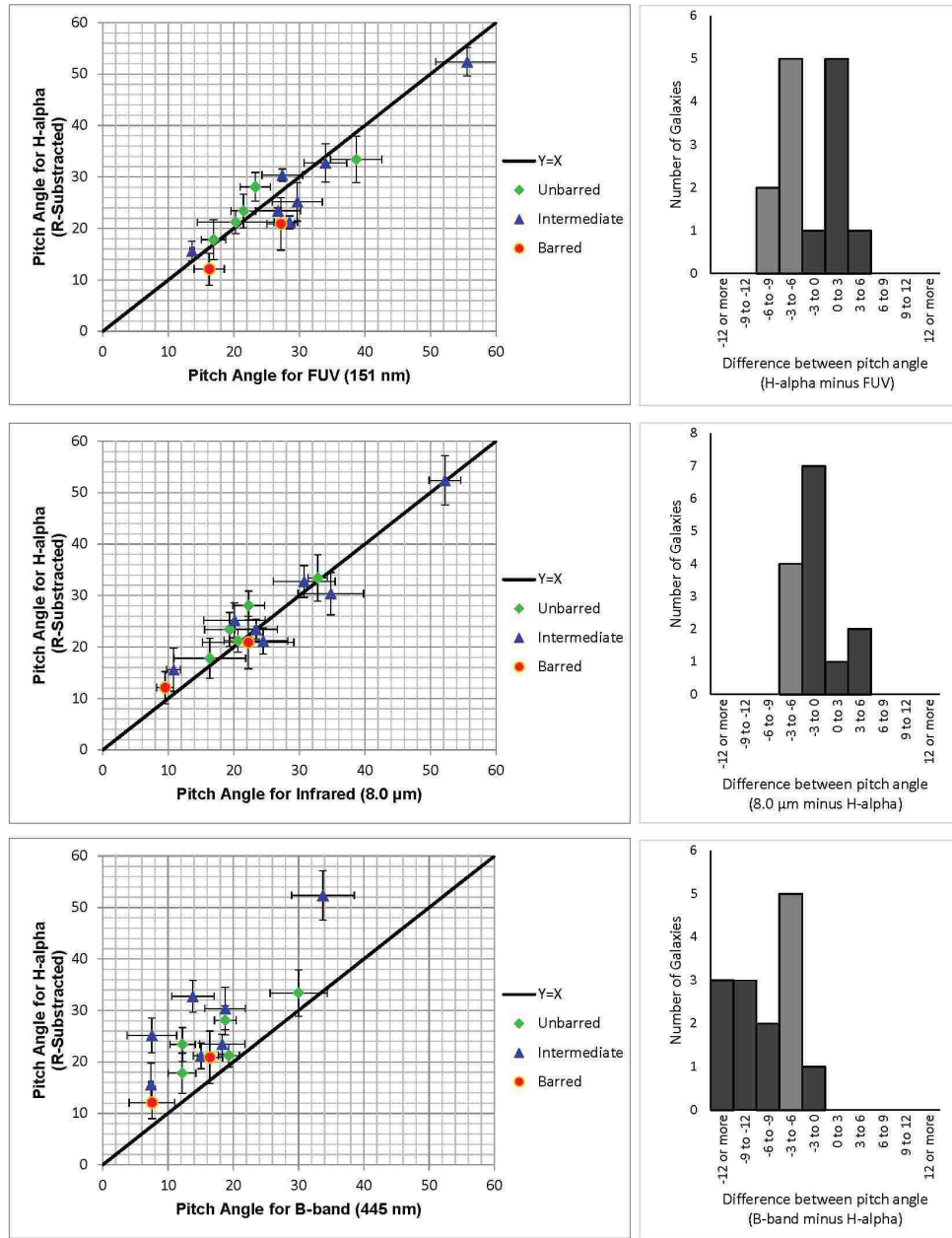


**Figure 4.5** Comparisons between pitch angles measured at different wavelengths. Each point on the plots represents an individual galaxy positioned according to the measurement of its spiral-arm pitch angle at two different wavelengths. The histograms show the distribution of pitch angle differences in terms of the number of galaxies found in each bin. The histograms for the top plot shows that the H- $\alpha$  and far ultraviolet (FUV) wavelengths are fundamentally equal since the greatest number of galaxies have pitch angles at these wavelengths that agree to better than  $3^\circ$ . The same is true for the second plot, comparing H- $\alpha$  with  $8.0 \mu\text{m}$  images. In contrast, we can see that H- $\alpha$  pitch angles and B-band pitch angles (bottom plot) are different from each other, since in both cases the greatest number of galaxies have a pitch angle difference of more than  $5^\circ$  (see the relevant histograms), with very few found below  $5^\circ$ . Images of 14 galaxies were used at H- $\alpha$ , 445 nm,  $8.0 \mu\text{m}$ .

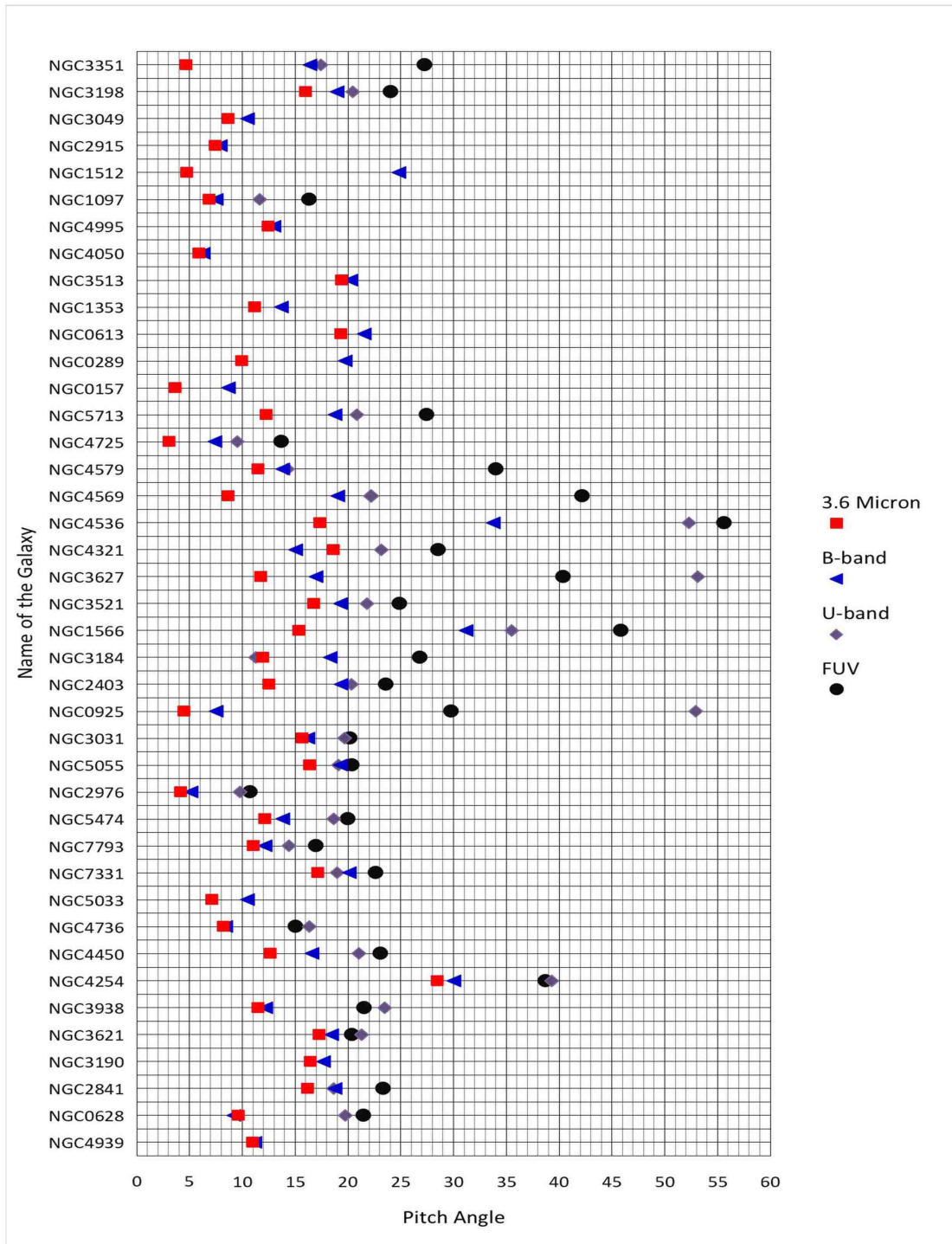


Figure 4.6 The Evolution of Pitch Angle from FUV (151 nm) to 3.6  $\mu\text{m}$

would be that the stars that emit most strongly in the far UV are sufficiently short-lived (O-type stars, for example) that they do not have time to move far from the star-forming region before they die. These stars simply form more quickly and live less long than other stars. Their great luminosity also increases the chance of their being seen while young, in spite of extinction. We see little in the way of measurable pitch angle differences within these two complexes. That is to say, the pitch angles measured in the FUV, H- $\alpha$  and 8.0 microns wavebands all seem to be more or less the same (see Figures 4.4, 4.5 and 4.6). Theoretically there is an evolutionary relationship between these wavebands, with the order running from 8.0 microns initially, then H- $\alpha$ , then FUV (tracking initially warmed dust, followed by clouds heated from within by young stars and proto-stars, ending with very bright newly formed O-type stars). However, the truth is that this process takes place in a very short space of time, at most a few million years for the most luminous stars, and one would not expect to see a measurable difference in pitch angle between these different wavebands. Meanwhile, whatever differences exist between pitch angles measured at different optical and near-infrared wavelengths (that is to say, the light produced by stars) they are small compared to the clear difference separating these optical pitch-angles from the pitch-angles measured in wavebands associated with the star-forming region. The fact that we see a looser pitch angle associated with the star-forming region and a tighter pitch angle associated with stars is entirely consistent with the stars being seen downstream of the star-forming region. The usual prediction of the density-wave theory is that star formation occurs close to the position of the density-wave (which compresses clouds of gas and sparks star-formation) and that new stars, which may take some time to form and emerge from the clouds of gas and dust characteris-

tic of the star-forming region, should be visible downstream of the density-wave. Inside the co-rotation radius downstream means ahead of the density-wave and outside the co-rotation radius means behind (see Fig. 4.1) so, in pitch-angle terms, downstream means a higher pitch angle. At all optical and near-infrared wavelengths, we measure a tighter pitch angle than we do for star-forming wavelengths. Therefore all our stellar light is “downstream” of the star-forming region. There are, however, two regions where density-wave theory predicts an enhancement of stellar light. One is the current position of the density-wave itself. At that location the density-wave may compress not only clouds of gas, but also the distances between stars so that the starlight from that region is brighter than from other parts of the disk. However, it has to be kept in mind that though the old disk population contains much of the stellar mass, it is not very bright, because of the predominance of M-type stars. It is actually by no means guaranteed that we can see the current position of the density-wave by looking in the near infrared red in search of the old disk stars. The principal way in which density-wave theory has always claimed that our eye picks out a the spiral pattern is via the appearance of new stars. Star formation takes place near the location of the density-wave and then, downstream of that position, we expect to see starlight enhanced by the turning on of young stars. We argue that this is true not only in the  $B$ -band but also into the NIR. Stellar evolution models certainly suggest that a great deal of red light is produced by young stars. Therefore the NIR light might also be best viewed downstream of the star-forming region. As mentioned previously, it is also quite plausible that the density-wave itself is downstream of the star-forming region, in which case the new stars and the wave itself are found in roughly the same spot.

To summarize, we argue that we are seeing a star-forming region close to (but very likely still upstream of) the density-wave. Still, within the star-forming region, we see those stars which live less than 10 million years. They cannot move far enough to be seen downstream of where they were born. Downstream from the star-forming region we see light from recently born stars visible in the near UV, optical and NIR. In a separate work (Abdeen et al, forthcoming) we use rotation-curve data to show that the typical time elapsed in moving from, say, the FUV spiral arm to the  $B$ -band spiral arm is on the order of 50 million years. This is certainly consistent with idea that we are seeing stars that were recently born since many bright blue stars can be expected to live on the order of 100 million years.

#### 4.6 Pitch Angle Differences Between Optical and NIR Wavelengths

Looking at the optical and near-infrared wavebands, we do see some evidence of a pitch angle difference from  $B$ -band to 3.6 microns in the NIR. In my sample there is a tendency for them to be clustered to one side of the line of pitch-angle equality, with the  $B$ -band pitch angles being slightly looser on average. However, the histogram in Fig. 4.4 shows that the differences measured between the pitch angles at these two wavelengths is typically less than the average measurement error. There is a conflict here with some other experimental results. One theoretical expectation is that 3.6 microns would be sensitive to old red disk stars and thus should see a spiral arm at the current position of the density-wave itself. In most scenarios, this would be the most upstream position and therefore the loosest pitch angle of all. Yet we find it to be perhaps the tightest of all. Some previous observers (Martinez-Garcia, 2012; Grosbol & Patsis, 1998) have indeed found NIR waveband

pitch angles to be looser than  $B$ -band, or other optical or  $u$ -band, pitch angles. We do not see this (see Fig. 4.3). While Grosbol & Patsis (1998) reported a significant increase in pitch angle in the  $K$ -band over the  $B$ -band, our results for the same galaxies show that the pitch angle is lower in the  $K$ -band than in the  $B$ -band. Notably, this difference is much smaller than the difference reported by Grosbol & Patsis (1998)(see Fig. 4.7). In order to get the best possible sense of how things stand, let us carefully examine all of the available observational evidence. Two previous papers have insisted that there is little or no variation in pitch angle across optical and NIR wavelengths (Davis et al., 2012; Seigar et al., 2006). We share the overall assessment of these papers in that we find that any difference between optical and NIR wavelengths is smaller than that of our typical measurement error. However, there is a statistically significant difference between all of these wavelengths and the ones associated with the star-forming region. As already stated, we do see a tendency towards the 3.6 microns (redder) waveband being tighter than the  $B$ -band. This differs from the work of Martinez-Garcia (2012), Martinez-Garcia et al. (2014), and Grosbol & Patsis (1998). However, we first of all draw attention to the fact that in one of these papers Martinez-Garcia (2012) the result is arguably compatible with the results of Davis et al. (2012) and Seigar et al. (2006). Most of the points in Fig.11 of that paper are actually close to the line of equality. Only a minority are noticeably distant from it. The same, obviously, is true of our data. So, looked at from a different point of view, most of the results to date are broadly compatible with the assertion that there is little variation of pitch angle across optical or NIR wavebands. Martinez-Garcia et al (2014) and Grosbol & Patsis do not agree with this, but their samples are small (only 5 galaxies each) and smaller still when one considers that

in both cases one or two of their galaxies do not follow the overall trend they report. So it is important to state that there is no conclusive evidence of a decisive trend in pitch angle between the optical and NIR wavebands. More work is clearly needed before a definite conclusion can be drawn. In Fig. 4.3, I have included on the same plot all the data from Martinez-Garcia (2012), Grosbol & Patsis (1998), Davis et al. (2012), Seigar et al. (2006) and Pour-Imani et al. (2016). Each of these give pitch angle measurements in the  $B$ -band and in some IR band (which one varies with the study). It seems to us that this combined plot is consistent with the conclusion that there is no significant difference between  $B$ -band and near-infrared wavelength pitch angle measurements.

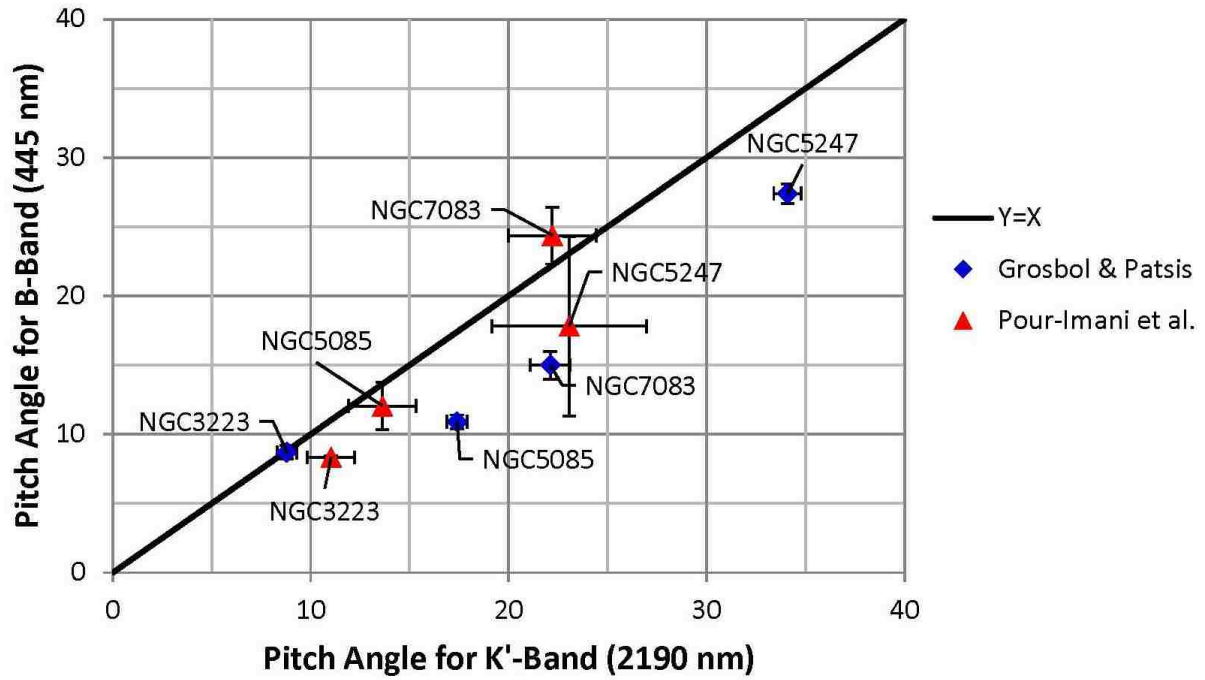


**Figure 4.7** Comparison between our results and Grosbol & Patsis (1998) for the same galaxies (NGC3223, 5085, 5247, 7083). The pitch angles measured at *B*-band (445 nm), *K*-band (2190 nm), *H*-band (1630 nm) and *J*-band (1220 nm).



How can this result be interpreted theoretically? A common expectation is that the reddest wavelengths, such as NIR, should show the current position of the density wave, since this is where the stars are bunched closer together by the action of the density-wave itself. Blue stars, however, being short-lived, are born in the star-formation region occasioned by the density-wave and are then observed downstream. But keep in mind that there is no proof that being downstream of the star-forming region means one is downstream of the density-wave. If star-formation kicks off upstream of the density-wave (as clouds become compressed upon approaching the wave) then the spiral arm of the new blue stars could be roughly in the same position as the density-wave.

Another point to consider is that some of the NIR light could be coming from red supergiants. Obviously the fact that redder light is seen in the vicinity of the blue light raises the possibility that one is seeing the same young stars, some of them have reached the end of their lives. James & Seigar (1999) have argued against this possibility but it could be a contributing factor to the red light being seen just slightly downstream of the blue light. An obvious question to ask is how long it takes for the newly formed stars to move from the star-forming spiral arm to the optical/NIR spiral arm? As mentioned above, in another publication (Abdeen et al, forthcoming) we have calculated this, using the same sample from this chapter and in Pour-Imani et al. (2016) and found it to be some tens of megayears. This is certainly consistent with the idea that the light coming from the optical/NIR spiral is made up of stars recently born in the star-forming region. It doesn't decide between the three scenarios just proposed, but it does provide an observation which the correct theory should be able to explain. To summarize, our conclusion is that we see the star-forming

region and, downstream of that light which is primarily produced by young stars recently born in that star-forming region. Since these stars are downstream of the star-forming region, they produce a more tightly wound spiral arm with a smaller pitch angle.

#### 4.7 Evidence From the $u$ -band

One way of investigating further is to examine the pitch angles in the  $u$ -band. This waveband falls between the  $B$ -band (which is part of the stellar complex) and the FUV (which is part of the star formation complex). It is hard to imagine a scenario in which the FUV emission is not due to newly born massive stars. If the  $B$ -band light is from stars born in the same burst of star formation, seen a little further downstream, then we might expect the  $u$ -band pitch angle to fall between these two values. I measured pitch angles for my sample in the  $u$ -band and the results are given in Fig. 4.4. We see that, predictably, the  $u$ -band pitch angle is not very different from either the FUV or the  $B$ -band. But it is arguably true that it tends to be a little tighter than the FUV pitch angle and a little looser than the  $B$ -band pitch angle. Since there is a clear difference between the FUV and  $B$ -band pitch angles (see the histogram in Fig. 4.4), the fact that  $u$ -band manages to be close to both, even though they are not close to each other, further suggests that  $u$ -band falls somewhere between them. But if this suggests that the  $B$ -band light is indeed coming largely from newborn stars, then what should believe about the 3.6 microns light? Elmegreens & Seiden (1989) argue that  $B$ -band and NIR spiral arms coincide and have a common origin, since their amplitudes are equal. Admittedly other observers have claimed that the amplitudes are not equal. Since we wish to point out the possibility that the light from new stars is

responsible for the spiral arm in the NIR as well as the optical let us discuss how this might be. Fig. 4.8 (Fig. 5 on p. 35 of Eufrazio (2015)) gives the spectrum of a cluster formed by a single burst of star formation at different stages of its evolution. The three relevant curves to note are the blue curve showing the spectrum of light from the cluster at age 10m yrs, the green curve for its spectrum at 100m yrs and the yellow curve for one at billion yrs. At any given position the luminosity at a given wavelength is essentially a sum of the new stars (10m yrs or less for the Star Formation pitch angle, and up to 100m yrs for the stellar pitch angle) plus the background of old disk stars (the 1 bn year line or more). At 151 nm (FUV) we see that there is a very high contribution from the new stars at 10m yrs and an essentially zero contribution from background stars. There is a sharp drop in the contribution from 100m yr old stars, so it is not surprising that at 151 nm we see the stars in the position of the Star Formation region. By the time 100m yr has passed the luminosity has greatly decreased. Note that the speed at which stars move out of the star-forming region is slow because it is the relative speed of the star to the pattern speed that counts, which is typically some 26 pc/Myrs. Looking at *u*-band, which is at 365 nm, we see that the gap from 10m yr to 100m yr is a little less, but actually only a little. The background contribution is more significant (1 bn yr line) but significantly down again. Certainly, this suggests that the *u*-band spiral arm might not be too dissimilar from the far-UV arm and this is what we see. Now looking at *B*-band (445 nm) we see that there is a noticeably smaller gap between the 10m yr and 100m yr curves, because of the bump in the 100m yr curve that falls between *u*-band and *B*-band. The wavelength difference between *u*-band and *B*-band is not great, but there is still a difference in the reduction from the 10m year curve to the 100m yr curve. Of course, it

is not a huge difference, not surprisingly given how close the two wavelengths are. Therefore one might also expect that there would not be a big difference between the  $u$ -band and  $B$ -band pitch angles and this is again what we see. Since  $u$ -band is close to both FUV and  $B$ -band, but these two are distinguishable from each other, this suggests that, on average,  $u$ -band pitch angles are a little tighter than the FUV but a little looser than the  $B$ -band, and this is indeed suggested by Fig. 4.4. Therefore we conclude that, as expected,  $u$ -band pitch angles do fall between the values for these other two wavelengths. Since  $B$ -band is part of the optical complex of pitch angles and FUV is part of the star-forming complex this suggests that it is in the  $u$ -band that we see a wavelength which falls between these two. One is tempted to see an evolution here (which would require further scrutiny and more data) from FUV to  $u$ -band to  $B$ -band to NIR with each step being a small decrease in pitch angle. Each step in this sequence is too small for the difference in pitch angle to be greater than our average measurement error (between two and three degrees for pitch angles in this sample), but a double step typically shows a large enough difference to be greater than our measurement errors (as shown by the histograms in Figs. 4.4 and 4.5. Thus there is a decisive difference between FUV and  $B$ -band and between  $u$ -band and 3.6 microns. This tends to strengthen our belief that what we are seeing is a looser pitch angle in the star-forming spiral arm, which is most likely close to where the density-wave lies, and then tighter and tighter pitch angles as one moves redward of the FUV.

Turning to the 3.6 microns images, the expectation has generally been that here one is sensitive primarily to the old red stellar population in the disk. These older disk stars have orbiting the galaxy more than once and no longer display any enhanced density

associated with clustering, because they have long since moved out of their original open clusters. However, when they pass through the density-wave they presumably are compressed somewhat closer together by it. However, as mentioned already, this isn't the only place where one expects to find a higher density of stars. Downstream of the star-forming region sparked by the density-wave, the old disk population is augmented by a population of young stars. Looking at Fig. 4.8, we see that this younger population does produce plenty of red light. So, in fact, it is not out of the question that the wake is visible in red light, through a combination of old red disk stars and younger stars. One explanation of our results is that we are seeing this wake created by newly formed stars in all of our optical and NIR wavelengths. In this context, it is worth noting that a few galaxies in Figure 4.4, all barred, have very large changes in pitch angle that are hard to reconcile with our scenario. These anomalies could be due to difficulties in measurement (pitch angles of these galaxies all have large error bars). Looking at Fig. 4.4, we see that our outliers are not greater than the outliers from other studies. Increasing the sample size may help in identifying the reason for these odd results.

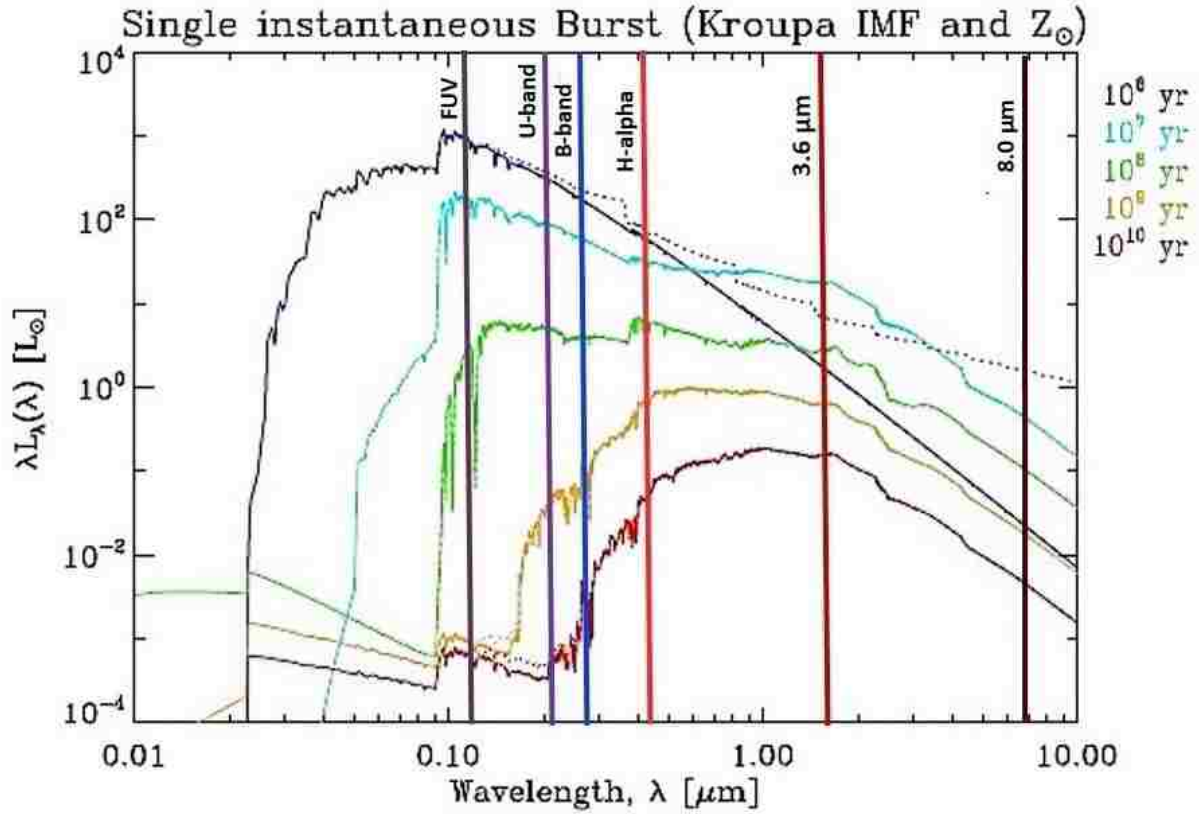


**Figure 4.8** Spectral evolution for a single burst of star formation, for a Kroupa IMF and Solar metallicity,  $Z=0.02$ . The total initial stellar mass is normalized to  $1M_{\odot}$ . Solid lines show photospheric emission from the stellar population. Spectra are color-coded, with respective ages shown in the upper-right corner. Models with nebular continuum emission are shown with the same color-coding. Only the youngest age shows significant difference due to its large ionizing photon rate. Figure by Eufrazio (2015).

## 4.8 Conclusion

I have presented clear evidence in favor of a prediction of the density-wave theory that there is a tighter pitch angle in the  $B$ -band than is found for wavelengths associated with the star-forming region. I have built upon the result in our earlier paper (Pour-Imani et al., 2016) by adding one more star-forming wavelength, the  $H-\alpha$ , which fits the pattern established by the 8.0 micron and FUV wavelengths from the earlier paper. I have also found that the  $u$ -band light seems to show pitch angles tending to fall between those of the star-forming region and the  $B$ -band, consistent with our standard interpretation of the density-wave theory. We, therefore, regard our results as strongly in favor of the density-wave theory. We additionally find evidence to support those earlier works which see only small differences in pitch angle between optical and NIR wavelengths. Broadly we see two different systems, a star-forming region visible in the 8.0 micron,  $H-\alpha$  and FUV and stellar light downstream visible in the  $B$ -band and the NIR. The  $u$ -band light, predictably, falls between these two systems. Thus we argue that we are seeing the star-forming region and then light from recently-born stars moving downstream from that position. This is consistent with the density-wave theory of spiral structure.

This research has made use of the NASA/IPAC Extragalactic Database, which is operated by the Jet Propulsion Laboratory, California Institute of Technology, under contract with the National Aeronautics and Space Administration.

## Bibliography

- Athanassoula, E., Romero-Gómez, M., Bosma, A. and Masdemont, J. J. 2010, MNRAS, 407, 1433-1448
- Abdeen, M.Shameer and Kennefick, D. and Kennefick, J. and Pour-Imani, H. and Shields, D. W. and Eufrazio, R. and Medina, J.B. and Monson, E. 2017, in Preparation
- Berlind, A. A. and Quillen, A. C. and Pogge, R. W. and Sellgren, K. 1997, AJ, 114, 107-114
- Bertin, G. & Lin, C. C. 1995, Spiral structure in galaxies a density-wave theory, The MIT Press
- Choi, Y. , Dalcanton, J. J. ,Williams, B. F. ,Weisz, D. R. ,Skillman, E. D. ,Fouesneau, M. and Dolphin, A. E 2015, ApJ, 810, 9
- Davis, B. L., Kennefick, D., Kennefick, J., Kyle, B. W., Shields, D. W. 2015, ApJ, 802, L13
- Davis, B. L., Berrier, J. C., Shields, D. W., Kennefick, J., Kennefick, D., Seigar, M. S., Lacy, C. H. S., & Puerari, I. 2012, ApJS, 199, 33
- Egusa, F. and Kohno, K. and Sofue, Y. and Nakanishi, H. and Komugi, S. 2009, ApJ, 697, 1870
- Elmegreen, B. G. and Seiden, P. E. and Elmegreen, D. M. 1989, ApJ, 343, 602
- Elmegreen, D. M., Elmegreen, B. G., Yau, Andrew, et al. 2011, ApJ, 737, 32
- Eufrazio, R. T. 2015, Ph.D. Thesis, The Catholic University of America
- Fazio, G. G., Hora, J. L., Allen, L. E., et al. 2004, ApJS, 154, 10
- Foyle, K. and Rix, H.-W. and Dobbs, C. L. and Leroy, A. K. and Walter, F. 2011, ApJ, 735, 101
- Gittins, D. M. and Clarke, C. J. 2004, MNRAS, 349, 909-921
- Goldreich, P. and Lynden-Bell, D. 1965, MNRAS, 130, 125
- Grosbol, P. J. & Patsis, P. A. 1998, A&A, 336, 840
- James, P. A. and Seigar, M. S. 1999, A&A, 350, 791
- Julian, W. H. and Toomre, A. 1966, ApJ, 146, 810
- Kendall, S. and Kennicutt, R. C. and Clarke, C. and Thornley, M. D. 2008, MNRAS, 387, 1007-1020



- Kennicutt, Jr., R. C. 1981, *AJ*, 86, 1847
- Kim, Y. and Kim, W.-T. 2013, *MNRAS*, 440, 208-224
- Lin, C. C. and Shu, F. H. 1964, *ApJ*, 140, 646
- Louie, M. and Koda, J. and Egusa, F. 2013, *ApJ*, 763, 94
- Martínez-García, E. E. 2012, *ApJ*, 744, 92
- Martínez-García, E. E. and Puerari, I. and Rosales-Ortega, F. F. and González-Lópezlira, R. A. and Fuentes-Carrera, I. and Luna, A. 2014, *ApJ*, 793, L19
- Martínez-García, E. E. and González-Lópezlira, R. A. 2015, *Highlights of Astronomy*, Vol 16, p323
- Pour-Imani, H. and Kenefick, D. and Kenefick, J. and Davis, B. L. and Shields, D. W. and Shameer Abdeen, M. 2016, *ApJ*, 827, L12
- Rix, H.-W. R. 1991, Ph.D. Thesis, Univ. Arizona
- Rix, H.-W. and Rieke, M. J. 1993, *ApJ*, 418, 123
- Roberts, W. W. 1969, *ApJ*, 158, 123
- Savchenko, S. S., and Reshetnikov, V. P. 2011, *AstL*, 37, 817
- Seigar, M. S., Bullock, J. S., Barth, A. J., & Ho, L. C. 2006, *ApJ*, 645, 1012
- Seigar, M. S., Kenefick, D., Kenefick, J., & Lacy, C. H. S. 2008, *ApJ*, 678, L93
- Sellwood, J. A. and Carlberg, R. G. 2011, *ApJ*, 785, 137
- Shields, D. W., Davis, B. L., Pour-Imani, Hamed., Kenefick, D., & Kenefick, J. 2015, arXiv:1511.06365
- Shu, Frank H. 2016, *Six Decades of Spiral Density-Wave Theory*, *Annual Review of Astronomy and Astrophysics*, Vol 54, Sep 2016
- Wright, G. S. and Casali, M. M. and Walther, D. M. and McLean, I. S. 1991, *Astronomical Society of the Pacific Conference Series*, Vol 14, p44
- Yuan, C. and Grosbol, P. 1981, *ApJ*, 243, 432

## Chapter 5

# The Connection Between Shear and Pitch Angle Variation in Different Wavelength

### 5.1 Abstract

Grand et al. (2013) first showed that, there is a correlation between shear rate and spiral arm pitch angle. They found that higher shear rates correlate to more tightly wound spiral arms (smaller pitch angle). An implication of the density-wave theory is that higher shear rate should cause a bigger difference between pitch angles at different wavelengths. In this chapter, we present a sample of 41 galaxies for which we have calculated the pitch angle variations for different wavelengths of light. We show that for barred galaxies, a correlation exists between the shear rate, lower pitch angle and pitch angle variation. For example, when we compare the pitch angle difference between *B*-band and  $8.0 \mu\text{m}$ , there is a greater difference for lower pitch angle (higher shear rate).

### 5.2 Introduction

The density-wave theory of spiral structure in disk galaxies was proposed in the mid-1960s by C.C. Lin and Frank Shu (Lin & Shu, 1964; Bertin & Lin, 1996; Shu, 2016). Their theory envisaged long-lived quasi-stationary density waves (also called heavy sound), which impose a semi-permanent spiral pattern on the face of the galactic disk. This theory makes a striking prediction that the pitch angle of spiral arms should vary at different wavelengths

of light (Chapter 3). The spiral arm is a pattern which rotates rigidly, while the physical components of the galactic disk (including stars and gas clouds) rotate differentially. The spiral arms predicted by this theory, and those actually observed in disk galaxies, are approximately logarithmic spirals. Logarithmic spirals are characterized by a constant pitch angle that has been proposed as a quantifiable feature suitable for theory testing between different explanations for galactic spiral structure (Athanasoula et al., 2010; Martinez-Garcia, 2012; Davis et al., 2015). A disk galaxy’s rotation curve (also called velocity curve) presents a relation between orbital speeds of visible stars or gas in the galaxy and their radial distance from the center of the galaxy. The shear rate,  $S$ , is a dimensionless quantity and is derived from the galaxy’s rotation curve as follows:

$$S = \frac{A}{\omega} = \frac{1}{2} \left( 1 - \frac{R}{V} \frac{dV}{dR} \right) \quad (5.1)$$

Where  $A$  is the first Oort constant,  $\omega$  is the angular velocity and  $V$  is the measured line-of-sight velocity at a radius  $R$ . The value  $A\omega$  is the shear rate  $S$ . The shear rate depends upon the shape of the rotation curve. For flat rotation curve we have  $S=0.5$ ; for a continually rising rotation curve we have  $S < 0.5$ , and for a falling rotation curve,  $S > 0.5$ . The density-wave theory predicts that the pitch angle of galactic spiral arms should vary with the wavelength in which the spiral pattern is observed (Chapter 3). An implication of the density-wave theory is that higher shear rate should cause a bigger difference between pitch angles for different wavelengths. This is an excellent opportunity for theory testing and checks the correlation between pitch angle variation in different wavelength and shear rate. We make use of *Spitzer* images of galaxies taken at 8.0 and 3.6  $\mu\text{m}$ . At 8.0  $\mu\text{m}$ , which

images warmed dust in clouds where star formation is occurring, we are capable of seeing the region of star formation in the gaseous spiral arm.  $3.6 \mu\text{m}$  and  $B$ -band images are sensitive to starlight. It is clear that the  $B$ -band images are showing young stars that have recently left the gaseous arm where they were formed and  $3.6 \mu\text{m}$  images are showing old stars.

### 5.3 Shear Rate, Mass Distribution, and Pitch Angle

As the mass distribution in a disk galaxy can affect the shape of the rotation curve, the shear rate at any given position depends on the mass distribution within that radius and the concentration of the mass at the center of the galaxy. So the spiral arm pitch angle depends on the central mass concentration as the expectations of the density-wave theory model for spiral galaxies (Bertin & Lin, 1996). The correlation between spiral arm pitch angle and rotation curve shear rate found by Seigar et al. (2006), suggested that there is a link between the spiral arm pitch angle and the central mass concentration in spiral galaxies. In Figure 5.1, Seigar et al. (2006) show that a correlation exists between shear rate and spiral arm pitch angle, no matter what waveband the pitch angle is measured in. Their correlation shows galaxies with higher shear rate present a larger central mass concentration and smaller pitch angle that means more tightly wound arms and they derive the following expression relating these terms

$$P = (64.25 \pm 2.87) - (73.24 \pm 5.53)S \quad (5.2)$$

Where  $P$  is the pitch angle in degrees and  $S$  is the shear rate. Their data and galaxy's name are listed in Table 5.1.

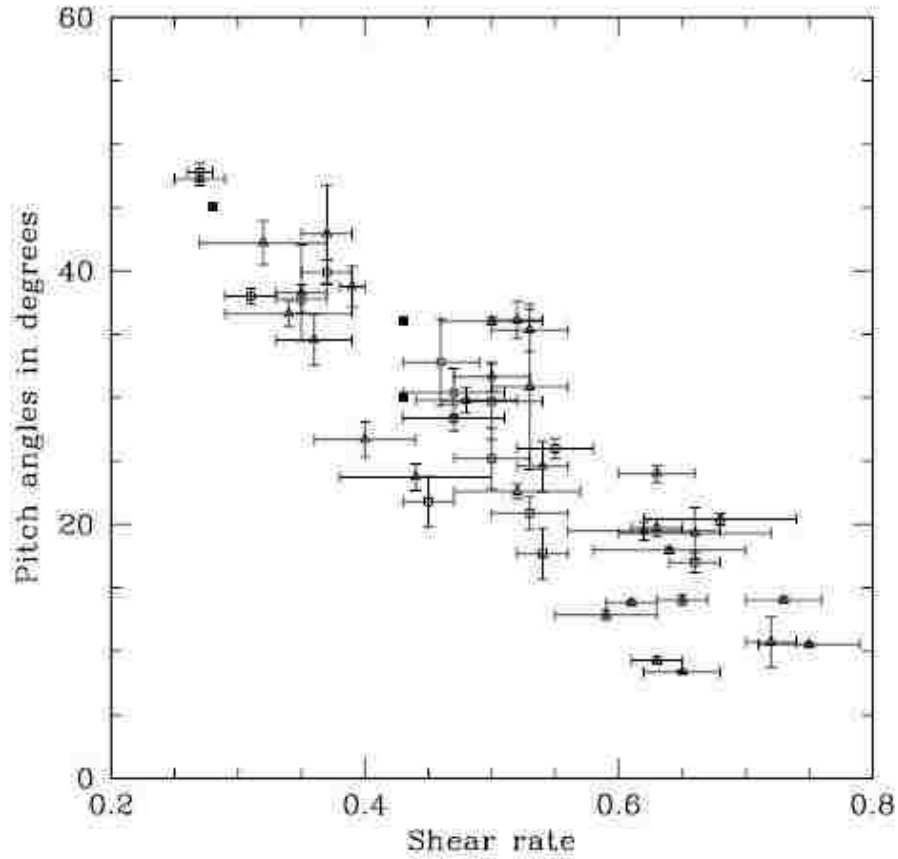


**Figure 5.1** Spiral arm pitch angle versus rotation curve shear rate, showing a strong correlation. The solid squares present the galaxies with data measured by Block et al. (1999), the open squares are galaxies from Seigar (2005) and the open triangles represent the data from Seigar et al. (2006).

Table 5.1. Pitch Angle and Shear Rate For 31 Spiral Galaxies, Reported by Seigar et al.  
(2006)

Galaxy Name	Type	Pitch Angle (degrees)	Shear Rate
(1)	(2)	(3)	(4)
ESO 9-G10	SAC	$23.7 \pm 1.1$	$0.44 \pm 0.06$
ESO 121-G26	SBc	$10.5 \pm 0.2$	$0.75 \pm 0.04$
ESO 582-G12	SAC	$22.6 \pm 0.6$	$0.52 \pm 0.05$
IC 2522	SACd	$38.8 \pm 1.6$	$0.39 \pm 0.01$
IC 2537	SABc	$9.3 \pm 0.3$	$0.63 \pm 0.02$
IC 3253	SAC	$24.6 \pm 2.0$	$0.36 \pm 0.03$
IC 4538	SABc	$38.3 \pm 3.8$	$0.35 \pm 0.02$
IC 4808	SAC	$14.1 \pm 0.4$	$0.65 \pm 0.02$
NGC 150	SBbc	$8.4 \pm 0.1$	$0.65 \pm 0.03$
NGC 151	SBbc	$36.1 \pm 1.5$	$0.52 \pm 0.02$
NGC 578	SABc	$18.0 \pm 0.2$	$0.64 \pm 0.06$
NGC 908	SAC	$12.9 \pm 0.4$	$0.59 \pm 0.04$
NGC 1232	SABc	$19.3 \pm 0.2$	$0.66 \pm 0.06$
NGC 1292	SAC	$29.8 \pm 1.0$	$0.48 \pm 0.04$
NGC 1300	SBbc	$31.7 \pm 1.1$	$0.50 \pm 0.03$
NGC 1353	SAbc	$36.6 \pm 1.0$	$0.34 \pm 0.05$
NGC 1365	SBb	$35.4 \pm 1.7$	$0.53 \pm 0.03$
NGC 1559	SBcd	$20.4 \pm 0.4$	$0.68 \pm 0.06$
NGC 1566	SABbc	$36.0 \pm 0.3$	$0.50 \pm 0.04$
NGC 1964	SABb	$13.8 \pm 0.2$	$0.61 \pm 0.02$
NGC 2280	SACd	$24.2 \pm 1.7$	$0.32 \pm 0.05$
NGC 2417	SABbc	$24.0 \pm 0.7$	$0.63 \pm 0.03$
NGC 2835	SABbc	$19.5 \pm 0.7$	$0.62 \pm 0.06$
NGC 2935	SABb	$14.1 \pm 0.2$	$0.73 \pm 0.03$
NGC 3052	SABc	$19.8 \pm 0.7$	$0.63 \pm 0.02$
NGC 3054	SABbc	$42.9 \pm 3.9$	$0.37 \pm 0.02$

Table 5.1 (cont'd)

Galaxy Name	Type	Pitch Angle (degrees)	Shear Rate
(1)	(2)	(3)	(4)
NGC 3223	SAbc	$10.7 \pm 0.2$	$0.72 \pm 0.02$
NGC 3318	SABb	$36.9 \pm 6.5$	$0.53 \pm 0.03$
NGC 5967	SABc	$47.3 \pm 0.5$	$0.27 \pm 0.02$
NGC 7083	SABc	$26.7 \pm 1.4$	$0.40 \pm 0.04$
NGC 7392	SBab	$24.6 \pm 2.0$	$0.54 \pm 0.02$

Note. — *Columns:* (1) Galaxy name; (2) Hubble morphological type; (3) Pitch angle in degrees; (4) Shear rate.

Grand et al. (2013) found this correlation in N-body simulations by calculating and comparing pitch angle of both individual density-waves and overall spiral structure in a suite of N-body simulations. They found the higher shear rates produce more tightly wound spiral arms (smaller pitch angle).

#### 5.4 Data

Our sample of 41 galaxies is drawn from the Spitzer Infrared Nearby Galaxies Survey, which consists of imaging from the Infrared Array Camera Fazio et al. (2004), selecting those galaxies with imaging at both 3.6 and 8.0  $\mu\text{m}$  and that had available optical imaging in the *B*-band (445 nm) as found in the NASA/IPAC Extragalactic Database.

Table 5.2. Pitch Angle's Variation for  $B$ -band, 3.6 and 8.0  $\mu\text{m}$

Galaxy Name	Type	P (3.6 $\mu\text{m}$ )	P ( $B$ -band)	P (8.0 $\mu\text{m}$ )	$\Delta$ (3.6, 8.0 $\mu\text{m}$ )	$\Delta$ ( $B$ -band, 8.0 $\mu\text{m}$ )
(1)	(2)	(3)	(4)	(5)	(6)	(7)
NGC 0157	SABb	$3.58 \pm 0.13$	$8.66 \pm 0.89$	$9.32 \pm 1.01$	5.74	0.66
NGC 0289	SBbc	$9.89 \pm 1.20$	$19.71 \pm 1.94$	$23.36 \pm 2.61$	13.47	3.65
NGC 0613	SBbc	$19.27 \pm 2.22$	$21.57 \pm 1.76$	$25.67 \pm 2.30$	6.40	4.10
NGC 0628	Sac	$9.58 \pm 0.60$	$9.20 \pm 0.83$	$20.60 \pm 2.28$	11.02	11.40
NGC 0925	SABd	$4.45 \pm 0.65$	$7.51 \pm 3.81$	$20.10 \pm 4.69$	15.65	12.59
NGC 1097	SBb	$6.84 \pm 0.21$	$7.54 \pm 3.49$	$9.50 \pm 1.28$	2.66	0.66
NGC 1353	SBb	$11.14 \pm 0.70$	$13.68 \pm 2.31$	$17.96 \pm 1.66$	6.82	4.28
NGC 1512	SBab	$4.70 \pm 2.24$	$24.80 \pm 3.43$	$30.20 \pm 4.64$	25.50	5.40
NGC 1566	SABbc	$15.29 \pm 2.37$	$31.20 \pm 4.80$	$44.13 \pm 11.94$	28.84	12.93
NGC 2403	SABc	$12.50 \pm 1.62$	$19.35 \pm 1.57$	$28.52 \pm 6.73$	16.02	9.17
NGC 2841	SAb	$16.13 \pm 1.63$	$18.77 \pm 1.66$	$22.25 \pm 2.42$	6.12	3.48
NGC 2915	SBab	$7.42 \pm 0.44$	$7.90 \pm 0.75$	$10.40 \pm 2.08$	2.98	2.90
NGC 2976	Sac	$4.14 \pm 0.34$	$5.13 \pm 0.43$	$8.36 \pm 0.40$	4.22	3.23
NGC 3031	SAab	$15.63 \pm 6.99$	$16.19 \pm 1.23$	$20.54 \pm 2.21$	4.91	4.35
NGC 3049	SBab	$8.60 \pm 0.46$	$10.50 \pm 2.05$	$16.10 \pm 2.59$	7.50	5.60
NGC 3184	SABcd	$11.92 \pm 1.77$	$18.30 \pm 3.45$	$23.40 \pm 3.27$	11.48	5.10
NGC 3190	SAap	$16.39 \pm 2.15$	$17.67 \pm 2.34$	$18.35 \pm 4.43$	1.96	0.68
NGC 3198	SBc	$15.97 \pm 1.38$	$18.95 \pm 2.69$	$20.59 \pm 5.95$	4.62	1.64
NGC 3351	SBb	$4.60 \pm 1.92$	$16.41 \pm 1.93$	$22.21 \pm 6.96$	17.61	5.80
NGC 3513	SBc	$19.35 \pm 2.85$	$20.27 \pm 1.67$	$22.20 \pm 2.29$	2.85	1.93
NGC 3521	SABbc	$16.74 \pm 1.32$	$19.28 \pm 1.92$	$21.48 \pm 2.19$	4.74	2.20
NGC 3621	SAd	$17.22 \pm 3.37$	$18.43 \pm 3.12$	$20.81 \pm 2.72$	3.59	2.38
NGC 3627	SABb	$11.71 \pm 0.78$	$16.97 \pm 1.54$	$18.59 \pm 2.85$	6.88	1.62
NGC 3938	SAc	$11.46 \pm 2.32$	$12.22 \pm 1.94$	$19.34 \pm 3.80$	7.88	7.12
NGC 4050	SBab	$5.82 \pm 0.51$	$6.32 \pm 1.89$	$9.00 \pm 1.01$	3.18	2.68
NGC 4254	SAc	$28.40 \pm 4.04$	$30.01 \pm 4.36$	$32.8 \pm 1.45$	4.40	2.91



Table 5.2 (cont'd)

Galaxy Name	Type	P (3.6 $\mu\text{m}$ )	P ( $B$ -band)	P (8.0 $\mu\text{m}$ )	$\Delta$ (3.6, 8.0 $\mu\text{m}$ )	$\Delta$ ( $B$ -band, 8.0 $\mu\text{m}$ )
(1)	(2)	(3)	(4)	(5)	(6)	(7)
NGC 4321	SABbc	$18.60 \pm 1.69$	$15.06 \pm 1.20$	$24.46 \pm 3.76$	5.86	9.40
NGC 4450	SAab	$12.59 \pm 2.63$	$16.62 \pm 1.45$	$21.2 \pm 3.87$	3.18	4.58
NGC 4536	SABbc	$17.3 \pm 1.75$	$33.74 \pm 4.8$	$52.22 \pm 2.42$	34.92	18.48
NGC 4569	SABab	$8.64 \pm 0.52$	$19.05 \pm 2.42$	$38.55 \pm 6.44$	29.91	19.50
NGC 4579	SABb	$11.44 \pm 0.57$	$13.8 \pm 3.25$	$30.73 \pm 4.73$	19.29	16.93
NGC 4725	SABab	$3.04 \pm 1.83$	$7.40 \pm 0.35$	$10.80 \pm 1.04$	7.76	3.40
NGC 4736	SAab	$8.19 \pm 2.94$	$8.41 \pm 1.34$	$14.09 \pm 5.11$	5.90	5.68
NGC 4939	SAbc	$10.93 \pm 3.60$	$11.20 \pm 1.07$	$16.25 \pm 4.94$	5.32	5.05
NGC 4995	SABb	$12.40 \pm 4.36$	$13.00 \pm 2.87$	$15.90 \pm 3.66$	3.50	2.90
NGC 5033	SAc	$7.09 \pm 0.46$	$10.46 \pm 2.66$	$13.91 \pm 4.42$	6.82	3.45
NGC 5055	SAbc	$16.35 \pm 1.78$	$19.31 \pm 1.63$	$20.63 \pm 2.11$	4.28	1.32
NGC 5474	SACd	$12.11 \pm 1.15$	$13.84 \pm 6.22$	$19.12 \pm 3.22$	7.10	5.28
NGC 5713	SABb	$12.20 \pm 0.32$	$18.76 \pm 3.10$	$34.79 \pm 5.01$	22.59	16.03
NGC 7331	Sab	$17.13 \pm 2.63$	$20.10 \pm 1.85$	$21.65 \pm 2.15$	4.52	1.55
NGC 7793	SAd	$10.98 \pm 1.6$	$12.16 \pm 2.1$	$16.34 \pm 5.47$	5.36	4.18

Note. — *Columns:* (1) Galaxy name; (2) Hubble morphological type; (3) Pitch angle in degrees for infrared 3.6  $\mu\text{m}$ ; (4) Pitch angle in degrees for  $B$ -band 445 nm; (5) Pitch angle in degrees for infrared 8.0  $\mu\text{m}$ ; (6) Pitch angle difference between 3.6 and 8.0  $\mu\text{m}$ ; (7) Pitch angle difference between  $B$ -band and 8.0  $\mu\text{m}$ ;

## 5.5 Shear rate and pitch angle variation for $B$ -band, 3.6 and 8.0 $\mu\text{m}$

### 5.5.1 Unbarred, Intermediate, and Barred Galaxies

The  $B$ -band images are sensitive primarily to newly born stars that have emerged from their stellar nurseries. By contrast, at 8.0 $\mu\text{m}$ , we can see details of gas and dust in spiral arms (Elmegreen et al., 2011), as this wave-band is sensitive to dust warmed by nearby

star formation. For the shear rate,  $S > 0.5$ , stars at the edge of a galaxy move slower than stars at the co-rotation radius. For  $S = 0.5$ , stars at the edge of a galaxy move at the same rate as stars at the co-rotation radius. So, when we compare the difference between  $B$ -band and  $8.0 \mu\text{m}$  pitch angle, we should see more difference in lower pitch (higher shear rate). Figure 5.2, shows the difference between pitch angle for  $B$ -band and  $8.0 \mu\text{m}$  versus  $B$ -band pitch angle and Figure 5.3, shows the difference between pitch angle for  $3.6$  and  $8.0 \mu\text{m}$  versus  $3.6 \mu\text{m}$  pitch angle for 41 NGC galaxies. These figures show there is no a specific correlation when we consider all type of galaxies (Unbarred, Intermediate, and Barred). For barred and intermediate galaxies, by the presence a bar, the pitch angle variation for different wavelength is higher than the unbarred case (Figures 3.2 & 3.3).

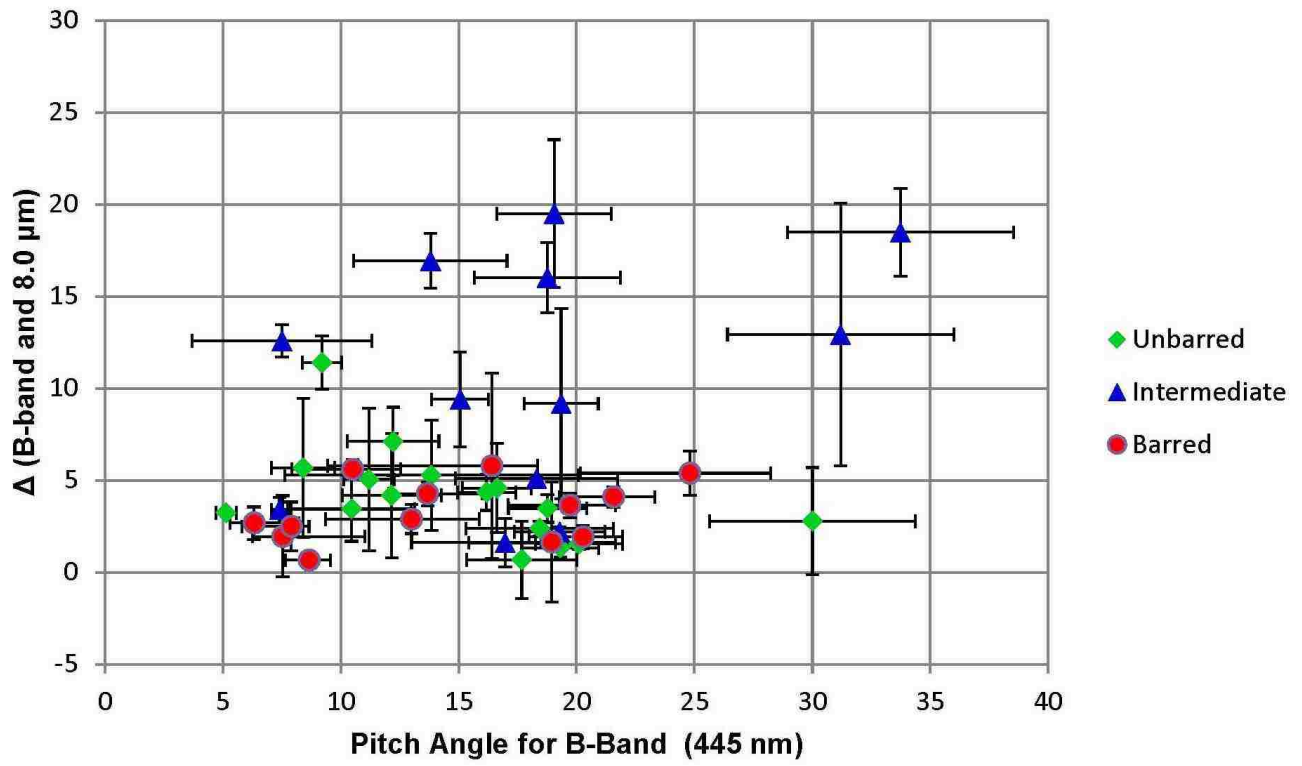


Figure 5.2 Pitch angle variation, *B*-band versus difference between *B*-band and 8.0 $\mu\text{m}$

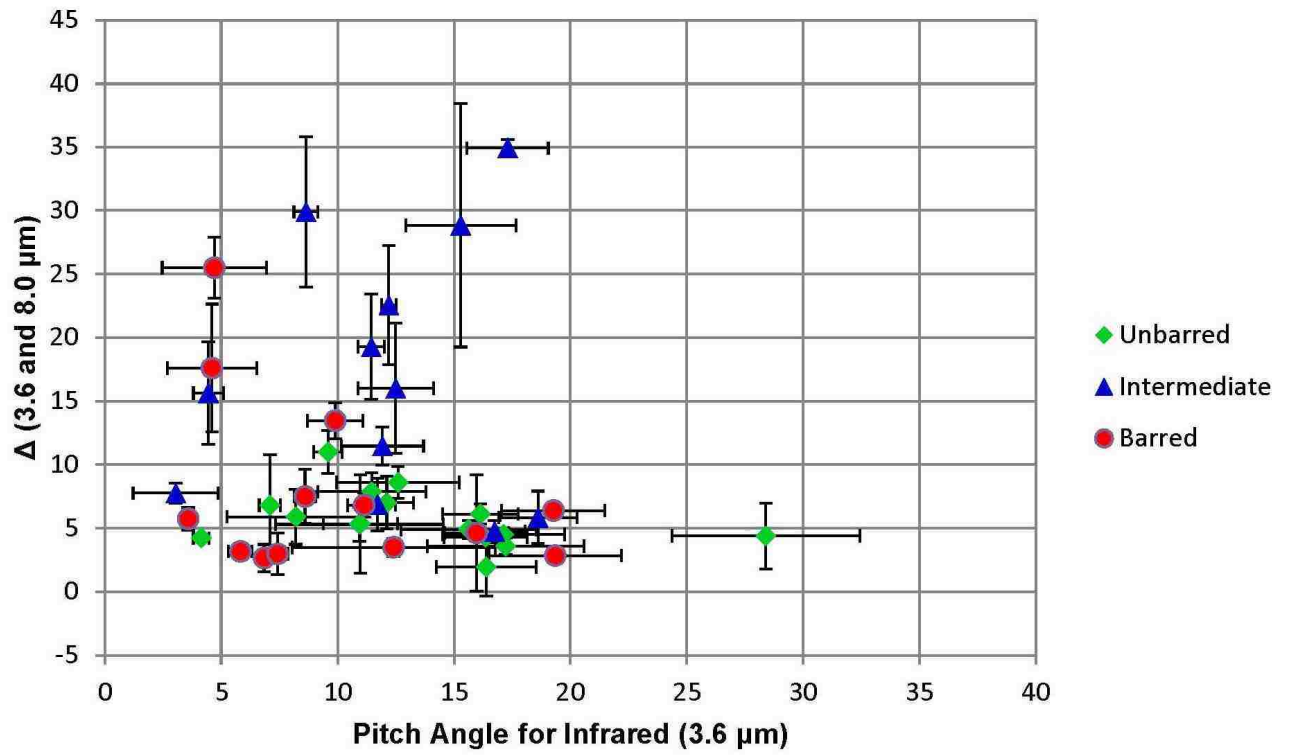
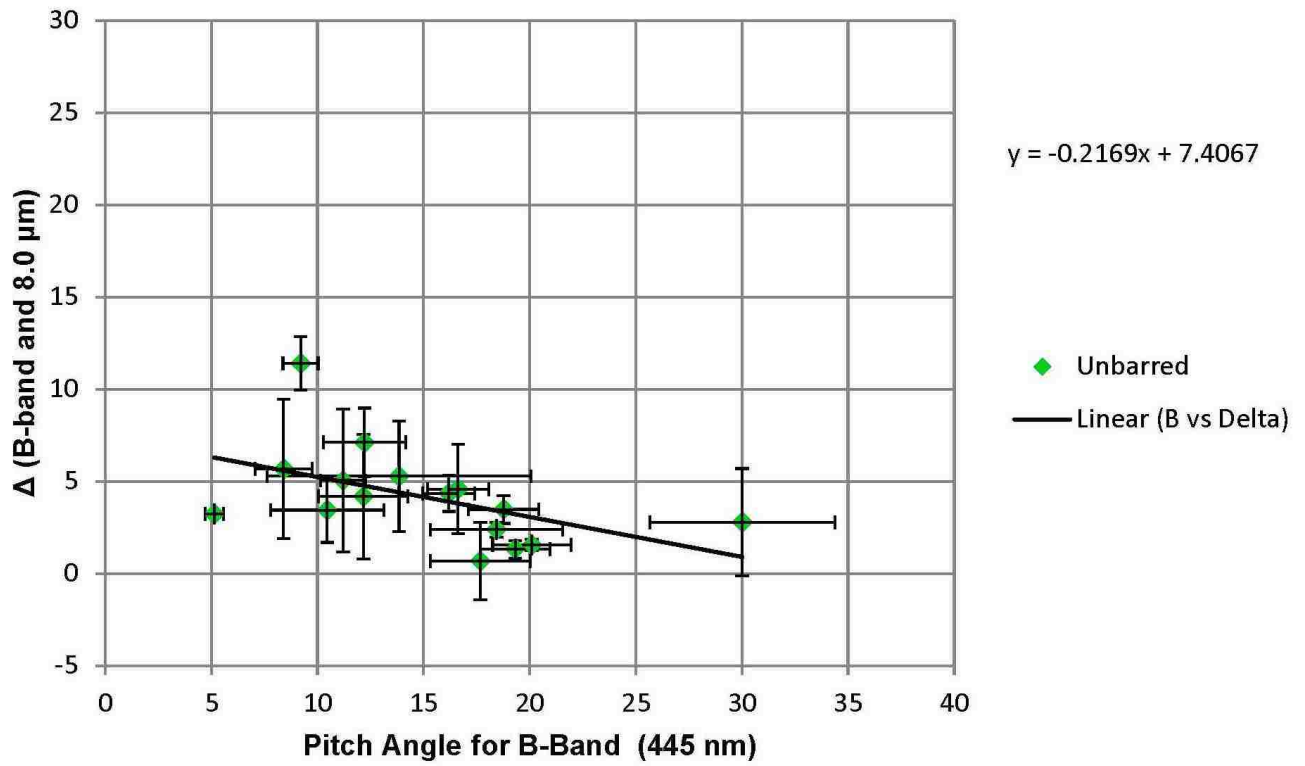


Figure 5.3 Pitch angle variation, 3.6μm versus difference between 3.6μm and 8.0μm

By the presence of a bar, its torque can affect the spiral arms pitch angle and we expect more variation by the presence of a bar at the center of a galaxy. In this context, it is worth noting that a few galaxies in Figures 5.2 & 5.3, all barred, have very large changes in pitch angle. As noted by Elmegreen et al. (2011), their results indicate that the presence of bars or ovals increases the amplitudes of the arms. These anomalies could be due to difficulties in measurement (pitch angles of these galaxies all have large error bars).

### 5.5.2 Unbarred Galaxies

When we consider the unbarred galaxies, results for 16 NGC galaxies show a good correlation between pitch angle, shear rate and pitch angle variation for different wavelength (Figures 5.4 & 5.5). Lower pitch angle (higher shear rate) has bigger pitch angle difference in different wavelength in agreement with a prediction of the density-wave theory and results by Seigar et al. (2006) and Grand et al. (2013).



**Figure 5.4** Pitch angle variation for unbarred galaxies, *B*-band versus difference between *B*-band and 8.0μm

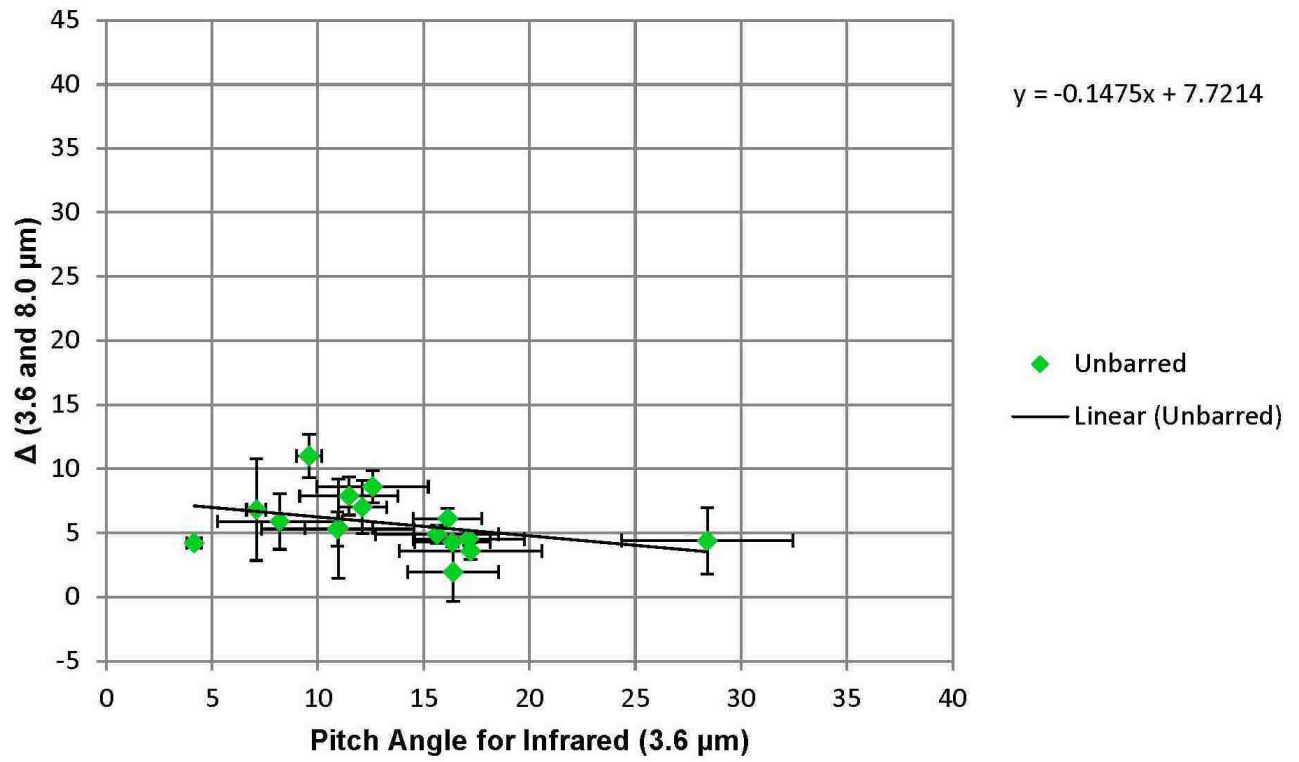


**Figure 5.5** Pitch angle variation for unbarred galaxies,  $3.6\mu\text{m}$  versus difference between  $3.6\mu\text{m}$  and  $8.0\mu\text{m}$

## 5.6 Conclusion

For the first time, to our knowledge, we have analyzed the pitch angle variations at different wavelengths of light and its correlation with shear rate. Amongst the mechanisms that form the spiral arms, a central bar and its structure is an important factor to study the pitch angles. We believe that the correlation in Figures 5.4 & 5.5 is a useful diagnostic tool for study the presence of a bar and its effect on forming the spiral arms. Figures 5.2 & 5.3 show that by considering all unbarred, intermediate and barred galaxies, there is no obvious correlation between pitch angles at different wavelengths, shear rate and morphological type of galaxies. But, when we consider unbarred galaxies, a good correlation exists (Figures 5.4 & 5.5). That means the presence of a bar at the center of galaxies could affect on pitch angle formation at different wavelengths. We are working to study this issue and understand how galaxy morphological classification (Table 1.1) can affect on spiral arm patterns, its pitch angle and galaxy's shear rate. Initial studies in this chapter show a correlation does exist.



## Bibliography

- Athanassoula, E., Romero-Gómez, M., Bosma, A. and Masdemont, J. J. 2010, MNRAS, 407, 1433-1448
- Bertin, G. & Lin, C. C. 1995, Spiral structure in galaxies a density wave theory, The MIT Press
- Block, D. L. and Puerari, I. 1999, A&A, 342, 627
- Choi, Y. , Dalcanton, J. J. ,Williams, B. F. ,Weisz, D. R. ,Skillman, E. D. ,Fouesneau, M. and Dolphin, A. E 2015, ApJ, 810, 9
- Davis, B. L., Kennefick, D., Kennefick, J., Kyle, B. W., Shields, D. W. 2015, ApJ, 802, L13
- Davis, B. L., Berrier, J. C., Shields, D. W., Kennefick, J., Kennefick, D., Seigar, M. S., Lacy, C. H. S., & Puerari, I. 2012, ApJS, 199, 33
- Egusa, F. and Kohno, K. and Sofue, Y. and Nakanishi, H. and Komugi, S. 2009, ApJ, 697, 1870
- Elmegreen, D. M., Elmegreen, B. G., Yau, Andrew, et al. 2011, ApJ, 737, 32
- Fazio, G. G., Hora, J. L., Allen, L. E., et al. 2004, ApJS, 154, 10
- Gittins, D. M. and Clarke, C. J. 2004, MNRAS, 349, 909-921
- Grosbol, P. J. & Patsis, P. A. 1998, A&A, 336, 840
- Kendall, S. and Kennicutt, R. C. and Clarke, C. and Thornley, M. D. 2008, MNRAS, 387, 1007-1020
- Kennicutt, Jr., R. C. 1981, AJ, 86, 1847
- Kim, Y. and Kim, W.-T. 2013, MNRAS, 440, 208-224
- Lin, C. C. and Shu, F. H. 1964, ApJ, 140, 646
- Louie, M. and Koda, J. and Egusa, F. 2013, ApJ, 763, 94
- Martínez-García, E. E. 2012, ApJ, 744, 92
- Martínez-García, E. E. and Puerari, I. and Rosales-Ortega, F. F. and González-Lópezlira, R. A. and Fuentes-Carrera, I. and Luna, A. 2014, ApJ, 793, L19
- Pour-Imani, H. and Kennefick, D. and Kennefick, J. and Davis, B. L. and Shields, D. W. and Shameer Abdeen, M. 2016, ApJ, 827, L12

- Roberts, W. W. 1969, ApJ, 158, 123
- Grand, R. J. J. and Kawata, D. and Cropper, M. 2013, , 553, A77
- Seigar, M. S. 2005, MNRAS, 361, L20
- Seigar, M. S., Bullock, J. S., Barth, A. J., & Ho, L. C. 2006, ApJ, 645, 1012
- Seigar, M. S., Kenefick, D., Kenefick, J., & Lacy, C. H. S. 2008, ApJ, 678, L93
- Savchenko, S. S., and Reshetnikov, V. P. 2011, AstL, 37, 817
- Shields, D. W., Davis, B. L., Pour-Imani, Hamed., Kenefick, D., & Kenefick, J. 2015, arXiv:1511.06365
- Shu, Frank H. 2016, Six Decades of Spiral Density-Wave Theory, Annual Review of Astronomy and Astrophysics, Vol 54, Sep 2016
- Yuan, C. and Grosbol, P. 1981, ApJ, 243, 432

## Chapter 6

### Conclusions

This dissertation has focused on finding a strong evidence for the density-wave theory of spiral arm structure in disk galaxies. As we discussed in Chapter 1, since the 1960s, there have been different models to explain the spiral structure. The density-wave theory of galactic spiral-arm structure (Lin & Shu, 1964) makes a striking prediction that the pitch angle of spiral arms should vary with the wavelength of the galaxy's image. Previous studies are not completely satisfied with the density-wave theory. For example, E. M Garcia et al (Martinez-Garcia et al., 2014) investigate the behavior of the pitch angle of spiral arms depending on optical wavelength. They examined five galaxies in two optical bandpasses and their results show that just three of those five galaxies comply with density wave theory. Their results and sample size are very similar to an earlier paper by Grosbol and Patsis (Grosbol & Patsis, 1998). Davis et al (Davis et al., 2012) consider the possibility of different pitch angles arising in different wavebands of light. Their results show a comparison of their pitch angle measurements for 49 NGC galaxies in optical wavelength (*B*-band: 445 nm, *I*-band: 806 nm) and in this comparison just 55% of galaxies have bigger pitch angle in *I*-band, so this result is not completely satisfied with the density-wave theory. We used a larger sample size than any previously used to study this issue with a greater variety and range of wavebands consulted.

Chapter 2 explains the density-wave theory of spiral structures, and gives some back-

ground to the theory testing method which involves measuring the pitch angle at different wavelengths of light and comparing them to see whether the pitch angle varies with wavelength.

Chapter 3 shows an exciting discovery we have made about a strong piece of evidence for the density-wave theory of spiral structure in disk galaxies. Images from deep infrared wavelength (3.6 and 8.0  $\mu\text{m}$ ) unlike images were taken at optical wavelengths show us the spiral arms patterns traced by old stars (near-infrared) and gas and dust (far-infrared). For each galaxy, we used images a wide range of wavelengths of light and we measured the pitch angle with two completely independent codes 2DFFT and Spirality (Davis et al., 2012; Shields et al., 2015). Our results for 41 NGC galaxies show that the spiral arm pitch angle for images with different wavelength are different and it completely satisfies the prediction of density-wave theory. These results constitute very strong evidence for this theory, made particularly impressive by using a larger sample size with a wider range of wavelength than used in previous studies.

In Chapter 4, I have presented clear evidence in favor of a prediction of the density-wave theory that there is a tighter pitch angle in the  $B$ -band than is found for wavelengths associated with the star-forming region. We have built upon the result in our earlier results in chapter 3 (Pour-Imani et al., 2016) by adding two more star-forming wavelengths, the  $H\text{-}\alpha$ , and  $u$ -band. We have found our results are even more consistent with the standard interpretation of the density-wave theory. We, therefore, regard our results as strongly in favor of the density-wave theory. We additionally find evidence to support those earlier works which see only small differences in pitch angle between optical and NIR wavelengths.

Broadly we see two different systems, a star-forming region visible in the 8 microns, H- $\alpha$  and FUV and stellar light downstream visible in the  $B$ -band and the NIR. The  $u$ -band light, predictably, falls between these two systems. Thus we argue that we are seeing the star-forming region and then light from recently-born stars moving downstream from that position. This is consistent with the density-wave theory of spiral structure.

In Chapter 5, I have presented one more possible prediction by the density-wave theory regarding the existence of a correlation between shear rate, pitch angle variations, and a galaxy's morphological type. For the first time, to our knowledge, I have analyzed the pitch angle variations at different wavelengths of light and its correlation with shear rate.

## Bibliography

- Athanassoula, E., Romero-Gómez, M., Bosma, A. and Masdemont, J. J. 2010, MNRAS, 407, 1433-1448
- Abdeen, M.Shameer and Kennefick, D. and Kennefick, J. and Pour-Imani, H. and Shields, D. W. and Eufrazio, R. and Medina, J.B. and Monson, E. 2017, in Preparation
- Berlind, A. A. and Quillen, A. C. and Pogge, R. W. and Sellgren, K. 1997, AJ, 114, 107-114
- Bertin, G. & Lin, C. C. 1995, Spiral structure in galaxies a density-wave theory, The MIT Press
- Choi, Y. , Dalcanton, J. J. ,Williams, B. F. ,Weisz, D. R. ,Skillman, E. D. ,Fouesneau, M. and Dolphin, A. E 2015, ApJ, 810, 9
- Davis, B. L., Kennefick, D., Kennefick, J., Kyle, B. W., Shields, D. W. 2015, ApJ, 802, L13
- Davis, B. L., Berrier, J. C., Shields, D. W., Kennefick, J., Kennefick, D., Seigar, M. S., Lacy, C. H. S., & Puerari, I. 2012, ApJS, 199, 33
- Egusa, F. and Kohno, K. and Sofue, Y. and Nakanishi, H. and Komugi, S. 2009, ApJ, 697, 1870
- Elmegreen, B. G. and Seiden, P. E. and Elmegreen, D. M. 1989, ApJ, 343, 602
- Elmegreen, D. M., Elmegreen, B. G., Yau, Andrew, et al. 2011, ApJ, 737, 32
- Eufrazio, R. T. 2015, Ph.D. Thesis, The Catholic University of America
- Fazio, G. G., Hora, J. L., Allen, L. E., et al. 2004, ApJS, 154, 10
- Foyle, K. and Rix, H.-W. and Dobbs, C. L. and Leroy, A. K. and Walter, F. 2011, ApJ, 735, 101
- Gittins, D. M. and Clarke, C. J. 2004, MNRAS, 349, 909-921
- Goldreich, P. and Lynden-Bell, D. 1965, MNRAS, 130, 125
- Grosbol, P. J. & Patsis, P. A. 1998, A&A, 336, 840
- James, P. A. and Seigar, M. S. 1999, A&A, 350, 791
- Julian, W. H. and Toomre, A. 1966, ApJ, 146, 810
- Kendall, S. and Kennicutt, R. C. and Clarke, C. and Thornley, M. D. 2008, MNRAS, 387, 1007-1020

- Kennicutt, Jr., R. C. 1981, *AJ*, 86, 1847
- Kim, Y. and Kim, W.-T. 2013, *MNRAS*, 440, 208-224
- Lin, C. C. and Shu, F. H. 1964, *ApJ*, 140, 646
- Louie, M. and Koda, J. and Egusa, F. 2013, *ApJ*, 763, 94
- Martínez-García, E. E. 2012, *ApJ*, 744, 92
- Martínez-García, E. E. and Puerari, I. and Rosales-Ortega, F. F. and González-Lópezlira, R. A. and Fuentes-Carrera, I. and Luna, A. 2014, *ApJ*, 793, L19
- Martínez-García, E. E. and González-Lópezlira, R. A. 2015, *Highlights of Astronomy*, Vol 16, p323
- Pour-Imani, H. and Kenefick, D. and Kenefick, J. and Davis, B. L. and Shields, D. W. and Shameer Abdeen, M. 2016, *ApJ*, 827, L12
- Rix, H.-W. R. 1991, Ph.D. Thesis, Univ. Arizona
- Rix, H.-W. and Rieke, M. J. 1993, *ApJ*, 418, 123
- Roberts, W. W. 1969, *ApJ*, 158, 123
- Savchenko, S. S., and Reshetnikov, V. P. 2011, *AstL*, 37, 817
- Seigar, M. S., Bullock, J. S., Barth, A. J., & Ho, L. C. 2006, *ApJ*, 645, 1012
- Seigar, M. S., Kenefick, D., Kenefick, J., & Lacy, C. H. S. 2008, *ApJ*, 678, L93
- Sellwood, J. A. and Carlberg, R. G. 2011, *ApJ*, 785, 137
- Shields, D. W., Davis, B. L., Pour-Imani, Hamed., Kenefick, D., & Kenefick, J. 2015, arXiv:1511.06365
- Shu, Frank H. 2016, *Six Decades of Spiral Density-Wave Theory*, *Annual Review of Astronomy and Astrophysics*, Vol 54, Sep 2016
- Wright, G. S. and Casali, M. M. and Walther, D. M. and McLean, I. S. 1991, *Astronomical Society of the Pacific Conference Series*, Vol 14, p44
- Yuan, C. and Grosbol, P. 1981, *ApJ*, 243, 432

# Appendix

## AMERICAN ASTRONOMICAL SOCIETY

This agreement must be signed and returned to the editorial office before the American Astronomical Society (AAS) can publish your paper. In the event the article is not judged acceptable for publication in the journal you will be notified in writing and the copyright and all rights conferred by this agreement shall revert to you.

PUBLICATION AND TRANSFER OF COPYRIGHT AGREEMENT Manuscript number: LET33933

Article title: Strong Evidence for the Density-wave Theory of Spiral Structure in Disk Galaxies

Names of authors: Hamed Pour-Imani Daniel Kennefick Julia Kennefick Benjamin Davis Douglas Shields Mohamed Abdeen

*Author Rights:* AAS grants to the author(s) (or their below-named employers, in the case of works made for hire) the following rights. All copies of the Article made under any of these rights shall include notice of the AAS copyright.

- (1) All proprietary and statutory rights other than copyright, such as patent rights.
- (2) The right after publication by the AAS to grant or refuse permission to third parties to republish all or part of the Article or a translation thereof. In the case of whole articles only, third parties must first obtain permission from the AAS before any right of further publication is granted. The AAS may choose to publish an abstract or portions of the Article before the AAS publishes it in a journal.
- (3) The right to use all or part of the Article in future works and derivative works of their own of any type, and to make copies of all or part of the Article for the authors' use for educational or research purposes.
- (4) In the case of a work made for hire, the right of the employer to make copies of the Article for the employer's internal use, but not for resale.

*Copyright Assignment:* Copyright in the Article is hereby transferred to the AAS for the full term of copyright throughout the world, effective as of date of acceptance of the Article for publication in a journal of the AAS. The copyright consists of all rights protected by copyright laws of the United States and of all foreign countries, in all languages and forms of communication, and includes all material to be published as part of the Article in any format or medium. The AAS shall have the right to register copyright to the Article in its name as claimant, whether separately or as part of the journal issue or other medium in which the Article is included.

Authorized signature \_\_\_\_\_

Date 5/21/2016

*Certification of Government Employment:* An article prepared by a government officer or employee as part of his or her official duties may not be eligible for copyright, if the authors are all employed by one of the governments of Australia, Canada, New Zealand, the UK, or the US. If all the authors of the article are such government employees, one of the authors should sign here. If any of the authors is not such a government employee, do not sign in this box.

Author signature \_\_\_\_\_

Date \_\_\_\_\_

After signing the form, please scan and upload via the peer review system at <http://ajjl.msubmit.net> or fax to 847-332-0702.

local\_p\_id: 516559

time: 1463801741

ip address: 162.211.129.46



## VITÆ

2017	Ph. D. in Physics & Astronomy, University of Arkansas
2016	M. Sc. in Physics, University of Arkansas
2004	B. Sc. in Physics, University of Isfahan

## PUBLICATIONS

Graphene's morphology and electronic properties from discrete differential geometry. Sanjuan, A.A.P., Wang, Z., **Pour-Imani, Hamed**, VaneviÄ, M., Barraza-Lopez, S. 2014, Phys. Rev. B 89, 121403(R)

Spirality: A Novel Way to Measure Spiral Arm Pitch Angle. Shields, D. W., Boe, B., Pfountz, C., Davis, B. L., Hartley, M., **Pour-Imani, Hamed**, Abdeen, M., Kenefick, D., & Kenefick, J. August 2016, Submitted to Publications of the Astronomical Society of the Pacifica

Strong Evidence for the Density-Wave Theory of Spiral Structure in Disk Galaxies. **Pour-Imani, Hamed**, Kenefick, D., Kenefick, J., Davis, B. L., Shields, D. W., & Abdeen, M. 2016, The Astrophysical Journal Letters, 827, L12